博 士 学 位 論 文

論文題目 Modeling, Simulation, and Optimization for Human-Centered Mobility Service and Crowd Management

提 出 者 東北大学大学院情報科学研究科

専攻 System Information Science

学籍番号 C0ID2007

氏 名 Ryo Nishida

TOHOKU UNIVERSITY
Graduate School of Information Sciences

Modeling, Simulation, and Optimization for Human-Centered Mobility Service and Crowd Management

（人・ユーザー中心の移動サービスと群集マネジメントのための
モデリング，シミュレーションと最適化）

A dissertation submitted to the degree of
Doctor of Philosophy in Information Sciences

Department of System Information Science

by

Ryo NISHIDA

January 10, 2023

Modeling, Simulation, and Optimization for Human-Centered Mobility Service and Crowd Management

Ryo NISHIDA

Abstract

Computer simulation can be used to advance mobility services design and crowd management. The processes consist of that to model actual mobility in a virtual space, analyzing various situations using simulation, optimizing services and measures for better mobility, and providing feedback information to improve real-world mobility. The motivation of this dissertation is to advance simulation-based mobility management by studying each process of modeling, simulation, and optimization of mobility.

In this dissertation, I base on agent-based simulation and focus on modeling, simulation, and optimization from a human or user perspective. Because people make decisions autonomously, simulation results will differ from reality unless the modeling takes those decisions into account. Therefore, the model of agents must reflect the actual users' behavior. In addition, because services and measures will not be accepted unless they are beneficial to users, unless it is shown that the new services and measures are valuable to users, they will end up being just an armchair philosophy. Therefore, when analyzing simulations, it is necessary to evaluate from multiple perspectives, including not only the supply side but also the user side. It is also important to take into account the fact that the objectives of the supply side and the users, e.g., service providers and users, are different and conflicting. If one objective function is used to optimize a service or measure, it may exacerbate other important objectives. Therefore, it is important to emphasize and incorporate the human/user perspective in the modeling, simulation analysis, and optimization processes.

Based on above, The objective of this dissertation is to contribute to more advanced and human-centered mobility service and crowd management by conducting research with a stronger emphasis on the human/user perspective in modeling, simulation, and optimization topics.

In research of modeling, I attempt to understand and model the characteristics of people's choice behavior from real data. I use travel mode choice modeling to identify

the selection bias of a new mobile service in the early stages of its introduction. I collected data on travel mode choice behavior on Mobility as a Service (MaaS) pilot in Shizuoka city. As a result of mode choice modeling, it was found that the user's choice behavior was in line with intuition even in the experimental environment, while selection bias toward a new mobility service was also observed. This suggests the importance of considering the selection bias for the new mobility service when verifying the effect of the initial introduction of the service, such as a demonstration experiment. In addition, I attempt to model pedestrians' route choice behavior. I show that route choice modeling from real crowd movement data can quantitatively reveal the existence of herding behavior and autonomous behavior that does not follow guidance, and that simulations that account for such behavior can improve the reproducibility of crowd movement. In addition to performing choice modeling for traffic/mobility service and crowds, I also attempt to extend the general method of choice modeling. I show that semi-supervised learning can be applied to estimate choice models even with a small amount of data.

In research of simulation analysis, I attempt to analyze whether the introduction of new mobility services really benefits users. I present a simulation analysis of the benefits that MaaS brings to users. The benefits to users of introducing on-demand shared mobility service (OSMS) in addition to railways and buses and increasing their transportation options were investigated in accordance with the setting of the MaaS demonstration experiment in Shizuoka. The results show that the introduction of MaaS, or in other words OSMS, increases the benefits to users, but the provider loses profit when the number of users is small. In addition, I analyze the benefits of introducing meeting points (MPs) in OSMS by simulation. OSMS generally provides door-to-door transportation between passengers' origins and destinations. In addition, services using specific pick-up/drop-off locations, which are called MPs, are also deployed. I conduct a static analysis under simple settings and a simulation analysis using actual road network data. Results showed that the introduction of MPs reduces vehicle kilometers traveled as well as the average travel time of passengers when the number of demands is greater than some threshold. As a research for crowd movement, I summarize the research trends in spatial design and crowd control from the viewpoint of crowd simulation and optimization. This survey will help event organizers and facility managers understand how spatial design and crowd control can help move crowds efficiently and safely.

Finally, I study multi-objective optimization in order to implement optimization from multiple perspectives, such as users and suppliers. I attempt to verify whether

multi-objective deep reinforcement learning (MODRL) can be applied to real-world problems, such as a crowd route guidance strategy optimization. I investigate problems of Pareto-DQN, one of the MODRL methods, and propose its improvement. I clarify the possibility of applying Pareto-DQN to real-problem and the advantages and disadvantages throughout the experiments using the problem of toy problem and crowd guidance strategy optimization problem.

In conclusion, This dissertation is summarized, and future works are described.

Contents

List of Figures

List of Tables

Chapter 1

Introduction

1.1 Background

We cannot build a time machine, but we can go to the future with a computer simulation. The most familiar and practical use case of simulation may be weather forecasting. Since the 1950s, with the widespread use of computers, computer simulation has been actively studied and can predict the weather with high accuracy. Simulation is also used in the design of automobiles and aircraft. For example, airflow around a vehicle is simulated under various conditions using numerical models, such as turbulence models. Sometimes, optimization with simulations is used to optimize the design. Product designs that would be costly in the real world can be repeated again and again using computer simulation. Design using computer simulations is now called computer-aided engineering or model-based development.

Targets of computer simulations have expanded to include not only natural phenomena such as weather and airflow around vehicles but also social phenomena. Fifty years ago, the Club of Rome, Swiss nonprofit, informal organization of scientists,

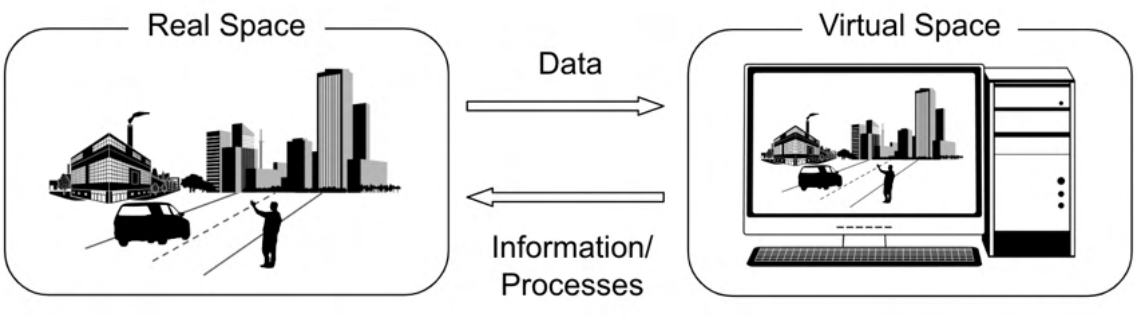

Figure 1.1: Concept of Digital Twin

economists, educators, business managers, etc., reported "Limits to Growth" [14]. They used system dynamics, which is a model based on differential equations, to simulate population, food, and pollution trends up to the year 2100, and reported the conclusion that "if trends such as population growth and environmental pollution continue at this rate, growth on Earth will reach its limits within 100 years due to resource depletion and environmental degradation". After this, simulations of various social phenomena and improvements in simulation methods have continued. Nigel Gilbert, a pioneer of agent-based models, stated "computer simulation has a similar role in the social sciences to that of mathematics in the physical sciences" [15]. Thus, computer simulation has become a powerful tool for understanding and improving society.

In 2003, the concept of simulation, which reproduces real entities and environments in the virtual space, was extended to the concept of Digital Twin [16]. The difference from the simulation is the close relationship between real and virtual space. As shown in Figure 1.1, data from the real space is measured, and the virtual space is modified to match reality at near real-time frequency. It then finds the desired state in the virtual space and feedback information or executes some process to the

real space in order to bring the real space closer to that desired state. The system then measures the real space that is updated by the feedback and modifies the virtual space again [17]. This continuous connection between the real and virtual spaces is the decisive difference from conventional offline simulation. The realization of Digital Twin has accelerated in recent years, driven by industrial developments such as Internet-of-Things (IoT), Big Data, and cloud computing.

Applications of Digital Twin are mainly in the manufacturing industry. It enables simulation and optimization of production systems, including logistics, and visualization of the manufacturing process. When a new order is received, production planning can be constructed in a virtual space. Real-time monitoring of the production system enables the user to grasp the condition of the machine and simulate future conditions in a virtual space, allowing the user to prepare for maintenance in advance [18]. Digital Twin is originally designed to improve manufacturing processes using simulations that have highly accurate models of individual components. However, with increasingly large and accurate building information models (BIM) combined with big data generated from IoT sensors in a smart city, it became possible to create Digital Twin for smart cities [19].

As mentioned above, computer simulations and Digital Twin are increasingly targeting societies and cities. The social simulation covers the economy, financial markets, SNS, infectious diseases, transportation, crowd movement, migration of population, power systems, and so on. The main domains of smart cities are transportation, environment, energy, healthcare, buildings, infrastructure, public safety, living, governance, and education [20, 21].

1.2 Motivation

"The road to hell is paved with good intentions." – – Unknown

Sometimes measures implemented to improve the current situation lead to worse results. For example, the Downs-Thomson paradox is a well-known example [22, 23]. A traveler can move from point A to point B either by public transportation or by car. When demand for public transportation increases, the number of services is increased, and travel time becomes shorter. When demand for car increases, the number of vehicles on the road increases, and the travel time get longer. Under these conditions, if the road is widened to reduce congestion on the road, car use will increase, public transportation demand will decrease, and public transportation service will decrease, resulting in a longer travel time than before the road was widened. Braess's paradox suggests the same thing [24].

Simulation allows for predicting results before the measures are implemented. In other words, simulation can be used to advance the design of mobility services and the management of crowd movement. Specifically, the processes are to model actual mobility in a virtual space, analyze various situations using simulation, optimize services and measures for better mobility, and provide feedback information to improve real-world mobility. The motivation of this dissertation is to advance simulation-based mobility management by studying each process of modeling, simulation, and optimization of mobility as shown in Figure 1.2.

In particular, in this dissertation, I base on agent-based simulation and focus on modeling, simulation, and optimization from a human or user perspective. Because people make decisions autonomously, simulation results will differ from reality unless the modeling takes those decisions into account. Therefore, the model of agents must

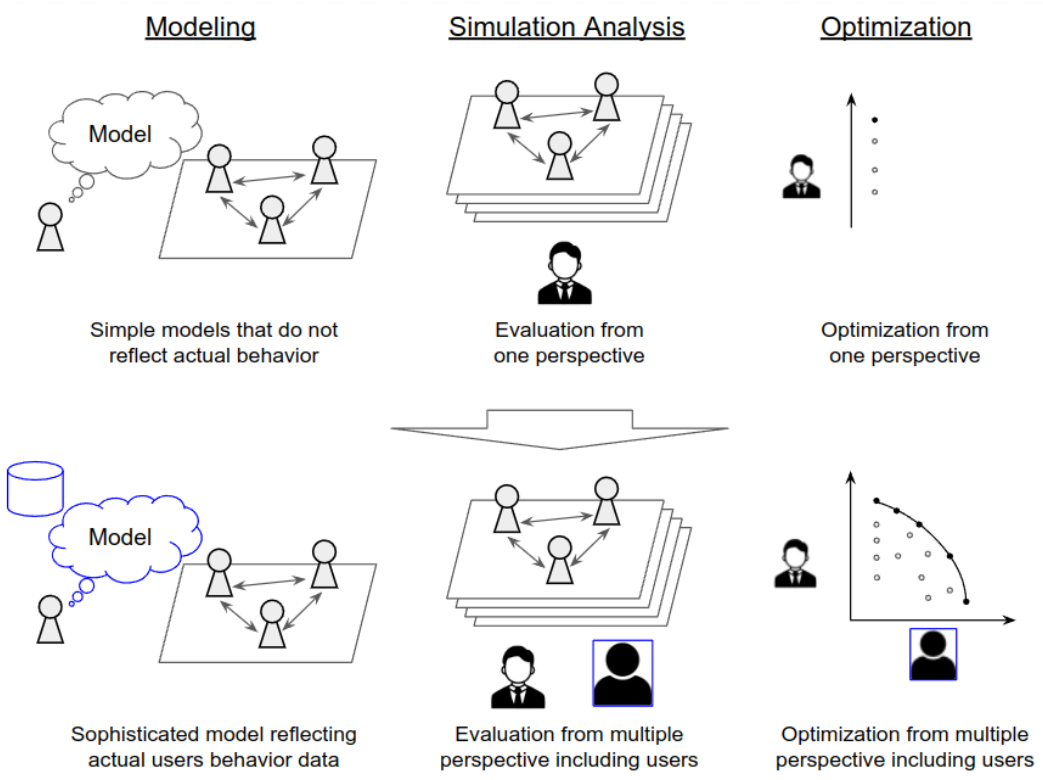

Figure 1.2: Concept of this dissertation.

reflect the actual users' behavior. In addition, because services and measures will not be accepted unless they are beneficial to users, unless it is shown that the new services and measures are valuable to users, they will end up being just an armchair philosophy. Therefore, when analyzing simulations, it is necessary to evaluate from multiple perspectives, including not only the supply side but also the user side. It is also important to take into account the fact that the objectives of the supply side and the users, e.g., service providers and users, are different and conflicting. If one objective function is used to optimize a service or measure, it may exacerbate other important objectives. Therefore, it is important to emphasize and incorporate the human/user perspective in the modeling, simulation analysis, and optimization processes.

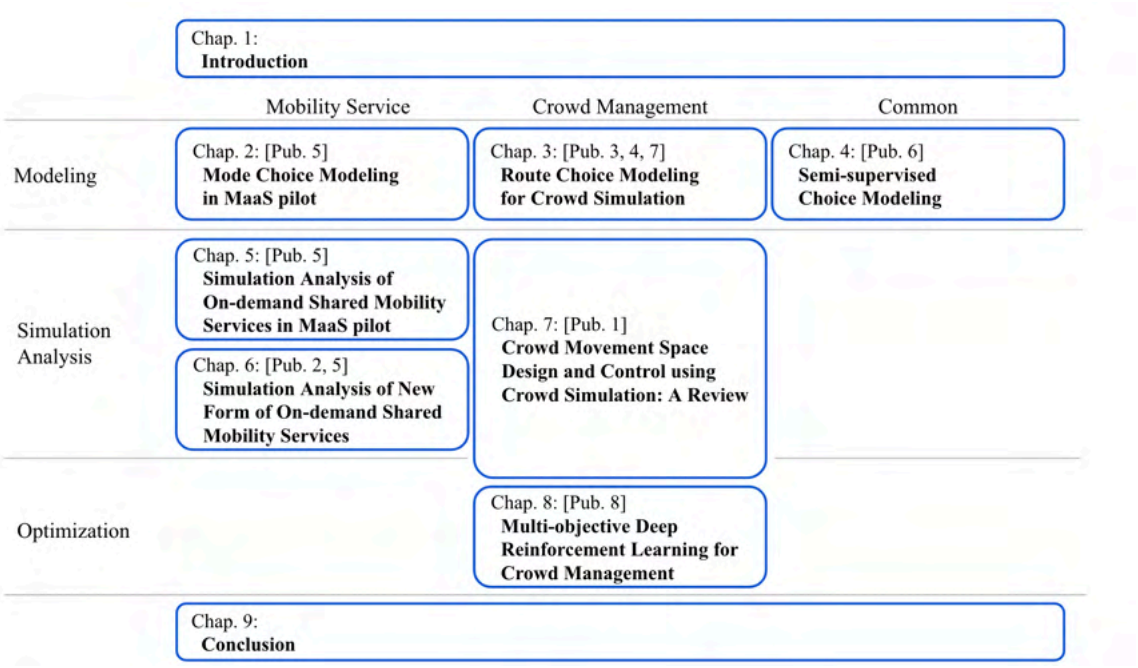

Figure 1.3: Overview of this dissertation.

1.3 Objective and Contributions

The objective of this dissertation is to contribute to more advanced and human-centered mobility service and crowd management by conducting research with a stronger emphasis on the human/user perspective in modeling, simulation, and optimization topics. The outline of this dissertation and its relation to the publication list are shown in Figure 1.3

This dissertation describes research in the order of modeling, simulation, and optimization. The modeling part consists of Chapters 2, 3, and 4, which attempt to understand and model the characteristics of people's choice behavior from real data. The simulation part consists of Chapters 5, 6, and 7, which attempt to analyze whether the introduction of new mobile services really benefits users and to organize the application of crowd simulation to clarify the findings. The optimization part

is Chapter 8, which attempts to verify whether multi-objective deep reinforcement learning (MODRL) can be applied to real-world problems, such as the crowd route guidance strategy optimization.

In Chapter 2, I model the travel mode choice behavior and identify the selection bias of a new mobile service in the early stages of its introduction. In Mobility as s Service (MaaS) demonstration experiment conducted in Shizuoka City in 2019, on-demand shared mobility service (OSMS) was introduced in areas where trains and buses are operating, and citizens used a smartphone App. that allows them to search for routes. I collected data on travel mode choice behavior from the usage history data of the App. As a result of mode choice modeling, it was found that the user's choice behavior was in line with intuition even in the experimental environment, while selection bias toward OSMS was also observed. This suggests the importance of considering the selection bias for the new mobility service when verifying the effect of the initial introduction of the service, such as a demonstration experiment.

In Chapter 3, I describe the choice modeling for pedestrians' route choices. I show that route choice modeling from real data can quantitatively reveal the existence of herding behavior and autonomous behavior that does not follow guidance, and that simulations that account for such behavior can improve the reproducibility of crowd movement. In experiments, we measure crowd movements during an evacuation drill in a theater and a firework event where tens of thousands of people moved and prove that the crowd simulation incorporating the route choice model can reproduce the real large-scale crowd movement more accurately.

In Chapter 4, I introduce a new paradigm of choice modeling. In recent years, neural networks (NNs) techniques have been developed in the field of artificial intel-

ligence to model human information processing with high accuracy. Therefore some choice models incorporating NNs have been proposed. NNs make it possible to represent heterogeneous preferences in decision-making more accurately. On the other hand, learning a model using NNs requires a large number of data. In this study, I show that semi-supervised learning can be applied to estimate choice models even with a small amount of data.

Chapter 5 presents a simulation analysis of the benefits that MaaS brings to users. The benefits to users of introducing OSMS in addition to trains and buses and increasing their transportation options were investigated in accordance with the setting of the MaaS demonstration experiment in Shizuoka. The results show that the introduction of MaaS, or in other words OSMS, increases the benefits to users, but the provider loses profit when the number of users is small. If the number of users increases and the number of OSMS vehicles and fares are adjusted, the provider also archives benefits. However, since the share of trains and buses is reduced by the introduction of OSMS, coordination between the different operators of each mobility service is necessary.

In Chapter 6, I analyze the benefits of introducing meeting points (MPs) in OSMS by simulation. OSMS generally provides door-to-door transportation between passengers' origins and destinations. In addition, services using specific pick-up/drop-off locations, which are called MPs, are also deployed. The operational efficiency of OSMS could be improved by asking passengers to walk to an MP. However, the travel time of passengers (i.e. passenger convenience) has not been sufficiently explored. I conduct a static analysis under simple settings and a simulation analysis using actual road network data. Results showed that the introduction of MPs reduces

vehicle kilometers traveled as well as the average travel time of passengers when the number of demands is greater than some threshold.

Chapter 7 summarizes the applications of crowd simulation. I summarize the research trends in spatial design and crowd control from the viewpoint of crowd simulation and optimization. I first introduce the evaluation indices of crowd movement in terms of efficiency and safety. Then, I explain the current findings on spatial design and categorize the methods of crowd control, ordered by the level of pedestrian behavior. In the end, the challenges and approaches are discussed based on the previous research. This survey will help event organizers and facility managers understand how spatial design and crowd control can help move crowds efficiently and safely.

In Chapter 8, I examine the applicability of MODRL, one of the approaches for coordinating multiple needs, to real problems. I investigate problems of Pareto-DQN, one of the MODRL methods, and propose its improvement. I clarify the possibility of applying Pareto-DQN to real-problem and the advantages and disadvantages throughout the experiments using the problem of toy problem and crowd guidance strategy optimization problem.

Chapter 9 concludes the dissertation. I discuss the future work and summarize the dissertation.

Chapter 2

Mode choice model in Mobility as a Services

2.1 Introduction

The modeling approaches of human mobility can be classified into macroscopic and microscopic. The macroscopic approaches treat and model people as a group. On the other hand, the microscopic approaches model each individual trip or behavior.

First, I describe macroscopic approaches of modeling human mobility. In the transportation research field, Four-step model has been mainly used to model human mobility and to forecast traffic demand [25]. This model predicts where people will move from where to where, when, by which modes of transportation, and by which route, divided into four stages: 1) trip generation, 2) trip distribution, 3) model split, and 4) traffic assignment. Four-step model was proposed in the 1950s and has been used for expressway demand forecasting.

Since the 1990s, Activity-based model has been developed based on the idea that

mobility is a derivative demand of individual activity [26]. It is a microscopic modeling approach because it focuses on individual activities. The model describes each activity of travel, including the trip destination choice and the travel mode choice. Hasnine et al. summarized the differences between Four-step model and Activity-based model, as shown in Table 2.1.

Assuming that the decision of the trip time of day is the choice of the start time of travel, we can see that some of this model, including trip destination choice, mode choice, and route choice in the part of network assignment, are based on people's choice behavior. By modeling people's choice behavior, we can understand the reasons for choice and preferences in choice behavior.

In recent years, new mobility services, such as on-demand mobility services and Mobility as a Service (MaaS), have begun to spread. MaaS is based on the concept of integrating multiple transportation modes as one service, such as railways, fixed-route buses, taxis, and new on-demand services like ride-hailing. MaaS is proposed by Heikkilä [27] and Hietanen [28] in Finland in 2014. In Helsinki, Finland, traffic congestion between a city and suburbs has become a problem, and the concept of MaaS was born as a solution to improve the convenience of public transportation that is necessary to reduce the dependence on private cars.

However, the analysis of travel mode choice behavior in such services is insufficient. Several studies have conducted questionnaires, collected data on people's choice behavior, and analyzed preferences in choice [29, 30, 31, 32, 33, 34, 35, 36, 37]. Since demonstration experiments and actual services are beginning to spread, it would be possible to analyze people's realistic behavior if actual data could be used for modeling.

Therefore, in this section, I attempt to model travel mode choice behavior in a MaaS demonstration experiment using actual data. A MaaS demonstration was conducted in Shizuoka City in Japan, in November 2019 where on-demand shared mobility service (OSMS) was introduced into public transportation modes such as railways, and fixed-route buses. To improve the convenience of public transportation, only railways and buses that are operated with fixed timetables and routes are not enough, so OSMS is an important key for MaaS. OSMS such as Via and UberPool are becoming popular. OSMS has the characteristic of riding people together who travel by a similar route. For users, the fare is cheaper than taxis, and it is possible to move more flexibly than buses, and for the provider, the demand can be processed with a small number of vehicles, which improves driving efficiency. I collect data and perform modeling in a MaaS demonstration experiment to understand choice behavior in the MaaS pilot and investigate the attractiveness of OSMS to users.

This chapter is organized as follows. Section 2.2 explains the choice modeling methods. Section 2.3 describes the MaaS pilot and data collection. Section 2.4 describes the estimation results of the mode choice model and summarizes the insights from the modeling. Finally, Section 5 provides a summary.

2.2 Choice Modeling

When we travel, we choose a transportation mode from among bus, train, taxi, and other options. Modeling such decision-making behavior is called ”choice modeling”. When the options are discrete, we call it ”discrete choice modeling”.

2.2.1 Discrete Choice Model

Discrete choice models (DCMs) can be applied to a wide range of fields, including marketing (e.g., product/service, brand choice), transportation (e.g., route, transportation mode choice), and economics (e.g., policy, migration location choice). Therefore, DCMs have been developed not only in economics but also in the field of transportation engineering.

DCMs are based on random utility maximization theory [38]. This theory assumes that when people make a choice, they choose the option that maximizes their utility. Figure 2.1 shows the process of a transportation mode choice. Utility basically consists of attributes of alternatives $\boldsymbol{x}$ such as travel time and monetary cost, and preferences $\boldsymbol{\beta}$ for those factors. The utility also depends on individual characteristics $\boldsymbol{z}$ such as age and gender. The utility function is consisting of two terms. The first is a deterministic term V that function of $\boldsymbol{x}, \boldsymbol{\beta}$, and $\boldsymbol{z}$. The second is a probability term ε. Since the true utility of the decision maker is unknown to the analyst, the probability term is used to represent utility probabilistically. The utility of each transportation mode and the choice probability are calculated, and the final selection is determined.

2.2.2 Multinomial Logit Model

In a basic model of DCMs, Multinomial Logit Model (MNL), the utility function is often represented by the linear sum of $\boldsymbol{x}, \boldsymbol{\beta}$, and $\boldsymbol{z}$. In MNL, the utility function U_{ij} for individual i choice j is shown below. The utility function consists of a deterministic term V_{ij} and a probability term ε_{ij}. In general, the deterministic term is expressed as a linear sum of the k observable factors x_{ijk} and preferences β_k. The probability term contains uncertainties such as unobservable factors, factors other than the

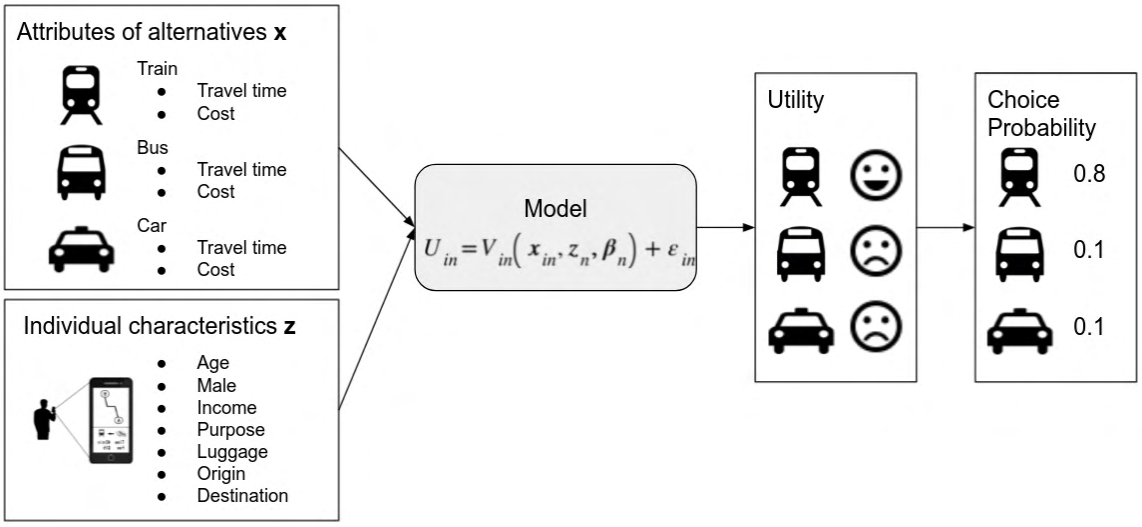

Figure 2.1: The process of choice

deterministic term, and measurement errors of the factors of the deterministic term.

$$U_{ij} = V_{ij} + \varepsilon_{ij} \tag{2.1}$$

$$= \beta_{ij,0} + \sum_{k=1} \beta_{ij,k} x_{ij,k} + \varepsilon_{ij} \tag{2.2}$$

where, x that describe the observed attributes of the choice alternative (e.g., the price or travel time associated with the mode), and the individual socio-demographic characteristics (e.g., the individual level of income or age) [39]. β_0 is an alternative-specific constant (ASC) and, it expresses a bias toward an alternative.

Assuming a Gumbel distribution for the probability term, the probability that an individual i will choose option j from a choice set C is as follows

$$P_i(j) = \frac{\exp(V_{ij})}{\sum_{l \in C} \exp(V_{il})} \tag{2.3}$$

The preference parameters β_k are estimated by maximizing the log-likelihood func-

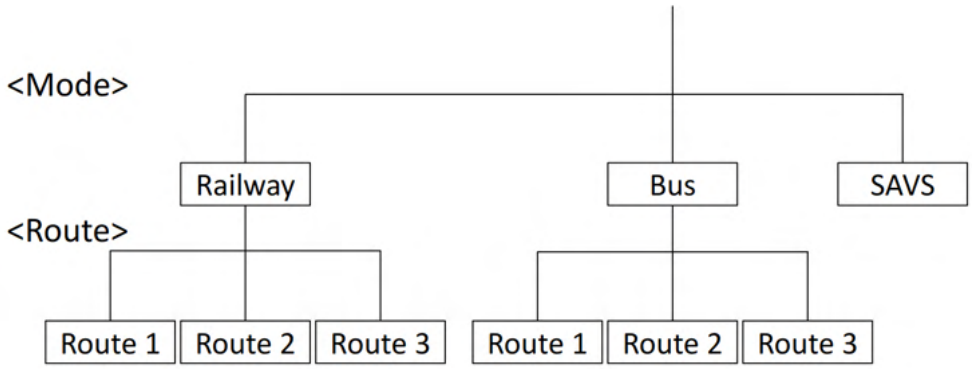

Figure 2.2: Nested tree. SAVS is correspondent to OSMS.

tion given by

$$LL(\boldsymbol{\beta}) = \sum_i \sum_j y_{ij} \log P_i(j) \tag{2.4}$$

where, y_{ij} is 1 when an individual i chooses option j, and 0 otherwise.

2.2.3 Nested Logit Model

MNL does not consider the correlation between choices and may overestimate the selection probability. Nested Logit (NL) model is also based on the principle of utility maximization, is derivation of a logit model, and nests similar options to consider the correlation between options [40].

In our case, the nested tree is as shown in Figure 2.2. Smart access vehicle service (SAVS) is the name of the OSMS service used in this MaaS demonstration experiment. The choice probability of the main mode m and the route r is defined by the following equation (2.5), and is the product of the route choice probability and mode choice probability.

$$\begin{aligned} P(m,r) &= P(r|m)P(m) \\ &= \frac{\exp\left(V_{mr}\right)}{\sum_{r'}\exp\left(V_{mr'}\right)}\frac{\exp\left(\eta_m\left(V_m+V'_m\right)\right)}{\sum_{m'}\exp\left(\eta_{m'}\left(V_{m'}+V'_{m'}\right)\right)}, \end{aligned} \tag{2.5}$$

where η_m is a scale parameter of a Gumbel distribution of a mode choice.

V_{mr} is the deterministic term of the route r whose main mode is m, and is defined as the linear sum of the price, travel time and number of transfers, and their weights, such as

$$V_{mr} = \beta_{\text{price}} * x_{\text{price}_{\text{mr}}} + \beta_{\text{time}} * x_{\text{time}_{\text{mr}}} + \beta_{\text{transfer}} * x_{\text{transfer}_{\text{mr}}}. \tag{2.6}$$

And V_m represents the utility peculiar to transportation mode. V'_m is called a logsum variable and represents the expected value of V_{mr} for each mode of transportation, and is defined as (5.4)

$$V'_m = \frac{1}{\eta_r}\ln\sum_r \exp\left(\eta_r V_{mr}\right), \tag{2.7}$$

where η_r is a scale parameter of a Gumbel distribution of a route choice.

Generally, the parameters of model such as the weights $\boldsymbol{\beta}$, η_m and η_r can be estimated by maximum likelihood estimation.

2.3 Data Collection

The MaaS demonstration was conducted in Shizuoka City in Japan, in November 2019 where OSMS (or SAVS) was introduced into public transportation modes such as railways, and fixed-route buses. For this demonstration, we developed a MaaS App that enables route search of such multiple transportations.

2.3.1 MaaS Pilot

The demonstration aims at the following four purposes

- Verification of social acceptability for paid operation of on-demand shared services
- Verification of the operability of the MaaS App
- Revealed preference survey of transportation mode choie in MaaS.
- Stated preference survey of MaaS schemes usage intentions

The MaaS App is a combined application of a "complex route search service" by Val Laboratory and "SAVS" by Mirai Share. With the MaaS App, users can search for multimodal routes such as railway, fixed-route buses, and SAVS, and only make reservations for a sole and immediate use of SAVS.

Figure 2.3 shows examples of App screenshots when a user is searching routes. The user can compare routes based on the service levels such as price, travel time, and number of transfer. As with a general route search service, once a destination is specified, the route from the origin to the destination will be displayed. The transportation modes are displayed as a icon at the bottom of the App screen. Press the blue button on the upper right to display the details of the option. The user can check the service level of the route. For a SAVS option, press the "Start reservation" button at the bottom to proceed to the reservation screen. The scheduled boarding time, scheduled getting-off time, and fare for SAVS are displayed. When the reservation is confirmed, the SAVS vehicle will be dispatched[1]. The user can check the current position of the vehicle on the App.

[1]Note that in this demonstration reservations can only be made for immediate use of SAVS, so it is not possible to make advance reservations for SAVS for routes that transfer from railways or fixed-route buses to SAVS.

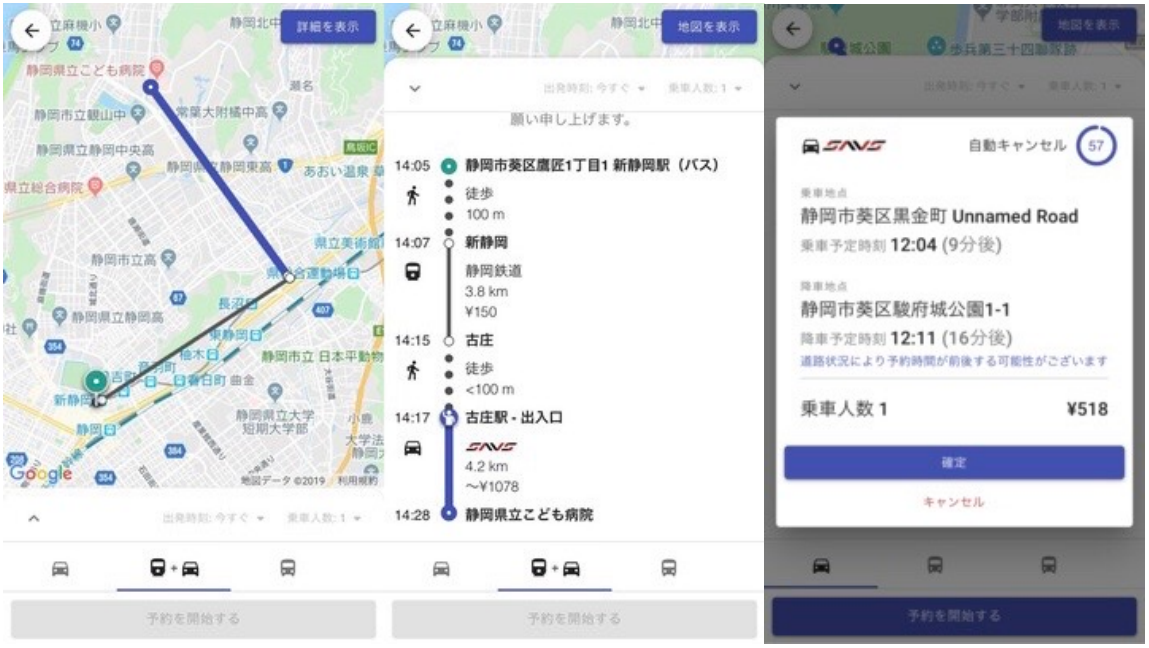

Figure 2.3: MaaS App screen examples

In this demonstration, to use the APP, participants were required to register a LuLuCa membership authorized by the Shizuoka Railway. The LuLuCa membership card offers the passengers a point card function, a credit card function, and a traffic IC card function. Traffic IC card records when and where traveler use railways or fixed-route buses.

The main purpose of this demonstration for this study is to acquire real travel behavior data, in particular mode choice behavior data, in a MaaS scenario. As mentioned above, a SAVS usage history can be specified from SAVS system's log of the MaaS App. However, the MaaS App doesn't provide the usage history of railways or fixed-route buses because the App does not link to the information of reservation and payment for those modes. Therefore, we try to specify the travelers' usage using traffic IC card history.

2.3.2 Usage of App and Travel Modes

This section describes the basic usage results such as the number of users, user characteristics, and changes in the number of searches, and then describes the usage results of each transportation.

App usage

This demonstration attracted 255 MaaS App users for a month. The anonymized user information was obtained via the registration data of LuLuCa card membership because the IDs of the App and the card are linked. Figure 2.4 shows the number of users classified by gender and age. More than 70% of users are male. In particular, among males, 45-54 years old are the most used (35%), while among females, 25-34 years old are the most used (36%). Only 3% of the users were elderly (65 years old or older), and only 5% were young people (24 years old or younger). There were no users under the age of 19.

In addition, Figure 2.5 shows the number of daily searches. The number of searches of the App. is 899 and the maximum number of searches was 73 per a day. More users used the route search function on weekdays rather than weekends and holidays. In the latter half duration of this demonstration, the number of searches increased especially in the last week, whereas the users, during these two weeks earned LuLuCa reward points for every access to the route search.

Each transportation mode usage

Next, we describe each transportation mode usage. From the App log, we calculated that 179 people used SAVS (315 times). On the other hand, when comparing

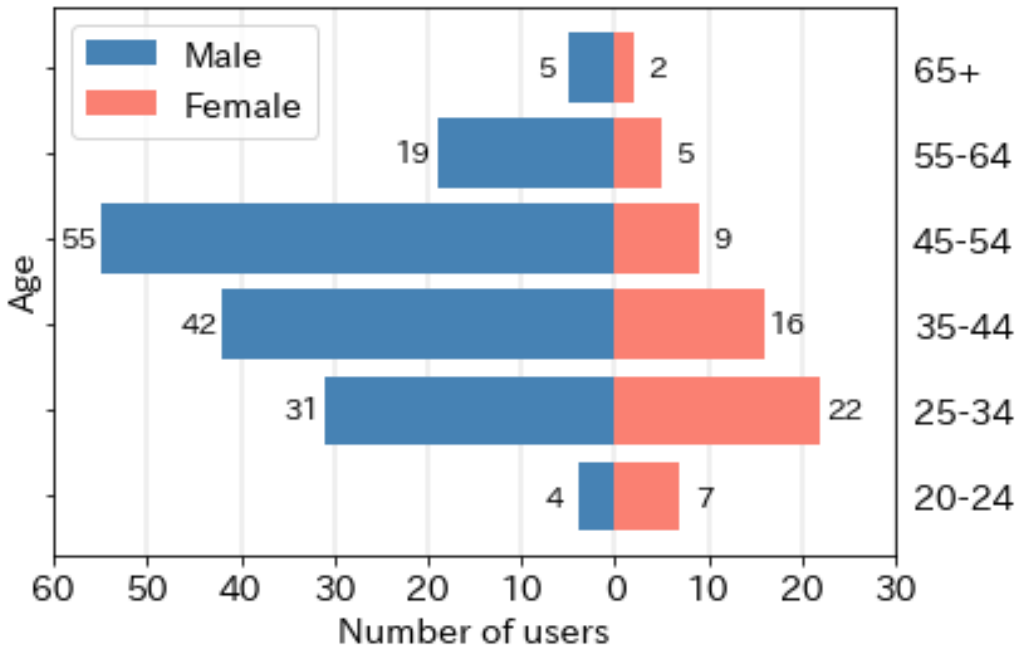

Figure 2.4: Number of MaaS App users by gender and age

the route search results of the App with the usage history by LuLuCa, only 44 out of 899 searches were confirmed to be used (75 cases were used during the same day, and 273 cases were using on any day during the experiment).

From a data analysis point of view, there are some limitations to modeling and simulation from only demonstration data. It seems that some users just used App as a trial for route search. In addition, some users who use public transportation as commuting has become a habit, are thought that use transportation without searching with the App. From these reasons, it was found more difficult than expected at this point to identify the route that searched with App and actually used.

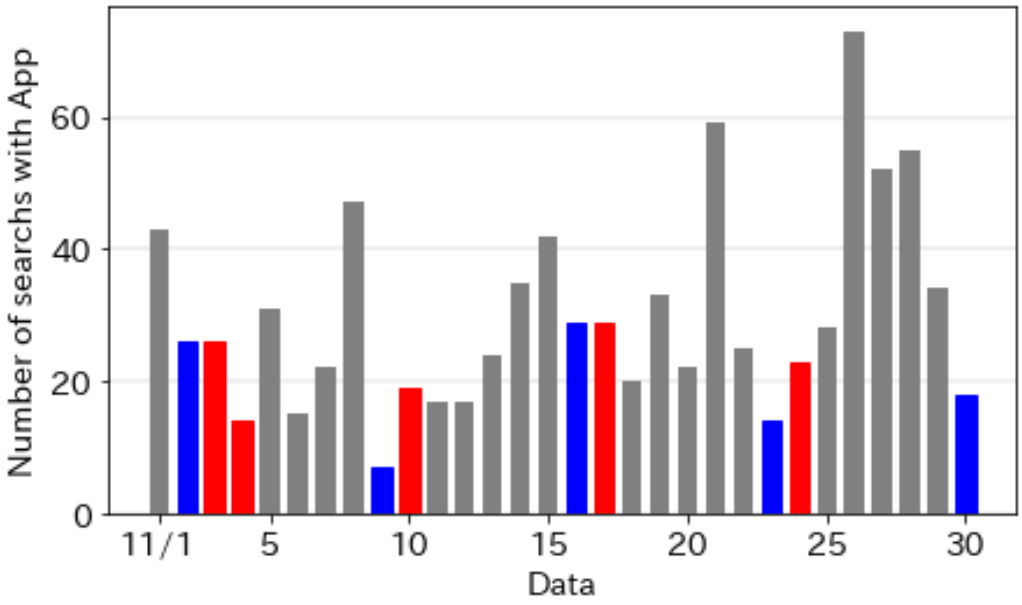

Figure 2.5: Number of daily searches

2.4 Estimation of Mode Choice Model

In this Shizuoka MaaS demonstration, we collected 390 mode choice behavior data that consist of mode/route choice set and choosed result. Of the 390 cases, 315 cases were identified that SAVS was used. Since the number of samples that can be specified that railways or fixed-route buses were used is small, we adopted 75 cases that could be identified as using the same route (at different times) as the recommended route.

Although the number of samples was small, we modeled the mode choice behavior using the NL model. As mentioned in Section 2.2.3, the explanatory variables $\boldsymbol{x}$ were price, travel time, and the number of transfers. In addition, we define V_m for SAVS as an alternative-specific constants (ASC) in order to consider the selection bias that can occur when a new mobility service is introduced. Therefore, the parameters to be estimated are weights $\boldsymbol{\beta}$ for the price, travel time, and the number of transfers,

constant to SAVS ASC_{SAVS}, and a scale parameter of Gumbel distribution η_m (we set $\eta_r = 1$). Table 2.2 is the estimation result. In the tables, $***, **$, and $*$, represent significance levels of 0.001, 0.01, and 0.1, respectively.

From the statistical values of each parameter and the value of the modified coefficient of determination of McFadden [41], $\bar{\rho}^2$, the estimation results are valid to some extent.

I find some knowledge from the estimation results as follows.

- The weights $\boldsymbol{\beta}$ were all negative values, and it was found that the sensitivity for each explanatory variable was reasonably valid even under the MaaS demonstration experiment.
- Since the SAVS constant (ASC_{SAVS}) is a positive value, it was found that SAVS was used more positively than railways and fixed-route buses. This is thought to reflect the concern that "in the MaaS demonstration experiment, there may be a bias toward using transportation that is not normally used." pointed out by Durand et al. [42].
- The time of value obtained from the parameter ratio of price and travel time was 17.8 [yen / minute], and the value is a generally reasonable value.

2.5 Conclusion

I analyze the usage history of apps and estimate a travel mode choice model for a MaaS demonstration experiment conducted in Shizuoka City in November 2019. In this demonstration experiment, we developed the App. that enables users to search for routes combining railroads, local buses, and OSMS. From the collected data, I analyzed the number of users of the MaaS app, user characteristics, trends in the

number of searches, and the usage history of each travel mode. The NL was used to represent the mode choice behavior and I identify the selection bias of OSMS in the MaaS demonstration.

Table 2.1: Comparison between Four-step model and Activity-based model [11]

Four-step model	Activity-based model	Objective
Trip generation	Activity generation and scheduling	Where are trips being generated and what types of activities are individuals participating in?
Trip distribution	Tour and trip destination choice	Where are individuals travelling to?
	Tour and trip time of day	When are they travelling and how long is each activity?
Trip mode choice	Tour and trip mode choice	What types of modes are individuals choosing?
Network traffic assignment	Network assignment	What route are they using and what is the travel time?

Table 2.2: Estimation result

variables	estimate	std error	t-value	p-value
β_{price} [100yen]	-1.144	0.373	-3.066	0.002 **
β_{time}[10min]	-2.035	0.595	-3.419	0.001 ***
β_{transfer}	-1.374	0.820	-1.677	0.094 *
ASC_{SAVS}	11.089	3.830	2.895	0.004 **
η_m	0.239	0.087	2.922	0.004 **
Initial log-likelihood	-400.144			
Final log-likelihood	-208.343			
$\bar{\rho}^2$	0.467			

Chapter 3

Route choice model for crowd simulation

3.1 Introduction

Crowd movement is an emergent phenomenon that results from the interaction of pedestrians. During disasters such as earthquakes and fires, and large-scale events such as music concerts and fireworks displays, many people gather in the same place and move individually at the same time. If someone collapses during crowd turbulence, stampedes may occur, leading to a serious crowd accident. So far, large-scale crowd movements have sparked crowd accidents [43, 44].

Crowd movement has also been modeled in macroscopic and microscopic approaches. Macroscopic models do not focus on the movements of individual pedestrians, but treats crowd in a unified and continuous manner. Applying the knowledge of fluid dynamics and potential fields, the movement of the crowd is reproduced [45, 46]. On the other hand, Microscopic models focus on the movement of individual pedes-

trians, and represents the interactions between pedestrians and the environment e.g. collision avoidance.

Since 1990s, many researchers have proposed Microscopic models such as the Cellular Automata model (CA) [47, 48], Social Force Model (SFM) [49, 50], and Reciprocal Velocity Obstacle (RVO) [51], but there are still challenges. Existing literature focus on only an *operational level*, in the pedestrian behavior levels defined by Hoogendoorn et al [12]. They define pedestrian behavior at three behavior levels as shown in Table 3.1. Behaviors are decided in order from the top to bottom. Microscopic models such as CA, RVO, SFM are *operational level* models are correspondent to the *operational level* models, and in almost simulation studies, the destination or route are pre-fixed. However, in general, pedestrians change their routes depending on the situation. Therefore, the decision-making of route choice should also be modeled in order to perform a more practical simulation.

Since 2010, modeling and simulation of route choice, which correspond to the *tactical level*, has increased. However, estimation of route choice models and the reproducibility evaluation of the crowd simulation incorporating the route choice model using real data are insufficient. Organizing modeling and simulation methodologies using real data and evaluating the reproducibility of simulations with real data are necessary for further refinement of crowd simulations, and further development can be expected based on these methodologies.

Therefore, the aim of this study is to propose and evaluate a crowd simulation incorporating a route choice model based on real crowd movement data. My contributions are: 1) I generalize and propose a crowd simulation framework that is consistent from actual crowd movement measurements to route choice model estima-

tion and crowd simulator construction, and 2) I measure the crowd movements during an evacuation drill in a theater and a firework event in which tens of thousands of people moved, and verify the reproducibility of the crowd simulation incorporating the route choice model using the measured real large-scale crowd movement data.

This chapter is organized as follows. Section 3.2 reviews studies that incorporate route choice models into crowd simulation. Section 3.3 describes my crowd simulations that incorporate a route choice model. Section 3.4 describes the reproduction of crowd movement during evacuation in a theater, and Section 3.5 describes the reproduction of crowd movement at a large fireworks display event. Finally, Section 3.6 provides a summary and discusses future work.

3.2 Route choice models in crowd simulation

In this section, I refer to several studies on route choice models in crowd simulation. The simplest model is to select the shortest path [52, 53]. However, the shortest path selection model (SP) cannot reproduce the actual movement of a crowd completely. Because pedestrians take into account factors such as route attractiveness, route width, congestion, and habits, in addition to distance [54, 55, 9]. Therefore, utility-based modeling is widely used. This model unifies the combination of factors involved in route choice in the form of utility (or cost), and assumes that the route with the maximum utility is chosen. Several models have been proposed that define their own utility functions and selection methods [56, 57, 58, 59]. In general, utility-based models have been formulated and widely used under the name of discrete choice model (DCM). The simulation of crowd movement, including route choice, is being proposed in combination with DCM as a route choice model and SFM or system

dynamics model as a walking model [60, 9, 61, 62, 63, 64, 65].

First, there are some studies in which the researchers determined the DCM parameters and combined to crowd simulators. For example, Liu et al. model route choice using a DCM with distance to the exit, attractiveness to the store, and movement of other people as factors [60]. SFM and RVO are used as the walking model. Crowd simulations are performed for evacuation, shopping, and movement during a riot. They reported that crowd simulation with DCM represent more complex crowd movement than with SP or random selection. Yang et al. simulate the crowd moving with the guide (navigator) during an evacuation [64]. The walking model is SFM. The destination of SFM is the location of the guide, and the part that selects which guide to follow is represented by DCM. Simulation is performed by changing the initial position of the guide, and the optimal initial position is obtained. Their study suggests the effectiveness of introducing a route choice model and provides examples of advanced simulation applications. However, the parameters of DCM were given by the authors, and the simulation results were not evaluated using real data, so it is unclear whether the model and simulation reproduce realistic crowd movements.

In addition, there are studies that collect route choice behavior through questionnaire surveys and surveys using VR, estimate DCM parameters, and incorporate them into simulations. Lovreglio et al. collect data on exit choice through questionnaires and estimate DCM [9]. The elements of DCM include the distance to the exit, the number of people near the exit, and the number of people in the vicinity of the decision maker. It is reported that the simulation can represent exit choice bias. Lu et al. collected data on route choice behavior in a VR experiment, and estimate DCM [65]. The factors are distance to the exit, density, and route guidance. They report that

using crowd simulation with response to guidance can be used to find more effective guidance methods. Data collection through VR experiments is an effective means, but there are concerns that the data may differ from actual behavior. These studies also did not evaluate simulations.

Other methods have been proposed to estimate the DCM parameters so that the simulated crowd movement matches the actual crowd movement. Gao et al. simulate the selection behavior of ticket gates at train stations and compare it with actual measured data. As in previous studies, the walking model is SFM and the route choice model is DCM. However, the parameters of the DCM are adjusted to match the simulation results to reality and are not estimated using actual route choice behavior data. In this case, it is possible that errors in the simulator are rounded into the parameters of the route choice model, and the model does not represent pure route choice behavior.

The work of Hahani et al. is closest to our goal. They conducted a subject experiment at a sports center, collected data on choice behavior, and used them to estimate the parameters of DCM. The experiments imitated emergency exit route decision-making when escaping from a threat in rooms with multiple exit alternatives [61]. The estimation results of DCM suggest that when the route or environment is partially unknown to the decision-maker, the movements of large numbers of pedestrians to the route increase the choice probability of the route. They also reported that the crowd simulation in which the estimated DCM and SFM combined can represent the crowd movement as in the experiment, from the perspective of the evacuation time [62]. Modeling route (or exit) choice with actual crowd movement data can provide a better understanding of crowd movement. The modeling with data obtained in

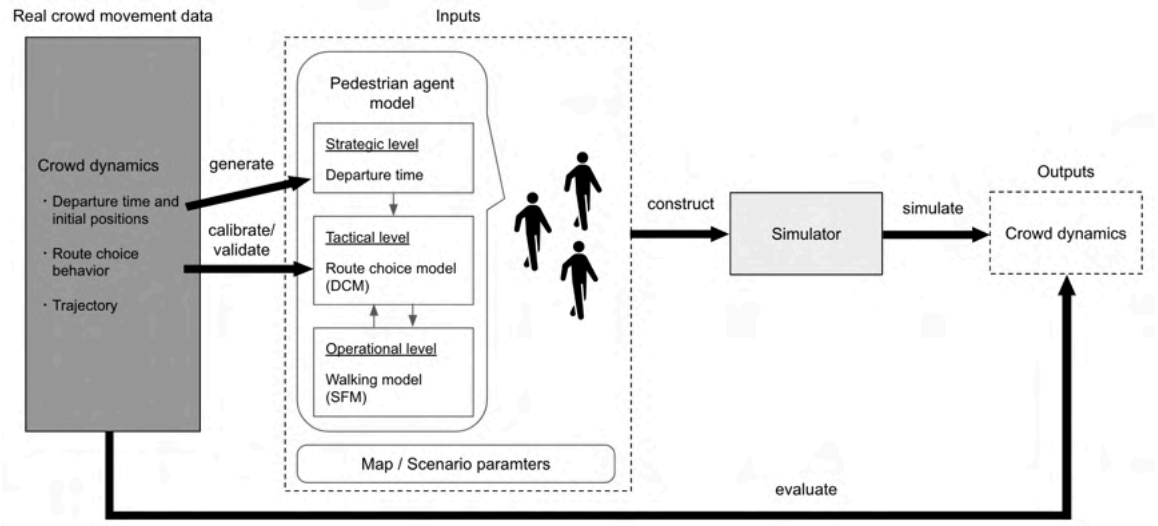

Figure 3.1: Our crowd simulation framework

more realistic situations may solidify the understanding, and the evaluation using real crowd movement data ensures the effectiveness of the crowd simulations.

In this study, therefore, I generalize and propose a crowd simulation framework that is consistent from actual crowd movement measurements to route choice model estimation and crowd simulator construction. In addition, I verify the reproducibility of the crowd simulation incorporating the route choice model using the measured real large-scale crowd movement data.

3.3 Crowd Simulation Framework

My crowd simulation framework is consistent from actual crowd movement measurements to route choice model estimation and crowd simulator construction, and the crowd simulator is agent-based and modeling pedestrian route choice and walking behavior. In this section, we describe the framework overview, the route choice

model, the walking model, measurement methods, and evaluation methods.

3.3.1 Simulation Framework Overview

I define our crowd simulation framework as shown in Figure 8.2. Measure the crowd dynamics such as trajectory and number of pedestrians, and calibrate the model based on measured data of crowd movement. Then, construct a simulator based on the pedestrian agent model, the map and other parameters, and run the simulation to output the crowd dynamics. Finally, the simulation is evaluated by comparing the actual crowd movement with the simulation results.

The pedestrian behavior can be categorized into *Strategic*, *Tactical*, and *Operational levels*. The model of the *Operational level* is mature, and the modeling of the *Tactical* and *Strategic levels* should be promoted. In this study, we focus on the modeling of route choice behavior at the *Tactical level*. Therefore, in our crowd simulation, the model represents the crowd movement after the decision at the *Strategic level* is made. In other words, the departure time of pedestrian movement is already determined, and pedestrian agents are generated accordingly. The agent then moves according to the route choice model and the walking model.

3.3.2 Route Choice Model

I apply DCM as the route choice model and define that DCM means MNL in this section. The definition of MNL is the same as in Chapter 2. The model builder can list the elements $\boldsymbol{x}$ involved in the route choice and define a utility function. Then, by measuring the variable $\boldsymbol{x}$ and the route choice result y, the route choice model, in other words, the parameters $\boldsymbol{\beta}$ of DCM can be calibrated. The variable $\boldsymbol{x}$, which

is involved in route choice, varies from scenario to scenario and is discussed in detail below.

3.3.3 Walking Model

I apply SFM as the walking model. SFM is a physical model that treats pedestrians as a point mass. The forces required to go to a destination and received from other pedestrians and the environment are defined as Social Forces, and the movement of pedestrians is formulated by these forces. In our simulations, we compute the Social Forces using the route direction determined by the route choice model as the destination.

3.3.4 Crowd Movement Measurement Methods

I describe a method for measuring crowd movement. The departure time, initial position, and route choice behavior of each pedestrian in a crowd can be calculated by measuring the trajectory of the pedestrians. Therefore, we describe a method for measuring pedestrians' trajectories.

I introduce the measurement methods using an RGB-depth camera or LiDAR. These sensors can measure point cloud information of three-dimensional objects such as pedestrians. The point clouds are clustered, and clusters with a large number of points are identified as pedestrians. The highest point in the cluster is the pedestrian's head, and the trajectory is extracted by discriminating that point in the time series [66]. The RGB-depth camera is capable of extracting the trajectories with a small error margin in bright indoor environments, but it has the disadvantage that it cannot be used outdoors with the sun since it actively emits infrared rays. On the other

hand, LiDAR can detect pedestrians even in outdoor since it measures the distance to surrounding objects from the time it takes for a laser beam to hit an object and bounce back, and noise related to sunlight can be cut. The disadvantage of LiDAR is that in bad weather conditions such as rain or snow, the laser is blocked, which degrades the performance of the measurement.

3.3.5 Evaluation

This section describes the evaluation of the route choice model and the evaluation of the crowd simulation. For the evaluation of the route choice model itself, we can use the evaluation method for general classification problems such as in machine learning. Separate the choice behavior data for train and test data, and evaluate the prediction accuracy of the test data.

For the evaluation of the crowd simulation, the number of people who choose the route is compared between the actual and the simulation. This is a reasonable evaluation index when focusing only on route choice behavior. In addition, the important indicators in crowd movement are efficiency and safety, and efficiency is often evaluated by travel time, and safety is often evaluated by congestion degree. Therefore, it is also necessary to evaluate the reproducibility of the crowd simulation using indicators related to travel time, such as the number of people completing the trip at each time point.

3.4 Evacuation Drill

To verify the reproducibility of the crowd simulation incorporating the route choice model, we collected crowd route choice behavior at an evacuation drill, which was

conducted at New National Theater in Japan. In the evacuation drill, the opera was actually performed, and during the performance, an evacuation order was issued and the audience evacuated out of the theater. The timing of the evacuation was not known in advance. Therefore, the situation was quite close to reality. Figure 3.2(a) and (b) show the layout of the theater and the evacuation route. The red route leading straight out of the auditorium is the correct evacuation route. It is also possible to choose the blue route and proceed toward the stairs.

3.4.1 Measurement

I measured crowd movement using RGB-Depth cameras at the locations shown in Figure 3.2(b) where pedestrians exit the hallway from the auditorium. 52 people were evacuated through this door. Figure 3.2(c) shows the trajectories extracted from the RGB-Depth camera data using the method described in Section 3.3.4. From these trajectories, we calculated the direction of the body per 0.5 [s]. Then, by defining the route in the direction of the pedestrian's body as the selected route, we obtained the pedestrian's chosen route per 0.5 [s].

At the locations, a phenomenon was measured in which the crowd flow changed depending on the choice of a few evacuees as shown in Figure 3.3. At first, they went straight out the door (a), but when two people chose the stairway (b), the pedestrians in the rear also chose the path to the stairway, following their choice (c). I attempt to model such route choice behavior and simulate crowd movement.

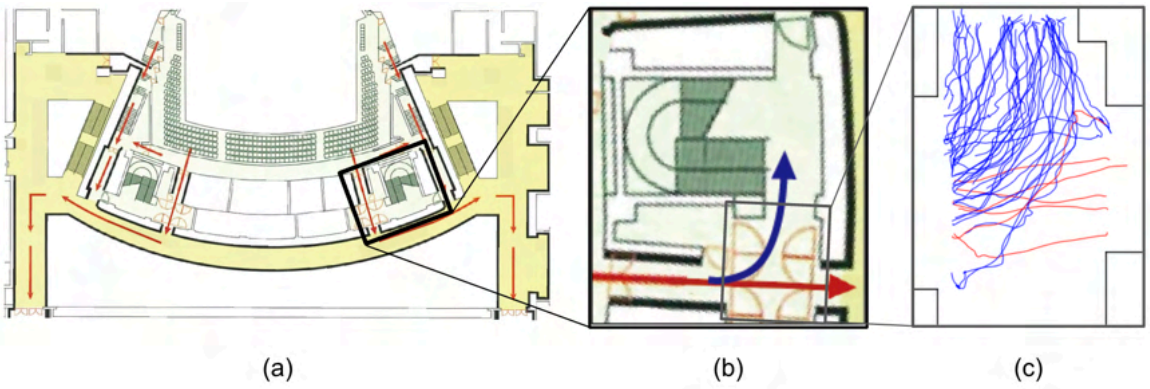

Figure 3.2: Measurement area and data. (a) The layout of the theater (b) details of measurement area (c) The pedestrians' trajectories. They are color coded according to the final route chosen.

(a) (b) (c)

Figure 3.3: The changes in pedestrians' route choice. The flow of pedestrians changes in (a), (b), and (c).

3.4.2 Modeling

I describe a method for modeling route choice behavior using DCM. As explained in Section 3.3.2, it is necessary to define the alternative attributes, i.e., the factors involved in route choice. The factors we considered are:

- **DIST**ance of the decision-maker from the start point of the route (DIST);
- **CH**osen at the previous step (1 second before) or not (CH);
- **N**umber of pedestrians choosing the route who are in **F**ront of the decision maker (NF);

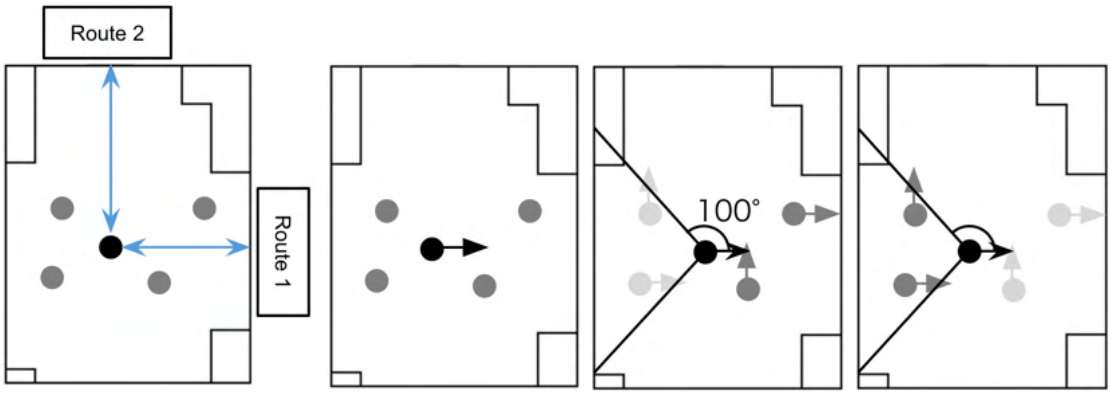

(a) DIST (b) CH (c) NF (d) NB

Figure 3.4: The factors involved in route choice in the evacuation

- **N**umber of pedestrians choosing the route who are **B**ehind of the decision maker (NB);

Figure 3.4 shows the graphical explanation of the factors. At the situation, the value of each factor in Route 1 is as follows. DIST is the distance from the pedestrian's position to the starting point of Route 1, CH is the selection made in the previous step, in this case the value is 1 because Route 1 was selected (otherwise the value is 0). Then NF is 1 and NB is also 1.

The determinant terms of the utility function are defined as follows. First, in this study, we change $\beta_{ij,k}$ in Eq. 2.1 to β_k by assuming that preference β does not vary from individual to individual and from option to option, so the determinant terms of the utility function is below.

$$V_{ij} = ASC_j + \sum_{k=1} \beta_k x_{ij,k} \tag{3.1}$$

Therefore, the determinant terms of the utility function in the case of evacuation drills is as follows.

$$V_{ij} = ASC_j + \beta_{DIST} DIST_{ij} + \beta_{CH} CH_{ij} + \beta_{NF} NF_{ij} + \beta_{NB} NB_{ij} \tag{3.2}$$

where j is Route 1 or Route 2 and $ASC_{Route1} = 0$. Assume that every step (every second), pedestrian i computes the utility of Route 1 and Route 2 and chooses a route.

I divide the measurement data into 5 parts per pedestrian unit, and estimate the route choice model through a 5-fold cross validation. The estimated parameters of the model and the prediction accuracy are shown in Table 3.2. The estimated parameters can be used to understand the route choice behavior of pedestrians. First, the negative value of β_{DIST} indicates that pedestrians are less likely to choose a route with a long distance to the starting point of the route. The positive value of β_{CH} indicates that pedestrians are more likely to make the same choice as the previous step. The fact that β_{NF} is positive indicates that the decision maker tends to choose the route with the greater number of choosers among the number of pedestrians in front of him/her. In other words, it indicates that the decision maker follows other pedestrians and it strengthens the evidence for the existence of herding behavior. Haghani et al. reported the existence of herding behavior in an empirical experiment imitating an evacuation situation [61], and our study supports that claim with data from more realistic evacuation situations. Interestingly, β_{NB} is negative and half the value of β_{NF}. This indicates that the choice of the pedestrian behind the decision maker has less impact on that decision maker than the choice of the pedestrian in front of the decision maker. Rather, it indicates that the decision maker is more likely to choose the opposite direction to the route chosen by most of the pedestrians behind him/her.

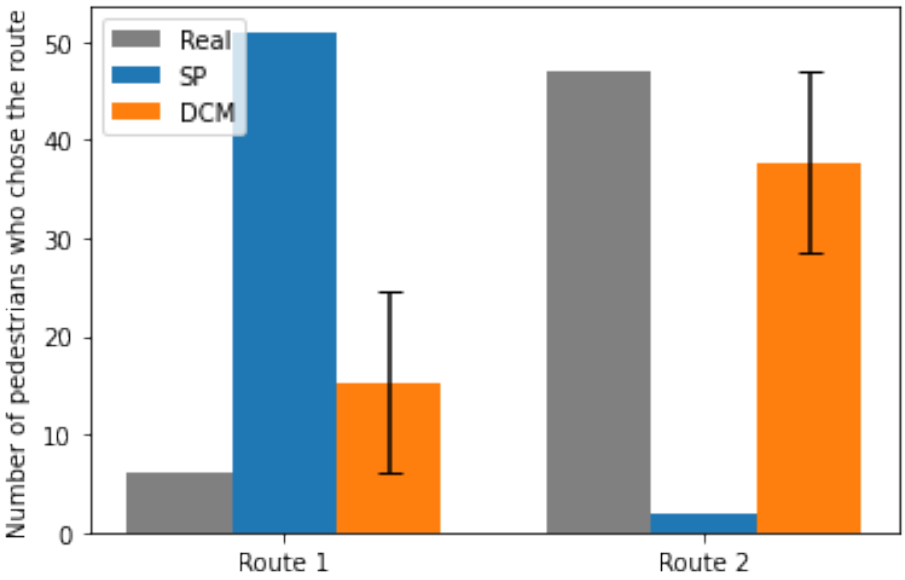

Figure 3.5: Number of pedestrians who chose the route

3.4.3 Simulation

I test whether a crowd simulation consisting of the estimated route choice model (DCM) and the walking model (SFM) can represent crowd movement during an evacuation drill. I use actual data of the pedestrians' initial positions and the time when they exit from the door. The first pedestrian to exit the door and the two pedestrians who chose Route 2 that triggered the change of the crowd flow are assumed to move in the simulation as they did in the actual situation. All other pedestrians move according to DCM and SFM after they are generated according to the actual initial position and timing. The SFM parameters are the same as in [49].

In this experiment, we evaluate the reproducibility of the simulation by the number of people selecting the route. A model that selects the shortest path (SP) at each step is used for comparison. The pedestrian's route choice is stochastic, so the simulation is run 50 times.

Figure 3.5 shows the number of people selected for Route 1 and 2. In case of that the route choice model is SP, most pedestrians choose Route 1. On the other hand, DCM takes into account the choices of other pedestrians choices in addition to distance. Therefore, the influence of the choice of the pedestrian who triggered the change in the flow of the crowd to Route 2 can be considered, and as a result, more pedestrians choose Route 2. Route selection is stochastic, and even if pedestrians start moving under the same conditions, the final route they choose will change. Therefore, the results of the simulation vary, but the actual crowd movement is one of the results of the crowd movement simulated by DCM.

3.5 Firework Event

In this section, we verify the reproducibility of the crowd simulation incorporating the route choice model using more large-scale crowd movement. During mass gathering events such as the haji, football matches, music festivals, firework events, crowd control is necessary [43]. Crowd simulation is a useful tool to test and improve crowd control strategies, and it is required to verify the crowd simulation using the crowd movement in such mass gathering events.

The target of this study is crowd movement at the firework event held at Moji Port in Kitakyushu, Japan. As the end of the fireworks display approaches, tens of thousands of people move from the event site to the nearest station. Security guards are in charge of guiding and controlling crowd at several points to avoid a risk of congestion and accidents which are occured if many people flow into the station simultaneously.

Figure 3.6 shows the route from the event site to the station and the control points.

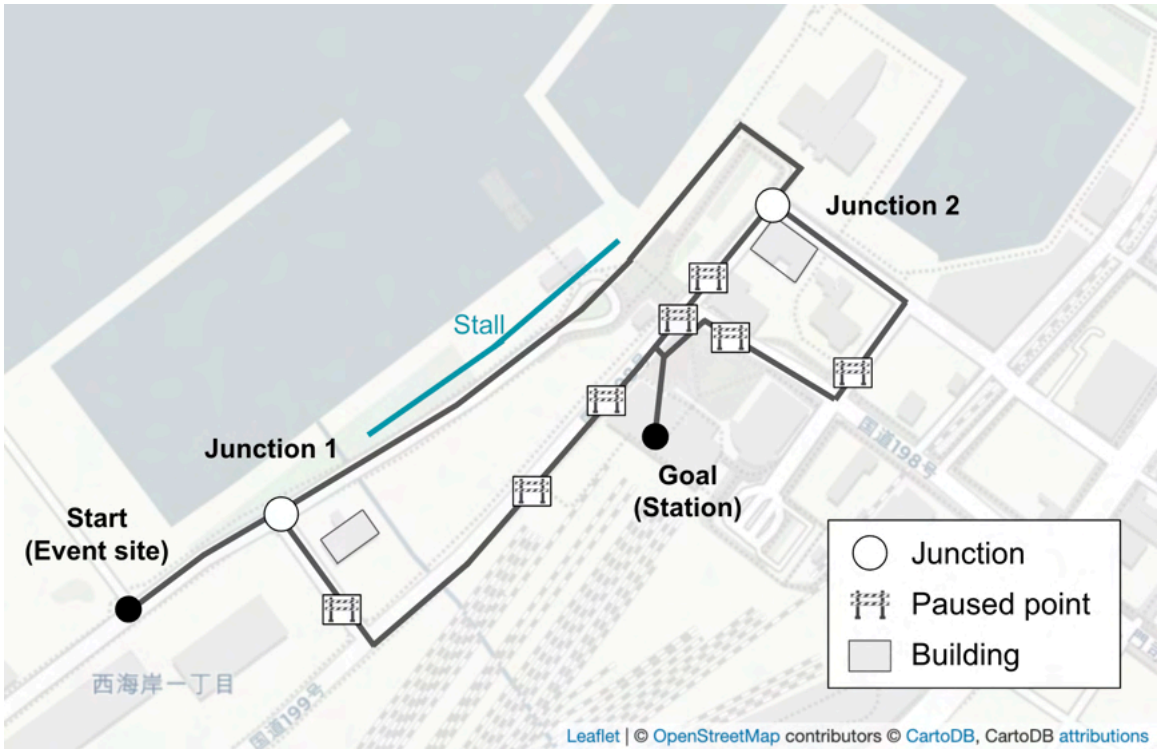

Figure 3.6: Routes and guidance control points in the firework event

There are two junctions and seven paused points. At the junctions, route guidance control is provided for going straight or detouring, and at the paused points, guidance control is provided for proceeding or stopping for a certain period of time. At the junction, in addition to the guidance control by security guards, guidance information is presented by guide projection on the building. In addition, food stalls are open on the route straight ahead from Junction 1.

3.5.1 Measurement

I measured route choice behavior at junctions and the number of pedestrians arriving at the station. In addition, we measured the control at each control point. Here, we describe each of the measured information.

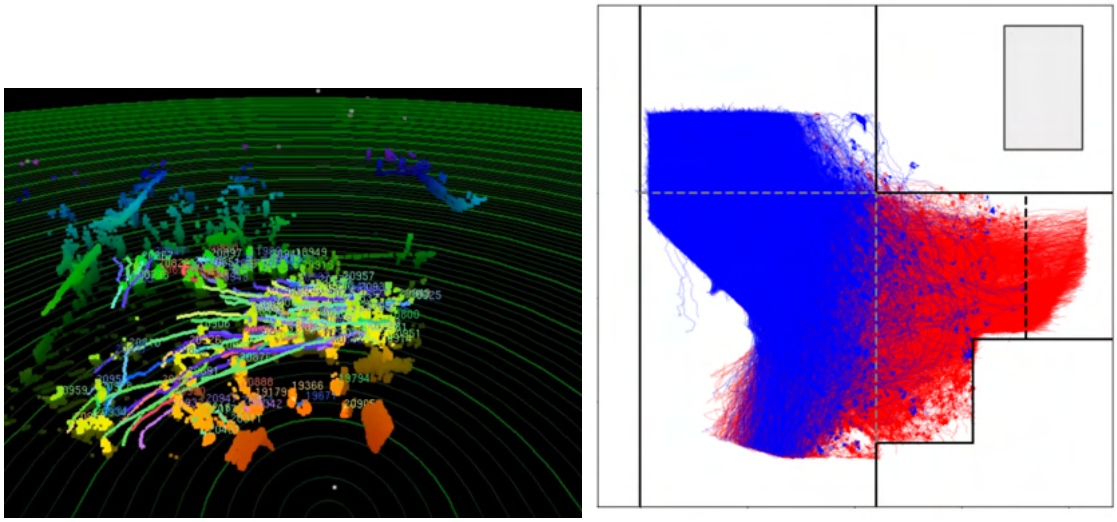

(a) Measurement of the pedestrian movement with LiDAR

(b) Trajectories

Figure 3.7: Measurement at Junction 1

First, we used LiDAR to measure route choice behavior at junctions. Figure 3.7(a) shows the state of measurement with LiDAR at Junction 1. I extracted the trajectories from LiDAR's data which is point cloud information, as shown in Figure 3.7(b). Then, identify the chosen route at the junction from the trajectory data. Here, instead of identifying a chosen route every second as in Section 4, we extracted a one-step route choice at the two junctions. As a result, a total of 34937 route choice behaviors at Junctions 1 and 2 were collected.

Second, the RGB-Depth cameras were also installed at the station to count the number of pedestrians arriving at the station, as shown in Figure 8.8(a) and the result is shown in Figure 8.8(b). The total number of people is 34839. The fireworks show ended at 20:40, but people started returning to the station at 20:00, and all arrived at the station by 23:00.

Finally, we installed cameras at junctions and paused points, and measured the

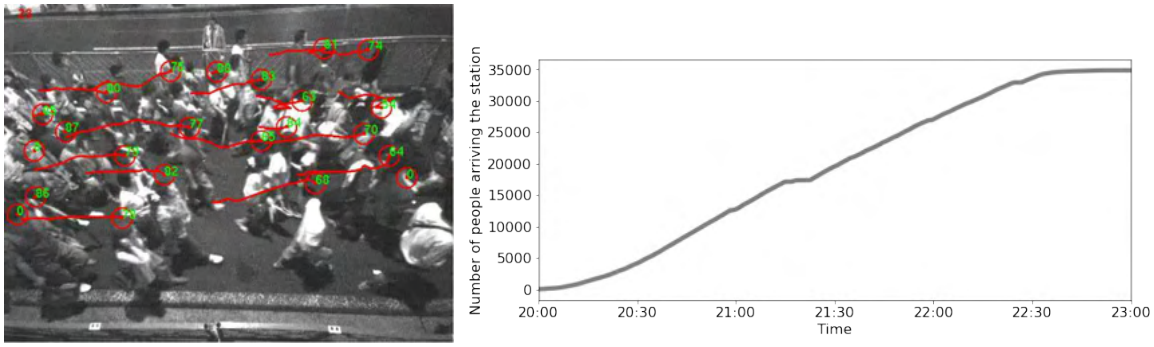

(a) Measurement of the pedestrian movement with RGB-Depth camera

(b) The number of people arriving at the station at each time

Figure 3.8: Measurement at the station

guidance that was actually carried out, as shown in Figure 3.9. The guidance was switched according to the situation by the guards on the point.

3.5.2 Modeling

I describe a method for modeling route choice behavior. Note that we assume that the pedestrian makes a route choice only once at a junction. The factors we considered are:

- **DIST**ance of the decision-maker from the junction to the station (DIST);
- **GUIDE**ance of the route (GUIDE);
- **ATT**raction of the route, such as stall (ATT);

Here, we define that the route closer to the station (red route in Figure 3.10) is Route 1, and the other route (blue route) is Route 2 at each junction. The distance to the station on each route at each junction is one of the factors. In addition, the presence or absence of route guidance is also considered a factor related to route

Figure 3.9: Guidance at each control point

selection. If there is an induction, set it to 1, otherwise 0. And we assume that the attraction of the route is influenced by the presence or absence of food stalls. If there is a stall on the route, it is set to 1, otherwise 0. Note that the stall close after 22:00.

Based on above, the determinant terms of the utility function in the case of the firework event is as follows.

$$V_{ij} = ASC_j + \beta_{DIST} DIST_{ij} + \beta_{GUIDE} GUIDE_{ij} + \beta_{ATT} ATT_{ij} \tag{3.3}$$

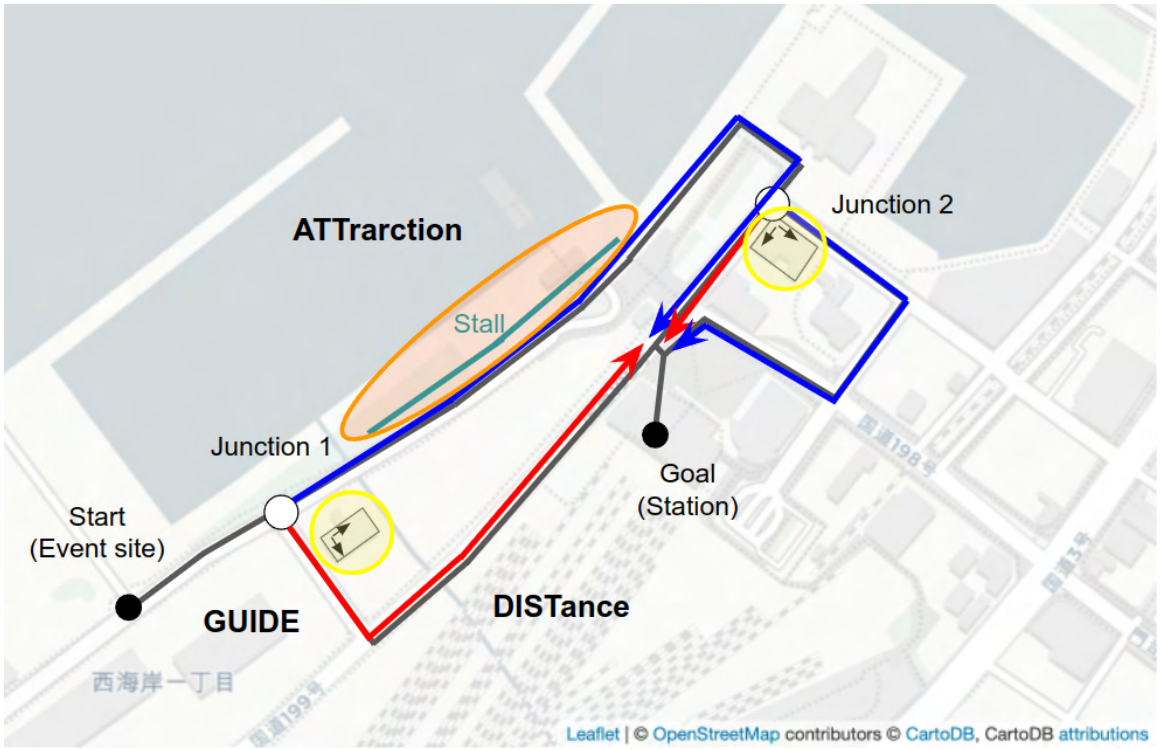

Figure 3.10: The factors involved in route choice in the firework event

where j is Route 1 or Route 2 and $ASC_{Route1} = 0$.

I divide the measurement data into 5 parts, and estimate the route choice model through a 5-fold cross validation as same as Section 4. The estimated parameters of DCM and the prediction accuracy are shown in Table 3.3. The following can be said from the estimated parameters. First, pedestrians are less likely to choose a route with a long distance. Second, pedestrians tend to choose guided routes and routes with stalls.

3.5.3 Simulation

I test whether a large-scale crowd simulation consisting of the estimated DCM and SFM can represent crowd movement during the firework event. I create the

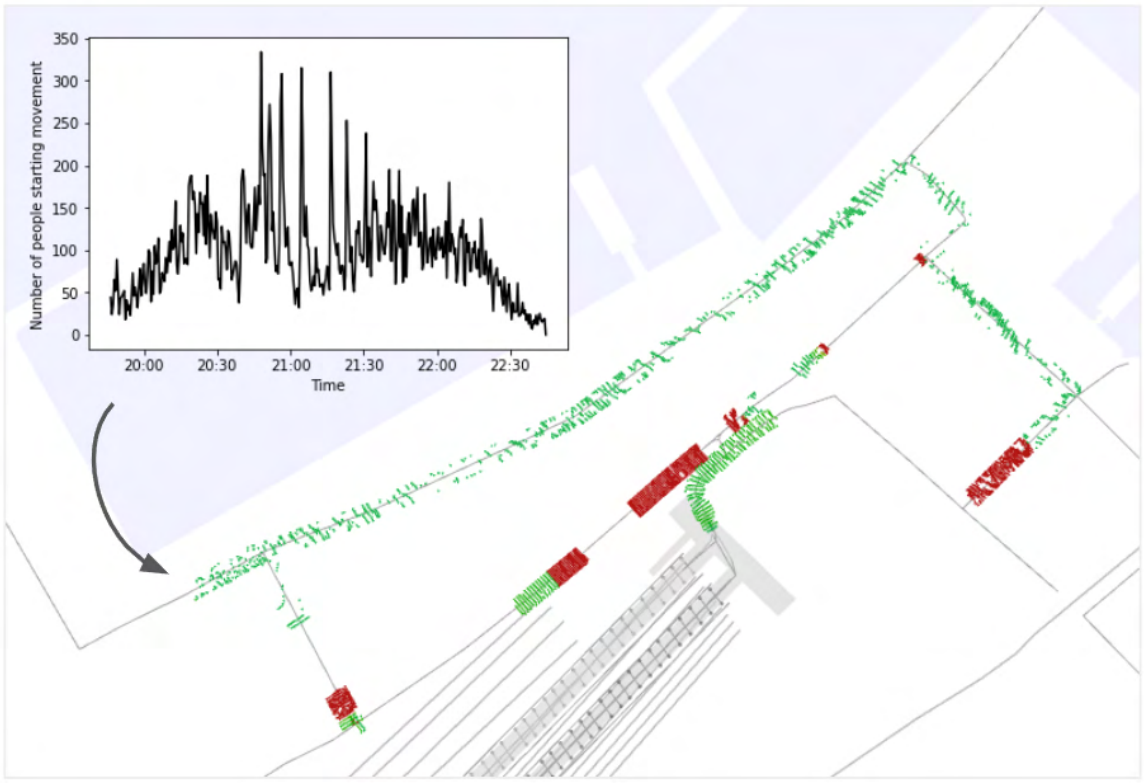

Figure 3.11: Simulation input and visualization. The dots represent pedestrians, and the color of the dots represents the pedestrian's speed. The speed decreases from green to red, and red means that the pedestrian is stationary at zero speed.

pedestrians' departure time from the event site and the number of people as follows. First, the number of pedestrians measured at Junction 1 at each time point measured by LiDAR is base. Then, multiply a constant by it so that the sum of it matches the total number of people measured at this firework event, 34839. The graph in Figure 5.1 shows the number of departure passengers at each time. In the simulation, agents are generated at the starting point according to this distribution. Then, select a route at junctions 1 and 2 according to DCM, and walk on the route according to SFM. In the simulation, guidance at junctions and stops is performed as the actual measured operation.

I use CrowdWalk, a multi-agent pedestrian simulator, as a base simulator [67].

CrowdWalk expresses the movable area using one-dimensional links and nodes, and it is light in memory consumption and calculation time. Therefore, CrowdWalk is suitable for large-scale simulations including tens of thousands of agents. CrowdWalk uses SFM as walking model of pedestrian agents. The default parameters of SFM of CrowdWalk are used in this experiment. The default route choice of agents in CrowdWalk is SP. Therefore, we extend the functionality of CrowdWalk to allow for utility calculation and DCM-based route choice. Figure 5.1 shows the visualization of crwod simulation using CrowdWalk.

In this experiment, we evaluate the reproducibility of the simulation by the number of people arriving the station at each time point. The evaluation index is MAE (Mean Absolute Error) and RMSE (Root Mean Square Error) with real data. RMSE tends to treat outliers (large deviations) as larger errors than MAE. Therefore, we use both as evaluation index. A simulation in which the pedestrian follows the guidance perfectly is used for comparison. This is called Follow. I also compare the effect on computation time of adding route choice to the agent's model in a crowd simulation of tens of thousands of people. I use Intel(R) Core(TM) i9-9900K CPU (3.60GHz) to run the crowd simulation. In the case of using DCM as the route choice model, the pedestrian's route choice is stochastic, so the simulation is run 50 times.

Table 3.4 lists the performance of the crowd simulation. The value for DCM represents the average and the standard deviation of each metric. It can be seen that the use of DCM improves the reproducibility compared to Follow case that did not consider pedestrians' decision-making. Compared to Follow, the use of DCM improved the error by 22.3% for MAE and 15.6% for RMSE. In addition, the computation time of the simulation with DCM is 1.13 times longer than Follow, which does not model

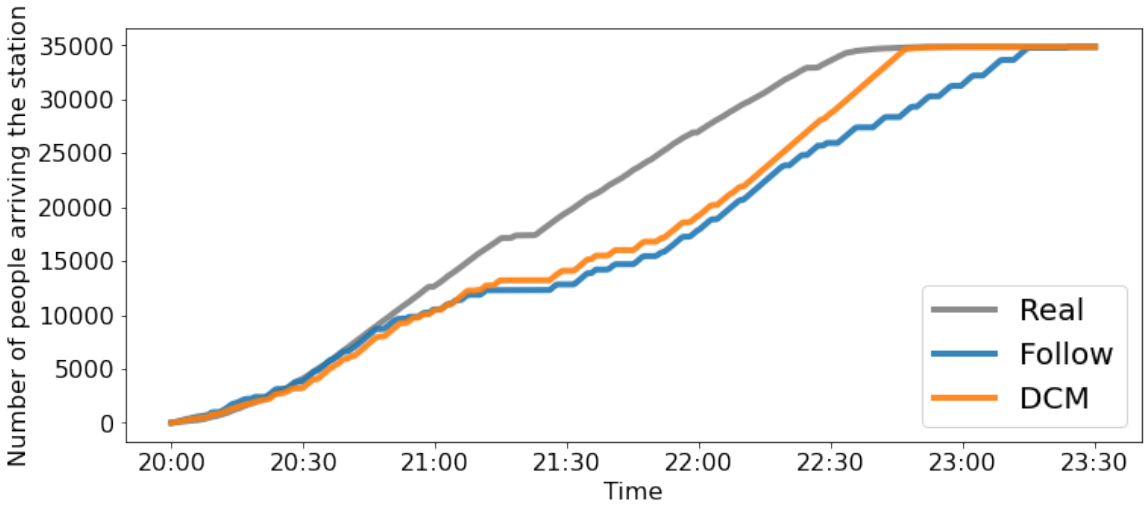

Figure 3.12: The number of people arriving at the station at each time.

route choice, but this is acceptable for improving reproducibility.

Figure 3.12 shows the distribution of the number of people arriving at the station at each time, where DCM is the average of 50 times. In the case of Follow, all pedestrians do not arrive at the station until after 23:00, while in the case of DCM, all pedestrians have completed their movements at 23:00, as in the actual case. In the case of DCM, pedestrians choose their route not only based on guidance, but also on the distance to the station and the attraction such as the food stalls. Therefore, pedestrians sometimes wait until the guidance changes to take the shorter route to the station. As a result, the crowd movement has completed faster than in the Follow case.

3.6 Conclusion

In this chapter, I generalized and proposed a crowd simulation framework that is consistent from actual crowd movement measurements to route choice model esti-

mation and crowd simulator construction. I use DCM as the route choice model and SFM as the walking model. In experiments, I measured the crowd movements during the evacuation drill in the theater and the firework event in which tens of thousands of people moved, and proved that the crowd simulation incorporating the route choice model can reproduce the measured real large-scale crowd movement.

The future work is to generalize and improve the accuracy of the route choice model. The walking models, such as SFM, are versatile for any environment or situation. On the other hand, the current route choice model needs to identify factors related to route choice and define utility functions according to the target situation. In recent years, many studies have been conducted to model choice behavior using neural networks. Such a model could reduce the cost of defining the utility function and improve the accuracy. In addition, it is also important to let the route choice model express the heterogeneity of pedestrians' preferences. Models that express heterogeneity have been well studied, and pedestrians' characteristics are recognized using recent measurement technology such as deep learning. Therefore, it is possible to construct more realistic crowd simulations. I believe that the evaluation using large-scale real data conducted in this study supports the use of realistic crowd simulations incorporating route choice models in building design and crowd control planning.

Table 3.1: Pedestrian behavior level [12]

Level	Behavior	Objective
Strategic level	Departure time choice Activity planning	Decision-making before starting travel, selecting the time to start moving or the activity
Tactical level	Activity scheduling Destination choice Route choice	After the selection at the strategic level, select the route and the exit (door) to go through
Operational level	Obstacle avoidance Interaction with other pedestrians and the environment	Walking while avoiding others and obstacles on the route selected at the Tactical level

Table 3.2: Estimation result of DCM in the evacuation drills

β_{DIST}	β_{CH}	β_{NF}	β_{NB}	ASC_{Route2}	Accuracy
-1.33	1.13	0.202	-0.105	2.33	82.2 [%]

Table 3.3: Estimation result of DCM in the firework event

β_{DIST}	β_{GUIDE}	β_{ATT}	ASC_{Route2}	Accuracy
-9.76	1.26	0.021	2.929	70.7 [%]

Table 3.4: The performance of the crowd simulation

	MAE	RMSE	Computation time
Follow	69.5	91.4	6 min 21 s
DCM	54.0 (0.31)	77.2 (0.33)	7 min 12 s

Chapter 4

Semi-supervised Choice Modeling

4.1 Introduction

In a basic model of DCMs, MNL, the utility function is often represented by the linear sum of $\boldsymbol{x}, \boldsymbol{\beta}$, and $\boldsymbol{z}$. In recent years, some researches have been conducted to improve the prediction accuracy of DCMs by representing the utility using neural networks (NNs).

However, most of the research are focused on improving the prediction accuracy [68, 69, 70, 71, 72]. Because interpretability is secondary, NNs have not been applied straightforwardly in economics and transportation engineering, where the focus is on making interpretable models. For example, in a random utility maximization model, the estimated parameters are considered as marginal utilities. In the field of transportation, the modeling can estimate the value of time (VOT) which is a willingness to pay for a change in time. The VOT is an important indicator used in the cost-benefit analysis of transportation projects, understanding people's transportation behavior, and analyzing and forecasting transportation demand.

Therefore, recent studies have attempted to achieve both predictability and interpretability [39, 13, 71]. The idea of recent studies is to divide the utility function into parts that do not need interpretation and parts that do, and express the former by NN and the latter by a linear function as same as MNL. These models are called neural-embedded choice models. Neural-embedded choice models archived both high prediction performance and interpretability, but learning models require a large number of data.

In choice modeling, a set of choices and selection results are treated as one data. It is possible that we know only the options but not the selected result. For example, to estimate the transportation mode choice model from the usage history data of the route search App, it is necessary to know the route set and the selected route (mode). However, it is unexpectedly difficult to obtain all data. Learning using a small amount of data is one of the problems in machine learning, especially deep learning, and many studies have been conducted as semi-supervised learning.

In this chapter, I consider the problem of learning choice models from a dataset that contains data that the selection result is unknown. I use Positive and unlabeled (PU) learning which is one of the semi-supervised learning methods, and which can be used for datasets containing unlabeled data. Using the transportation mode choice dataset ”swissmetro”, I experimentally show that PU learning is also useful in the field of choice modeling.

The rest of this chapter is organized as follows. In Section 4.2, I review the neural-embedded choice model. In Section 4.3, I introduce PU learning. In Section 4.4, I explain choice modeling using PU learning. In Section 4.5, I report experimental results. Finally, I summarize this study and discuss future work.

4.2 Neural-embedded choice models

With the development of machine learning technology, most researchers use NNs to improve predictability [73]. Although NNs achieve higher predictability than conventional DCMs in most cases [68, 69, 70, 71], the model interpretability has become almost secondary. Only recently, several models using NNs that also take interpretability into account have begun to be proposed [39, 13, 71]. Han et al. named the model that integrates NNs and DCMs to benefit from both: the flexibility of NNs and the interpretability of DCMs, as "neural embedded choice models". Learning-MNL (L-MNL) is the first example of the neural embedded choice model proposed by Sifringer et al., and TasteNet-MNL proposed by Han et al. is the second example. In L-MNL, utility function is divided into two parts: the "interpretable" part, which is specified manually, and the "representational" part, which is a non-linear representation learned by the NNs. However, L-MNL do not model the heterogeneity of preferences (taste) among individuals. In contrast, TasteNet-MNL models heterogeneous taste parameters as flexible functions by means of NNs. L-MNL and TasteNet-MNL alleviated the trade-off problem between predictability and interpretability. However, these neural embedded choice models require more data than traditional DCMs to learn.

TasteNet-MNL models heterogeneous preference (taste) parameters as flexible functions by means of NN.

$$\boldsymbol{\beta} = TasteNet(\boldsymbol{z}, \boldsymbol{\theta}) \tag{4.1}$$

where $\boldsymbol{z}$ describe the individual characteristics and $\boldsymbol{\theta}$ is parameter of NN, TasteNet. $\boldsymbol{\beta}$ is combined with variable $\boldsymbol{x}$ as Eq.(2). The estimation flow is the same

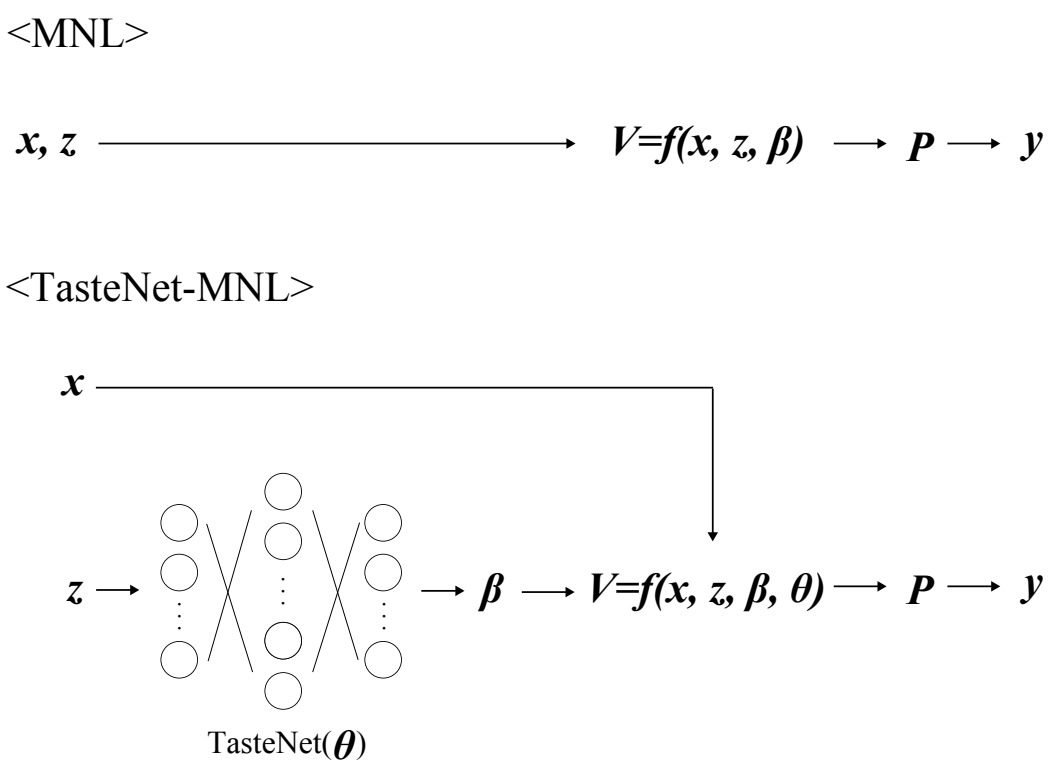

Figure 4.1: Diagram of MNL and TasteNet-MNL

as MNL, but $\boldsymbol{\beta}$ is estimated as the output of TasteNet, so estimate parameter of TasteNet-MNL is $\boldsymbol{\theta}$. figure 2 shows a graphical overview of MNL and TasteNet-MNL.

4.3 PU Learning

To learn some models, we need the input X and the output y of the model. For example, when learning an image recognition model, the image is X and the label representing the content of the image is y. When learning a transportation mode choice model, the service levels of the transportation modes and personal attributes are X, and the selected transportation mode is y. Annotating images is costly and obtaining transportation mode selection results is sometimes difficult, so there is a

lot of data in the world that is only X without y. We call such data as unlabeled data.

Learning models using a small amount of data is one of the problems in machine learning, especially deep learning. Therefore, many studies have been conducted to propose methods that use unlabeled data for learning, which is called semi-supervised learning. In this study, we pay particular attention to the learning of binary classification models, and we focus on PU learning which is one of the semi-supervised learning methods. In a normal binary classification problem, it is usually assumed that a positive or negative label is assigned. However, in PU learning problem, the negative label is not assigned, and only a part of the positive data is labeled. In other words, unlabeled data can be either positive or negative. In PU Learning, the classification problem using the Positive and Unlabeled datasets is reduced to the weighted classification problem [74], and details of this method are described in Section 4.4. In this study, I experiment with learning using PU learning for each of the linear DCMs and Neural-embedded choice model, and try to show the usefulness of PU learning in the field of choice modeling.

4.4 Learning DCM using Positive and Unlabeled data

In this section, we explain the method to learning DCMs such as MNL and TasteNet-MNL from datasets containing unlabeled data using PU learning. From now on, PU learning is simply called PU.

We define $X = (\boldsymbol{x}, \boldsymbol{z})$ as a data, X_1 as a positive data, X_0 as a positive data,

X_u as an unlabeled data. In PU, the classification problem using the positive and unlabeled datasets is reduced to the weighted classification problem. A dummy label is attached to unlabeled data X_u. Moreover, the reliability $w(X)$ of the label is also given. If the label is originally attached, the reliability is high, and if the label is a dummy one, the reliability is low. When training the model, parameter updates are weighted in consideration of reliability.

Using the training data, we first learn a classifier g that predicts whether the data is labeled or unlabeled. Use the classifier g to calculate the probability c that positive data is labeled. Use c to find the probability $w(X)$ that an unlabeled data is positive or negative. This probability is the reliability of the label (or called the weight).

Before defining the loss function to be minimized, change the notation of the log-likelihood of MNL. First, let X be the variables related to the choice of individual i, and $y_{X,1} = 1$ if the selection result of X is Positive, and $y_{X,0} = 1$ if the selection result of X is Negative. Second, let $P_X(1)$ be the probability that the selection result of X is Positive and $P_X(0)$ be the probability that it is Negative. Finally, the log-likelihood of Eq.(4) can be expressed as follows.

$$LL(\boldsymbol{\beta}) = \sum_X y_{X,1} \log P_X(1) + y_{X,0} \log P_X(0) \tag{4.2}$$

The loss function can be transformed as follows by multiplying the log-likelihood by a minus. Since this is a normal positive and negative binary classification, we expressed the loss function as $J_{PN}(\boldsymbol{\beta})$.

$$
\begin{aligned}
J_{PN}(\boldsymbol{\beta}) &= -LL(\boldsymbol{\beta}) \\
&= -\sum_{X} y_{X,1} \log P_X(1) + y_{X,0} \log P_X(0)
\end{aligned} \tag{4.3}
$$

In the case of PU, the value of $y_{X,1}$ and $y_{X,0}$ is unknown because some positive and all negative data are unlabeled. Therefore, the unlabeled data is duplicated and one is labeled as Positive and the other is labeled as Negative, which are $Xu, 1$ and $X_{u,0}$, respectively. And the loss of unlabeled data is weighted. In summary, the loss function of PU is as follows.

$$
\begin{aligned}
J_{PU}(\boldsymbol{\beta}) &= -\sum_{X_1} \log P_X(1) \\
&- \sum_{X_{u,1}} w(X) \log P_X(1) - \sum_{X_{u,0}} (1 - w(X)) \log P_X(0)
\end{aligned} \tag{4.4}
$$

where, the parameter of J is $\boldsymbol{\theta}$ instead of $\boldsymbol{\beta}$ if TasteNet-MNL is used.

4.5 Experiment: Swissmetro

I try to show the usefulness of PU learning in choice modeling. I learn linear DCMs, MNL, and neural-embedded choice model, TasteNet-MNL, using PU.

4.5.1 Setting

I use Swissmetro mode choice data [75]. This dataset consists of survey data collected on the trains between St. Gallen and Geneva, Switzerland, during March 1998. Transportation modes are existing train, new train, Swissmetro, and private carts.

Attributes of alternatives $\boldsymbol{x}$ are travel time, monetary cost, and more. Individual characteristics $\boldsymbol{z}$ are age, gender, and more.

From this original data, we created two types of datasets to be used in the experiment. I treat only two transportation modes, Swissmetro and Car. In this experiment, Swissmetro is positive and Car is negative. The variables are summarized in Table 1. The two types of datasets have different proportions of unlabeled data. The first is that labels of half of the positive data and labels of all negative data are removed. The second is that labels of all negative data are removed. The former is named dataset1, and the latter is named dataset2. The breakdown of training data and test data, labeled data, and unlabeled data are shown in Table 4.2.

The definition of the utility function is as follows. First, the utility of MNL is the linear sum of weights for choice-specific variables and personal attributes. This is the same as the definition in [13].

$$
\begin{aligned}
V_{X,SM} &= ASC_{SM} + \beta_{TT_{SM}} TT_{X,SM} - CO_{X,SM} \\
&+ \beta_{HE} HE_{X,SM} + \beta_{SEATS} SEATS_{X,SM} + \beta_{GA} GA_X \\
V_{X,CAR} &= \beta_{TT_{CAR}} TT_{X,CAR} - CO_{X,CAR} \\
&+ \beta_{LUGGAGE1} LUGGAGE1_X \\
&+ \beta_{LUGGAGE2} LUGGAGE2_X
\end{aligned}
$$

Second, the utility of TasteNet-MNL is the linear sum of variables and weights. The variable of the personal attribute is used as the input of NN and the weight is estimated, $\boldsymbol{\beta} = TasteNet(\boldsymbol{z}, \boldsymbol{\theta})$.

$$
\begin{aligned}
V_{X,SM} &= ASC_{SM} + \beta_{TT_{SM}} TT_{X,SM} - CO_{X,SM} \\
&+ \beta_{HE} HE_{X,SM} + \beta_{SEATS} SEATS_{X,SM} \\
V_{X,CAR} &= \beta_{TT_{CAR}} TT_{X,CAR} - CO_{X,CAR}
\end{aligned}
$$

Note that cost coefficients are fixed to -1.0 for directly reading VOT from time coefficients as same as [13]. TasteNet has hyperparameters such as the number of units and activation function. We use the parameter set with the highest prediction accuracy in the verification data when learning with all labeled data. In the training with all labeled data, the data was divided into train, verification, and test at a ratio of 7:1:2. Finally, the hyperparameters of TasteNet-MNL were as follows. The learning rate is 0.001, the number of middle layers is 1 and the number of units is 60, the activation function is ReLU, and we add the l2 regularization term to loss function and the coefficient is 0.0001. Also, since it is desirable that the preference for the travel time (time) and the time until the next train arrives (headway) is a negative value, a transform function is used in the output of TasteNet to make it a negative value as $-relu(-\beta)$.

I evaluate based on the prediction accuracy. Since the output of the choice model is the choice probability, we define that a transportation mode with a high choice probability is selected. Prediction accuracy is the percentage of accurate predictions of the selected transportation mode in the test data.

4.5.2 Result

Table 4.3 shows the prediction accuracy of the test data predicted by the MNL and TasteNet-MNL models trained using only labeled data, trained using dataset1

and dataset2 with PU, and trained using all labeled data as same as a normal dataset. From this result, it was found that the choice model can be learned from the dataset containing the unlabeled data using PU. The reason why the prediction accuracy of MNL learned using dataset2 with PU exceeds the prediction accuracy learned using full labeled data is due to the way of splitting train and test data. We do cross-validation in future work.

In the field of choice modeling, the estimated parameter values $\boldsymbol{\beta}$ are as important as the prediction accuracy. MNL estimates one preference value for each element such as time and headway. In other words, it is not possible to express the heterogeneity of preferences that changes depending on individual attributes. On the other hand, TasteNet-MNL can express the heterogeneity of an individual, and by inputting the individual attribute variables $\boldsymbol{z}$ in the learned TasteNet, the preference of the individual can be output. Since the preference value for the cost is fixed at -1, the value obtained by multiplying beta by -1 represents the monetary value. For example, the value obtained by multiplying the preference value of TT by -1 represents VOT, which is the value for changing the one-minute travel time.

Figure 4.2 shows histograms of preferences for variables such as travel time and time until the next train arrives. This is the result of learning MNL and TasteNet-MNl with dataset1, dataset2, and full labeled data. PU is used for learning dataset1 and dataset2. When the proportion of unlabeled data contained in the dataset becomes smaller, the preference values estimated by MNL are all the same as those learned with full labeled data. A similar tendency can be seen in TasteNet-MNL. However, the estimated preference value with dataset2 has a greater degree of heterogeneity among individuals than the estimated preference value with full labeled data.

The difference between dataset2 and full labeled datasets is whether the negative data is labeled or not. However, in PU, such that reduce the problem into a weighted classification problem, there is a degree of freedom in the part where attachment of dummy label and estimation based on the reliability of the label. Therefore, further investigation is needed relationship between this freedom of method and the misestimation of the heterogeneity of the preference value.

4.6 Conclusion

In recent years, some DCMs incorporating NNs have been proposed. NNs make it possible to more accurately represent the heterogeneity of preferences in decision making. On the other hand, learning a model using NNs requires a large number of data. In this study, I consider the problem of learning choice models from a dataset that contains data that the selection result is unknown. Using a transportation mode choice dataset "swissmetro", I try to experimentally show that PU learning is also useful in choice modeling.

I learn linear DCMs, MNL, and neural embedded choice model, TasteNet-MNL, using PU. As learning results, it was found that the choice model can be learned from the dataset containing the unlabeled data by using PU. However, there are still gaps in the representation of the heterogeneity of preference values, so further analysis is an issue for future work.

Table 4.1: Description of Variables in the Swissmetro Dataset (almost same as [13])

Alternatives	Alternative attributes
Swissmetro (SM)	time, cost, headway, seats (TT_{SM}, CO_{SM}, HE_{SM}, $SEATS_{SM}$)
private car (CAR)	time, cost (TT_{CAR}, CO_{CAR})
Individuals	**Variable levels**
GA (Swiss annual season ticket)	0: no GA, 1: owns a GA
LUGGAGE	0: none, 1: one piece, 2: several pieces
AGE	0: age 24, 1: 24 30, 2: 39 age 54, 3: 54 age 65, 4: 65 <age
MALE	0: female, 1: male
INCOME (thousand CHF per year)	0: under 50, 1: between 50 and 100, 2: over 100, 3: unknown
FIRST (First class traveler)	0: no, 1: yes
PURPOSE	0: Commuter, 1: Shopping, 2: Business, 3: Leisure
WHO (Who pays)	0: self, 1: employer, 2: half-half

Table 4.2: Breakdown of data (labeled / unlabeled)

		Swissmetro	Car
dataset1	Train	2077/2078	0/2450
	Test	1022/0	630/0
dataset2	Train	4155/0	0/2450
	Test	1022/0	630/0

Table 4.3: Prediction accuracy

Model	only labeled data	dataset1	dataset2	full labeled data
MNL	61.864	65.254	71.186	70.884
TasteNet-MNL	61.864	72.760	76.937	77.179

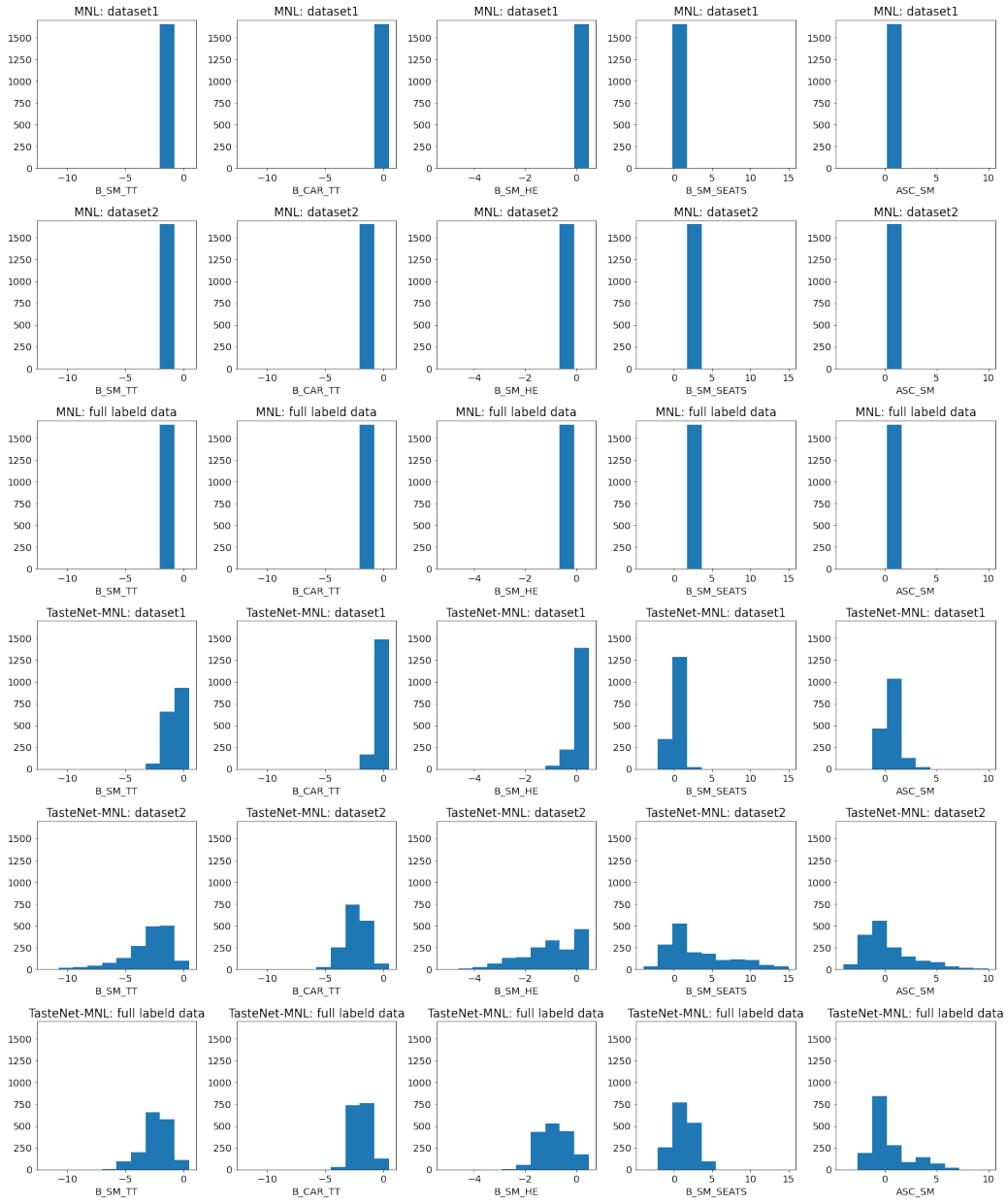

Figure 4.2: Histograms of preferences value $\boldsymbol{\beta}$ for some variables estimated by MNL and TasteNet-MNL using dataset1, dataset2, and full labeled data. The top three are MNL and the bottom three are TasteNet-MNl estimation results

Chapter 5

Simulation Analysis of Mobility as a Service

5.1 Introduction

When introducing new mobility services, service providers or city authorities require a tool that can analyze cost-benefit. Multi-agent simulation makes it possible to verify the effects of introducing new mobility services. For example, an analysis of the effectiveness of autonomous vehicles (AV) using agent-based simulation is conducted. The number of studies is increasing every year. The insight from simulation analysis is that one AV can replace approximately 10 conventional vehicles, although the waiting time is 5 minutes [76]. Simulations have also been conducted on electric vehicles (EV). The number of EV and the number of charging stations have a chicken-and-egg relationship. If the demand for EV is low, there is no incentive to increase the number of charging stations, but if there are few charging stations, EV will not spread. Simulation analysis shows that a sufficient number of charging stations are

necessary to increase the diffusion of EV [77], and that increasing the range of EV has a considerably greater impact on the diffusion of EV than the number of charging stations [78].

When service providers or city authorities plan to deploy MaaS, they want to know answers to questions such as "how many vehicles do we need?," "how much is the appropriate price?," and "will the convenience of users improve?" Multi-agent simulation can answer these questions. Jittrapirom et al. [79] review the modeling approach of demand-side (travelers behavior), supply-side (transport operation), and business model (demand and supply matching)on MaaS. In addition, Kamargianni et al. [80] proposed agent-based modeling and simulation framework including such models considering MaaS concept. However, since most of the MaaS services in each region are in the early stages of introduction and demonstration experiments, few studies model and simulate MaaS system which covers both fixed and flexible transportation, using actual travelers' behavior data and real map scenarios.

In this chapter, therefore, I produce an agent-based simulation framework that can analyze the cost-benefit of introducing MaaS or OSMS. I use the travel mode choice model described in Chapter 2 (demand side) and OSMS operations by an existing vehicle allocation optimization method (supply side), and integrate the demand and supply model with the traffic simulator, SUMO [81] to model demand-supply interaction. The proposed simulation framework can evaluate the impact of introducing new mobility services. In order to quantitatively evaluate the effects of introducing MaaS, I define various indicators from users' and providers' perspectives according to the cost-benefit analysis approach of economics.

This chapter is organized as follows. Section 5.2 explains the simulation analysis

methods. Section 5.3 describes the simulation analysis results based on the MaaS pilot. Section 5.4 provides a summary.

5.2 Simulation Analysis Method

I describe the simulation method and cost-benefit analysis.

5.2.1 Agent-based Simulation Framework

I propose a simulation framework that consists of the travel mode choice model, OSMS vehicle allocation optimization system, and traffic simulator SUMO. Figure 5.1 shows an overview of a simulation. This simulation framework treats users and vehicles as agents. User agents act based on OD data and the travel mode choice model described in Chapter 2. SAVS is provided by Mirai share [82] and is used for the vehicle allocation and route optimization system of OSMS. SUMO is used to simulate the movement status of Smart Access Vehicle (SAV). The "SAVS system" communicates with SUMO at each simulation step and gets the position information of the SAV. When a demand is generated, vehicle allocation optimization is performed and the SAV route and service level (price, travel time) are calculated. Then user calculates the choice probability of each mode with the travel mode choice model based on the calculated service level of SAVS and the service level of the railway/bus at the demand OD and chooses one mode according to the choice probability. If the chosen mode is SAVS, the calculated route information is sent to SUMO, and the vehicle moves according to that route on the SUMO. This is repeated to simulate the traffic of one day.

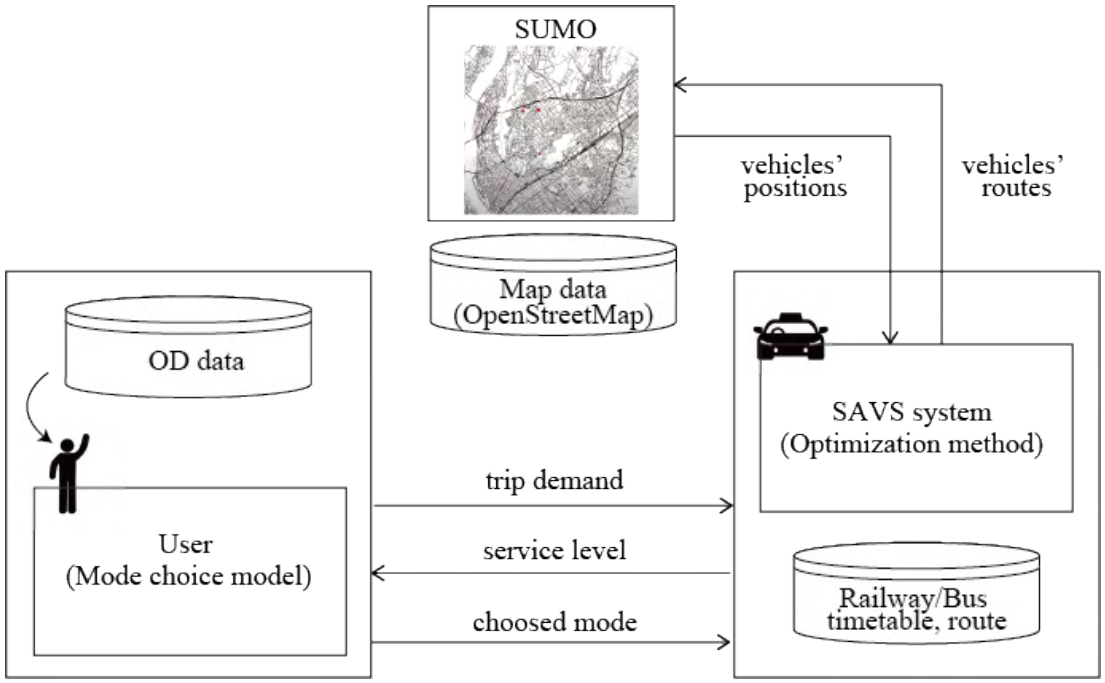

Figure 5.1: Overview of our simulator

5.2.2 Cost-benefit Analysis

Cost-benefit analysis is used to evaluate the effectiveness of MaaS introduction. As the name suggests, the cost-benefit analysis compares the costs and benefits of the introduction of MaaS, and determines the necessity of the introduction of MaaS. If the cost-benefit ratio (benefit/cost) is greater than 1, the policy or project (in this case, the introduction of MaaS) is effective. Costs are monetary, such as construction and operation costs, or social, such as traffic congestion, CO2 emissions, noise, and so on. The benefits may include improved convenience for users and increased fare revenues for suppliers. I define cost and benefit as follows.

Social Cost

The cost of operating MaaS and the cost of CO2 emissions from MaaS are defined as social costs. Since railroads and local buses are scheduled, fixed-route transportation, it is assumed that the introduction of MaaS will not change their operating costs. Therefore, operating costs are defined for each SAVS vehicle. These may include driver labor costs, vehicle management costs, fuel costs, and so on.

$$\text{Operating costs} = \sum_{\text{v}} \text{operating costs of vehicle v} \tag{5.1}$$

I assume that the cost of operating a SAVS is only the driver's labor cost, and that the daily labor cost for one driver is 10,000 yen.

For railroads and buses, no change in CO2 emissions is assumed for the same reason as for operating costs, and only SAVS is considered. The cost of CO2 emitted by SAVS is defined as follows.

$$\begin{aligned} \text{CO2 emission costs} &= \frac{\text{Total vehicle kilometers traveled of SAVS}}{\text{Fuel consumption}/1000} \\ &\times \text{ Unit heating value} \times \text{Emmsion coefficient} \\ &\times \text{ Monetary valuation unit} \end{aligned} \tag{5.2}$$

Assuming that the vehicle is a taxi and the fuel used is LP gas, the fuel consumption is 5.23[km/L], the unit heating value is 50.8[GJ/kL], the emission coefficient is 0.0161[t-C/GJ], and the monetary valuation unit is 2300[yen/t-C].

Social Benefit

I define the user benefits and supplier benefits from the introduction of MaaS as social benefits. The user benefit is defined as the reduction in the generalized cost of the user's travel. The generalized cost is defined by the following equation based on the determinant term of utility V_{mr} and the parameters β_{price} and η, which are described in Chapter 2.

$$GC = -\frac{1}{\beta_{\text{price}}}\frac{1}{\eta}\ln\left(\sum_{m}\exp\left(\eta V'_m\right)\right), \tag{5.3}$$

where V'_m is expressed by the following equation and is called the log-sum variable. This is the expected value of the maximum utility of transportation mode m.

$$V'_m = \ln\sum_{r\in R_m}\exp\left(V_{mr}\right) \tag{5.4}$$

In other words, in this study, the generalized cost is defined as the expected value of the maximum utility obtained by the user divided by the preference of the fare, β_{price}, in monetary units, with a minus sign.

The supplier benefit is defined as the amount of increase in the profit of the supplier of the mobility services (railroads, local buses, SAVS). Here, the supplier benefit is simply the amount of increase in revenue.

5.3 Simulation analysis of MaaS pilot

In this study, a cost-benefit analysis of the introduction of MaaS is conducted for one day of traffic in two settings. The first is a posterior evaluation of the MaaS pilot conducted in 2019, in which simulations and cost-benefit analyses are conducted

using the same number of vehicles and fares as in the pilot. The second is to conduct exhaustive simulations and cost-benefit analyses under various scenarios with different numbers of SAVS vehicles and fares, to investigate the conditions that maximize the benefit to the cost. Twenty simulations are performed for each scenario, and the average value is used in the analysis.

5.3.1 Posterior Evaluation of the MaaS Pilot

In the demonstration experiment, railroads and local buses operated on the same timetable and routes as usual, and in addition, MaaS was introduced, including SAVS as an option. 21 SAVS vehicles were used. OD data for the day with the highest demand (70 demand) was used. For comparison, a simulation was also conducted in which all data (824 demands) during the demonstration experiment were used as the daily demand.

The costs and benefits calculated from the simulations and the cost-benefit ratios are shown in Table 5.1. The cost-benefit ratio for the most demanding day (70 demand) was 0.066, a very low value. On the other hand, the cost-benefit ratio for the hypothetical high-demand scenario (824 demand) was 0.789, which is higher than the 70-demand scenario, but the cost-benefit ratio is less than 1. Based on this result, it can be said that the benefits of this experiment were not commensurate with the costs, i.e., the introduction costs cannot be recovered only from the fare revenue. However, since the cost-benefit ratio improves as the demand increases, it can be considered that the introduction of the MaaS can be expected to be effective by raising awareness of the MaaS and increasing the demand.

Note that the benefits do not necessarily increase in proportion to the demand.

Table 5.1: Cost-benefit evaluation

		70 demand	824 demand
Social cost	Operating cost	210000	210000
	CO2 emission cost	12.206	145.175
Social benefit	User benefit	6555.791	79092.289
	Provider benefit	7272.056	86656.399
Cost-benefit ratio		0.066	0.789

For reference, Figure 5.2 shows the changes in the share rates of railway, buses, and SAVS. The ratio of shifting from railway and local buses to SAVS is almost the same even if the demand increases. This is considered to be because the number of vehicles is sufficient for the number of demands, and the service level of SAVS did not change even if the number of demands increased. If the demand is further increased, the supply will not be able to catch up with the demand, waiting time will increase, and the benefit to the users will not increase.

5.3.2 Exhaustive Simulation

Simulations are performed for 70 demand scenarios, with the number of vehicles changed from 1 to 21 by 1 and the initial fare of SAVS changed from 0 yen to 1,400 yen by 100 yen. The cost-benefit ratios for each scenario, the cost-benefit ratio from the provider's perspective are shown in Figure 5.3. The cost-benefit ratio from the

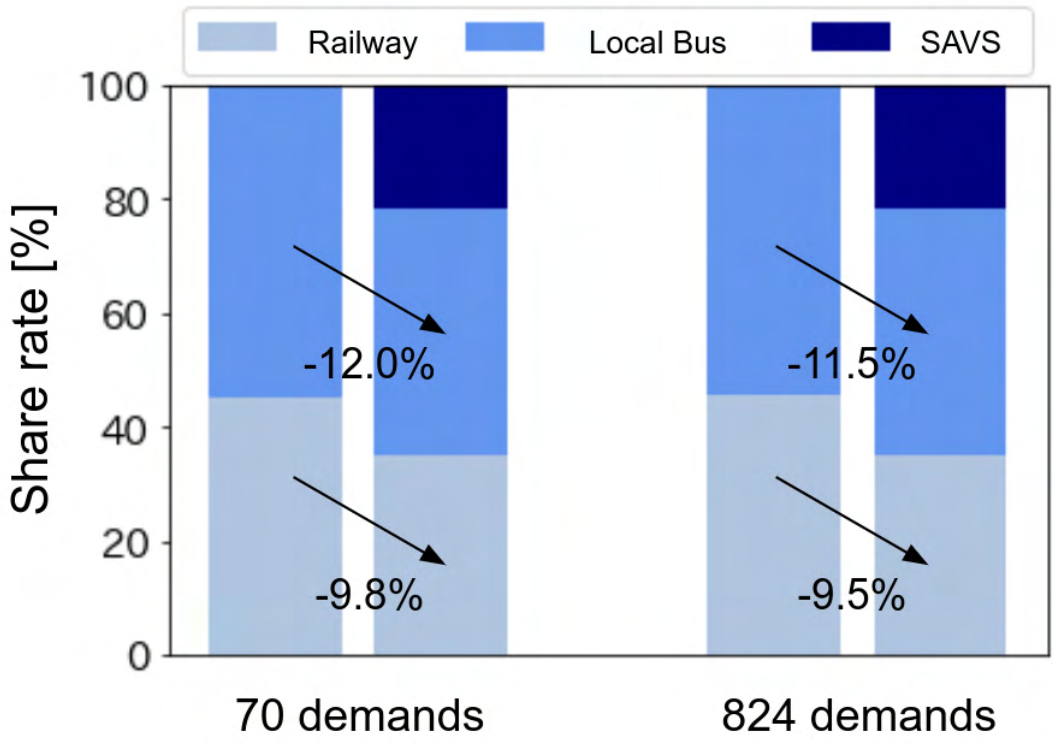

Figure 5.2: Mode share rate

provider's perspective is the value obtained by dividing the supplier benefit by the operation cost, and is referred to as the supplier cost-benefit ratio. This figure shows that the scenario in which the cost-benefit ratio exceeds 1 is the scenario in which the number of vehicles is 1 and the starting fare is between 0 yen and 700 yen. The cost-benefit ratio reached its maximum value of 1.583 when the number of vehicles was 1 and the starting fare was 200 yen. The supplier cost-benefit ratio never exceeded 1 in any scenario, and reached a maximum value of 0.743 when the number of vehicles was 1 and the starting fare was 800 yen.

A similar exhaustive simulation is performed for the 824-demand setting. The results are shown in Figure 5.4 The figure shows that if the demand increases and the number of vehicles and fares are adjusted, a profitable situation for the supplier

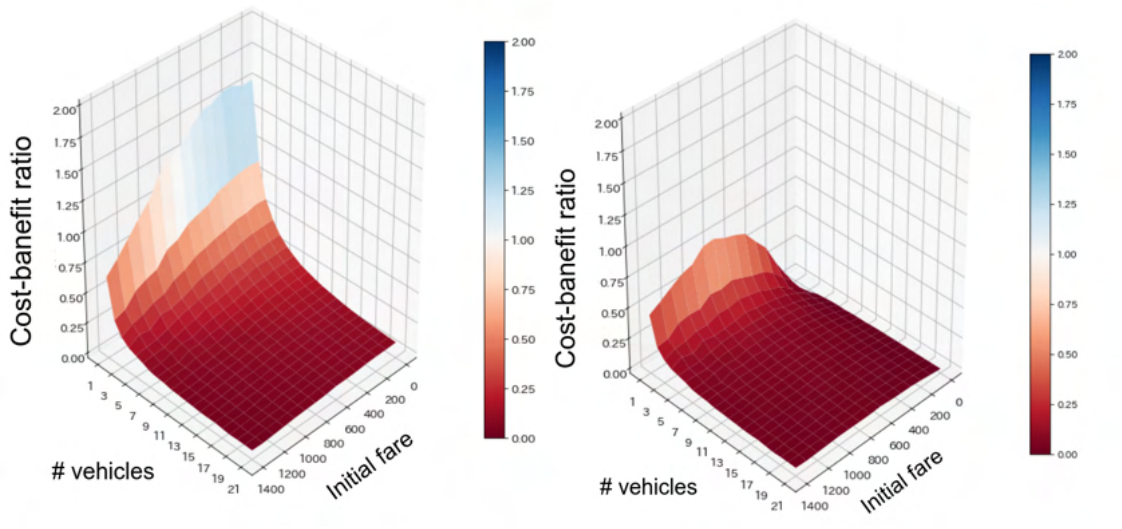

(a) Social cost-benefit

(b) Provider cost-benefit

Figure 5.3: The cost-benefit ratio (70 demand).

can be created. However, since the share of railways and buses is reduced by the introduction of SAVS (OSMS), coordination between the different operators of each mobility service is necessary.

5.4 Conclusion

This chapter presents a simulation analysis of the benefits that MaaS brings to users. The benefits to users of introducing OSMS in addition to trains and buses and increasing their transportation options were investigated in accordance with the setting of the MaaS demonstration experiment in Shizuoka. The results show that the introduction of MaaS, or in other words OSMS, increases the benefits to users, but the provider loses profit when the number of users is small. If the number of users increases and the number of OSMS vehicles and fares are adjusted, the provider also archives benefits. However, since the share of railways and buses is reduced by the

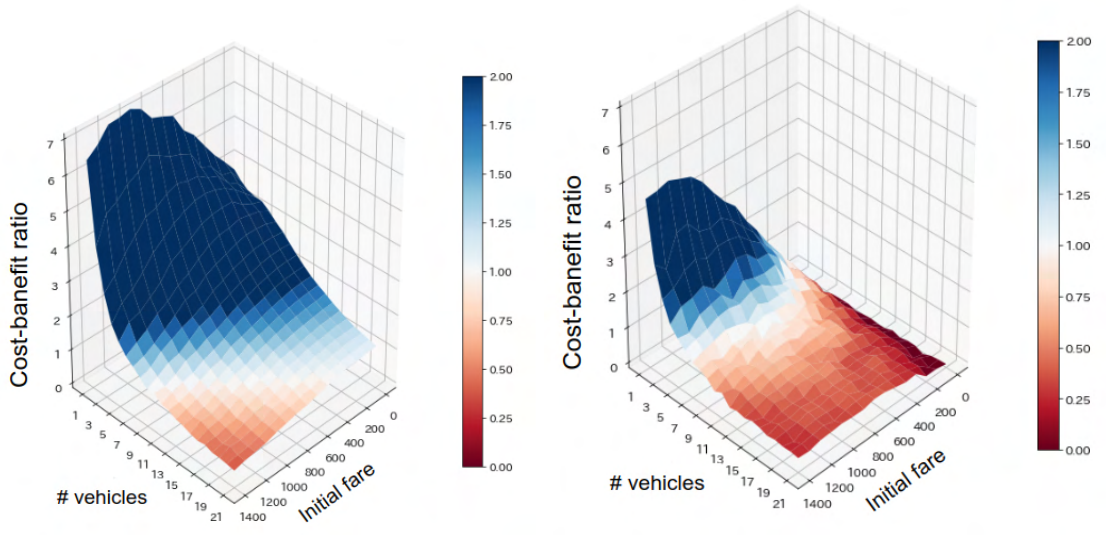

(a) Social cost-benefit

(b) Provider cost-benefit

Figure 5.4: The cost-benefit ratio (824 demand).

introduction of OSMS, coordination between the different operators of each mobility service is necessary.

Chapter 6

Simulation Analysis of On-demand Shared Mobility Services

6.1 Introduction

As smartphones are becoming prevalent and the accuracy of location-information data improves, on-demand mobility services, such as Uber, Lyft, and DiDi, are becoming more common. On-demand mobility services allow passengers to move from their current locations to their destinations. They make trips of passengers more convenient than conventional public transportation such as railways and buses. Furthermore, the population of early people is increasing in some countries, and the elderly are required to return their driver's licenses. Therefore, the number of people who are unable to travel conveniently is likely to increase in the near future, and on-demand mobility services are expected to provide for their mobility. However, the shift to on-demand mobility services by former public transit users and private vehicle users has increased the number of service vehicles and caused congestion. [83, 84].

On-demand shared mobility services (OSMS), such as UberPOOL (recently, called UberX Share), Lyft Shared, and Via, are viewed as more appropriate than others. OSMS can be operated with a small number of vehicles, thereby mitigating congestion caused by on-demand mobility services. In 2017, UberPOOL operated in 36 cities, and Lyft Shared was used in 16 cities in the United States [85]. OSMS can transport multiple passengers who move to similar destinations and routes at a time. OSMS serve as both a "bus" that can carry many passengers and a "taxi" that can move flexibly. It may take a longer travel time than for a regular taxi due to the detours of shared passengers. On the other hand, the fare is cheaper than a regular taxi. One vehicle can carry multiple passengers, so operating costs can be reduced as well as congestion.

Researchers have analyzed the effects of OSMS, that is, the effectiveness of sharing, but only few studies have used actual usage data. Generally, a small amount of OSMS data is available, and the specific impact of OSMS cannot be quantified [86, 85]. The only research in which actual data were used was that of Li et al. who analyzed DiDi's operation data [87]. From their findings, OSMS saved an average of 22% on vehicle hours traveled compared with regular taxis. However, passengers' average travel time and travel distance increased by 30% (10 [min]) and 15% (1.5 [km]), respectively. They stated that the usage rate of OSMS was as low as 6%-7% due to reduced passenger convenience. Other studies based on simulations suggested that OSMS improve operational efficiency. For example, Sun et al. used taxi-usage data in Washington, D.C. to compare taxi trips with simulated OSMS trips [88]. From their findings, total vehicle hours traveled decreased by 18% if passengers were willing to increase their travel time by an average of 25% and four passengers share a vehicle.

OSMS improve operational efficiency but increase the travel time of passengers. Because OSMS are generally door-to-door (D2D) services that transports passengers from their current locations to their destinations. It causes detours, one-way streets, traffic jams, and so on, extending the travel time of passengers [89, 90]. This is undesirable for both the operator and passengers.

Recently, meeting points (MPs)-based OSMS have been developed. MPs-based OSMS allow passengers to walk near specific pick-up/drop-off points (MPs), as shown in Figure 8.2. The benefits of introducing MPs are as follows [89].

- *Operational efficiency*: Services can be established with fewer vehicles and shorter VKT by reducing the number of extra detours. More passengers' requests (hereafter, passengers' requests are termed as demands) can be handled under the same setting.
- *Passengers convenience*: When multiple passengers are riding simultaneously, the total travel time may be reduced because fewer stops are required.
- *Safety*: Pick-up and drop-off on residential roads can cause accidents. Placing MPs on arterial roads and parking lots makes pick-up and drop-off safe.
- *Health*: Incorporating walking into a trip can be seen as a healthier and more sustainable mobility service.
- *Privacy*: Because passengers are not picked up and dropped off at their actual origin and destination, their home or workplace addresses are not revealed.
- *Easier rendezvous*: In D2D, the driver and passengers cannot identify each other's location easily. By clearly defining the meeting place, drivers can easily recognize passengers' boarding and destination and passengers can easily recognize the location of the vehicle.

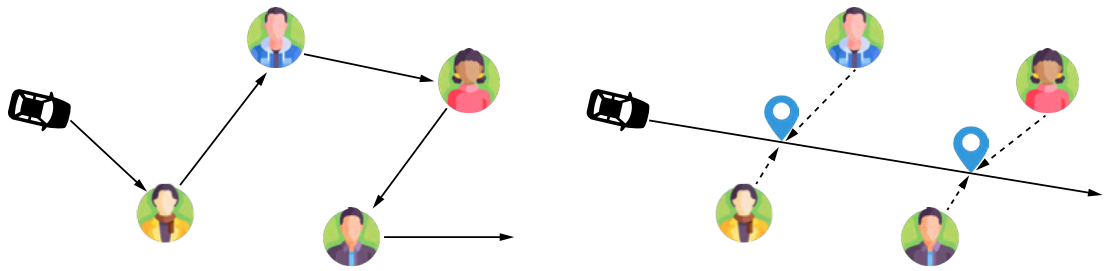

(a) D2D-based (b) MPs-based

Figure 6.1: Illustration of the differences between D2D-based and MPs-based OSMS.

Previous studies have demonstrated that the introduction of MPs into OSMS can improve operational efficiency from the perspectives of the number of vehicles, VKT, and the rejection rate of demands [89, 91]. However, the benefits in terms of passenger convenience have not been thoroughly investigated. OSMS increase the travel time of passengers more than non-shared services, and the introduction of MPs mandates passengers to walk. Therefore, some companies have attempted to address these issues by discounting the fare. For example, Uber offers MPs-based OSMS, called Uber ExpressPOOL, which is 25% lower than UberPOOL [92].

In this chapter, I examine the impact of the introducing MPs into OSMS on the travel time of passengers by asking the question: "Is there any possibility that the introduction of MPs will shorten the travel time of passengers?" Intuitively, as the number of passengers increases, the average travel time of passengers will be shorter if passengers are picked up and dropped off at MPs rather than using D2D-based services. It is crucial to determine whether there is an advantage in terms of the travel time of passengers, and if so, under what conditions can it be achieved.

I evaluate the introduction of MPs in terms of operational efficiency and passenger convenience through agent-based simulations. First, I compare D2D-based OSMS with MPs-based one, which mandates passengers to walk to MPs. Moreover, I analyze

the benefits of introducing MPs and the conditions under which those benefits occur in synthetic and static situations. This is called static analysis because all requests are generated at the same time and no sequential route optimization. Then, I conduct a simulation analysis on the basis of the hypotheses obtained from the static analysis. This is an agent-based simulation, where requests are generated each time, and vehicle allocation route optimization is performed dynamically. In the simulation analysis, I use actual road network and demand data to verify the benefits of introducing MPs. Simulations were performed by varying parameter combinations such as MP locations, the number of demands, the number of vehicles, and vehicle capacity.

The remainder of this chapter is organized as follows. Section 6.2 reviews the literature related to MPs; Section 6.3 describes the static analysis; Section 6.4 explains the configuration of the simulator used in our simulation analysis and a vehicle assignment algorithms; Section 6.5 describes the setup and results of the simulation analysis; finally, Section 6.6 summarizes the study, along with future works.

6.2 Meeting Points-based On-demand Shared Mobility Services

In this section, I review the literature related to MPs-based OSMS (on-demand shared mobility services).

According to Czioska et al. [89], most studies on MPs assumed a ride-sharing case. Each driver has their origin and destination and does not act as a service provider. The popular study by Stiglic et al. have reported that introducing MPs in a setting with one driver and multiple passengers improves the number of matches and reduces

the total VKT [93]. Subsequently, many variations have been studied, such as the recommendation of MP locations in long-distance ride-sharing [94], allocation-route optimization when MPs are included in ride-sharing [95], and optimization of MP locations in ride-sharing situations when passengers do not reveal their origin and destination for privacy reasons [96].

Zheng et al. analyzed the effect of introducing MPs on Flex-route buses [97], where routes between bus stops are not fixed and can be changed flexibly within the constraints of the timetable at bus stops. Timetable constraints of bus stops sometimes reject some demands. Zheng et al. attempted to solve this problem by introducing MPs into Flex-route buses. MPs are installed in the area between bus stops. Passengers are picked up and dropped off at either bus stops or MPs. They formulated this problem as a two-stage optimization problem. First, demand rejection is determined, and then, the route is optimized. An experiment using an artificial map shows that the demand rejection rate decreases with the introduction of MPs. In other words, the number of detours and stops can be reduced by introducing MPs, and more demand can be handled within the time schedule constraints. However, the travel time of passengers is increased. It is noted that the total travel time of rejected passengers was excluded, so there was no direct comparison with D2D-based services.

Few studies have investigated the effects of introducing MPs on OSMS. Czioska et al. proposed bi-level optimization for MP-based OSMS in a setting in which all demands are known in advance [89]. First, demands are clustered on the basis of the origin, destination, and departure time. Then, the demands in each cluster are further divided into subgroups on the basis of the walking distance to MPs and assigned to MPs. Candidate MPs are located at parking lots, train stations, and

other locations for easy pick-up and drop-off. In an experiment using a map of the city of Braunschweig, Germany, MPs-based OSMS improved operational efficiency in terms of the number of vehicles, vehicle hours traveled and VKT; however, the travel time of passengers was increased. This is consistent with the results of Stiglic et al. for simple ride-sharing. The reason for the increase in passenger travel time is that passengers have to walk to an MP and wait for other passengers to arrive at the MP.

Czioska et al. assumed a static situation in which the demand is known in advance, but Fielbaum et al. investigated the optimization of routes for MP-based OSMS in dynamic situations [91]. Passengers can move to their desired pick-up and drop-off locations or MPs. The waiting time, walking time, on-boarding time, and additional waiting and on-boarding time due to the acceptance of new demands are defined as passenger travel costs. Moreover, the cost of demand rejection is also considered a cost that should minimize. Demand acceptance and routing are optimized to minimize these costs. Experiments using actual maps and demands in Manhattan have shown that introducing MPs improves VKT and demand rejection rates. The experiment results also show that the passenger cost (including demand rejection) is less in MPs-based OSMS than in D2D-based OSMS. However, since these results depend on the cost definition of demand rejection, it is necessary to compare the travel time of passengers in D2D-based OSMS with that in MPs-based OSMS in a setting where all demands are accepted. In addition to reducing VKT, it has also been reported that the introduction of MPs can reduce congestion at curbsides [98] and noise [99].

In summary, studies on introducing MPs into OSMS and similar studies have confirmed operational efficiency improvement in terms of the number of vehicles, VKT, and demand rejection rate. However, the benefits to passengers are unclear.

Therefore, the purpose of this study is to investigate the benefits of introducing MPs from the perspective of not only operational efficiency but also passenger convenience, especially travel time.

6.3 Static Analysis

This section analyzes the effect of introducing MPs in a static situation.

6.3.1 Setting

As shown in Figure 6.2, I consider a trip between two areas. There is only one vehicle and no capacity constraint. All passengers request a trip simultaneously, and they go in the same direction (from left to right). In D2D-based OSMS, a vehicle moves through the origin and destination of each passenger. In MPs-based OSMS, passengers walk to an MP, board and alight a vehicle at an MP, and then walk to their respective destinations. The passengers' travel time is equal to the time it takes to arrive at their respective destinations because they call a vehicle simultaneously. In this analysis, I compare the average travel time of passengers in D2D-based OSMS with that in MPs-based OSMS and examine the effect of introducing MPs. In the case of a three-area trip, passengers board a vehicle at the first MP and alight at the second or third one.

D2D-based OSMS route is calculated by solving an optimization problem formulated as a 0-1 integer programming problem similar to the traveling salesman problem. Let $G = (V, E)$ be a graph consisting of a node set V and an edge set E connecting each node. Let the number of passengers be n. Let V be a node set of node 0 representing the initial position of the vehicle and nodes $\{1, 2, ..., 2n\}$ representing the

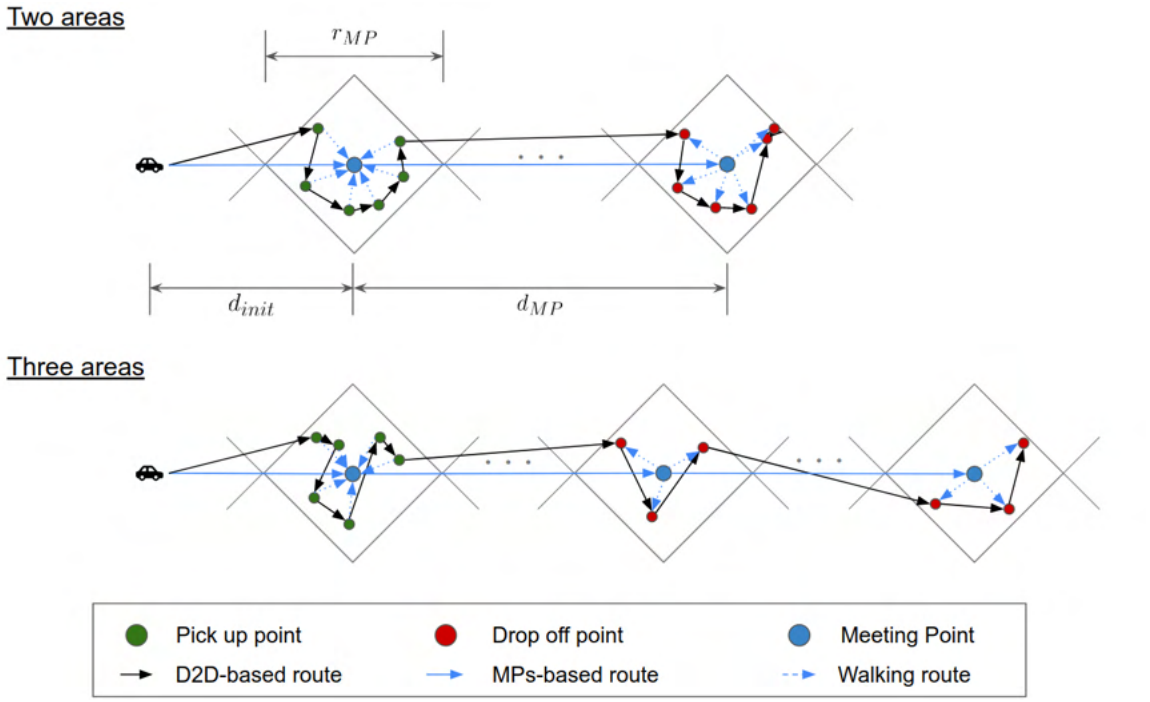

Figure 6.2: Static analysis situations.

pick-up and drop-off locations of each passenger. The edge-connecting nodes i and j are denoted as $e_{ij} \in E$. The travel cost between nodes i and j is c_{ij}, where the Manhattan distance is used to account for the structure of the road. Let x_{ij} be the decision variable to be optimized. It is set to 1 if the vehicle passes through the edge e_{ij}; otherwise, it is set to 0. From the above explanation, the optimization problem formulation to search for D2D-based OSMS route is as follows.

$$\min \sum_{(i,j)\in E} c_{ij}x_{ij} \tag{6.1}$$

subject to

$$\sum_{i \in V, i \neq j} x_{ij} = 1 \qquad \forall j \in V \setminus \{0\} \tag{6.2}$$

$$\sum_{j \in V \setminus \{0\}} x_{0j} = 1 \tag{6.3}$$

$$\sum_{i \in V, i \neq j} x_{ij} - \sum_{i \in V} x_{ji} = 0 \qquad \forall j \in V \tag{6.4}$$

$$\sum_{(i,j) \in E, i \neq j} x_{ij} \leq |S| - 1 \qquad S \subseteq V \setminus \{0\} \tag{6.5}$$

$$x_{ij} \in \{0, 1\} \qquad \forall (i,j) \in E \tag{6.6}$$

where Eq. 6.1 represents the objective function to minimize the travel cost of a vehicle. Eq. 6.2 is the constraint that the vehicle visits each passenger location only once. Eq. 6.3 is the constraint that the vehicle starts from an initial location. Eq. 6.4 is the constraint that the number of vehicle coming to a passenger location is the same as that leaving that location. Eq. 6.5 is a sub-tour elimination constraint. The sub-tour S is a round tour that returns to where the vehicle starts without visiting all the points, and is a set consisting of combinations of nodes that do not contain a depot. Eq. 6.6 is a constraint on the decision variables. Note that a constraint to remove routes such that the vehicle goes to drop-off locations before the passenger's pick-up locations is excluded in the formulation. Such routes are removed from the candidate solutions automatically during the optimization process because they do not minimize the cost.

Furthermore, I describe the specific setup. The number of passengers is $n = \{1, 2, ..., 15\}$. In the three-area trip, $n = 1$ is the same as in the two-area case, so $n = \{2, ..., 15\}$. I define a walking speed of 3 [km/h] as assumed for elderly users because OSMS is assumed to replace private cars as transportation for the elderly. Additionally, let the vehicle speed be 30 [km/h]. The size of the rhombus determines

how far passengers should walk to/from an MP and is $r_{MP} = \{200, 400\}$ [m]. The r_{MP} is also the interval between MPs. I chose this setting because bus stops are generally 300-500 [m] apart. In other words, if $r_{MP} = 200$ [m], passengers will walk up to 100 [m] to the MP. The distance d_{init} from the initial position of the vehicle to the first MP is set to $\{1, 2\}$ [km], depending on r_{MP}. This is the same distance that a vehicle can travel in the time it takes a passenger to walk $\{100, 200\}$ [m], and it is set to prevent the vehicle from departing before the passengers at the farthest MP in the rhombus arrive. In the two-area trip, the distance d_{MP} between the first and second MPs is set to 2 [km], and in the three-area trip, it is set to 1.5 [km].

The vehicle stop time includes the acceleration/deceleration time and passenger pick-up/drop-off time. Since the acceleration/deceleration time is 11 [s] in a previous study [100], I assume that it takes an additional 5.5 [s] each to stop and start the vehicle at the pick-up/drop-off point. In addition, according to the same study [100], the passenger pick-up and drop-off times are proportional to the number of passengers, n_{ba}, and each is assumed to be $5 + 2.75n_{ba}$ [s].

From the above information, I compare the average travel time of passengers in D2D-based and MPs-based OSMS using varying n and r_{MP}. Passengers' origin and destination locations are generated randomly within the rhombus, and an average of 200 calculations are performed for the comparison. D2D-based OSMS route optimization is modeled using PuLP, a Python optimization library, and the CBC solver is used for optimization.

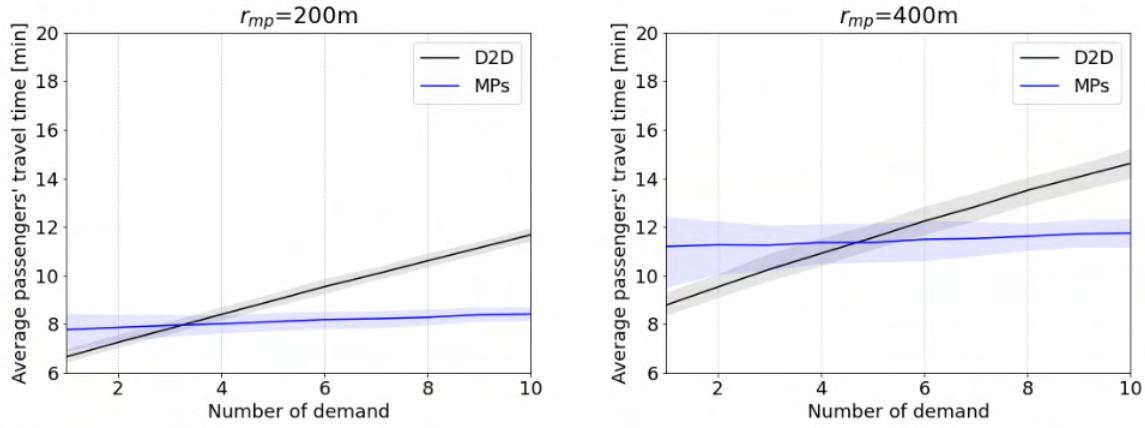

(a) Two areas

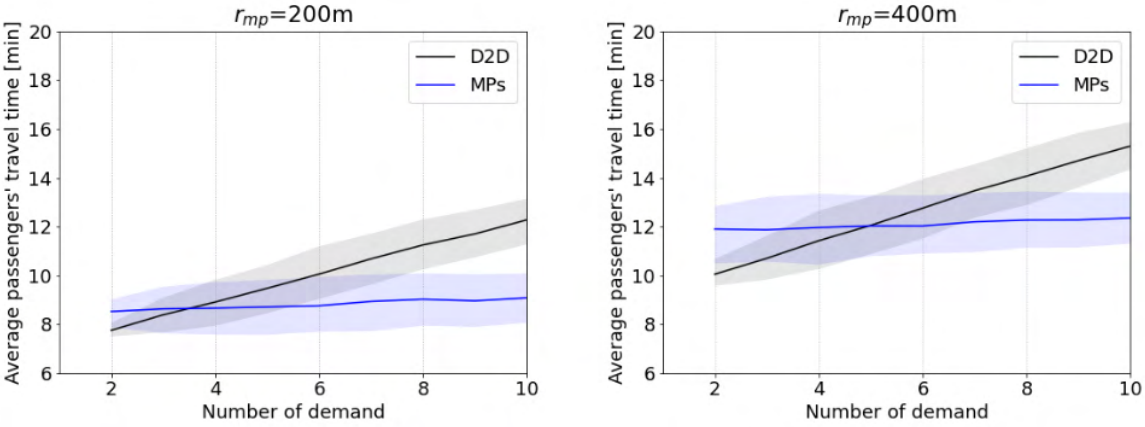

(b) Three areas

Figure 6.3: Average travel time of passengers in D2D-based and MPs-based OSMS.

6.3.2 Results

The results for the two-area trip are displayed in Figure 6.3(a). Each graph corresponds to $r_{MP} = \{200, 400\}$ [m], respectively. The solid line represents the average value, and the widths represent the maximum and minimum values in 200 trials. Specifically, when $r_{MP} = 200\,[\mathrm{m}]$, four or more passengers are picked up and dropped off at the MP; when $r_{MP} = 400\,[\mathrm{m}]$, five or more passengers are picked up and dropped off at the MP, the average travel time of passengers becomes shorter

in MPs-based OSMS than inD2D-based one. The same results are obtained for the three-area trip (Figure 6.3(b)). The VKT is reduced when the pick-up and drop-off locations are aggregated at one MP.

I found that the introduction of MPs reduces the VKT and, if the number of demands n exceeds a certain number, the average travel time of passengers in MPs-based OSMS is shorter than that in D2D-based OSMS. Since, in this static analysis, there is one vehicle and all passengers ride together, n represents the number of shared passengers. Therefore, in other words, the introduction of MPs reduces the average travel time of passengers if the number of shared passengers is greater than a certain number.

However, there are limitations to this static analysis.

- Demands are generated in the same one direction simultaneously. However, in the real world, trips are requested from various directions at various times, so it is difficult to share rides.
- Passengers wait for other to arrive. In this static analysis, passengers are assumed to wait until other passengers arrive at the aggregation MP. However, waiting for other passengers is not typically considered in a case without a timetable because it would negatively affect convenience.
- The capacity of a vehicle. Although more passengers boarding/alighting a vehicle at an MP simultaneously reduces their average travel time, depending on the vehicle capacity, the effect may not be seen.

In the real world, MPs-based OSMS charge a smaller fare than D2D-based OSMS because of reduced passenger convenience caused by the condition requiring passengers to walk to MPs. For example, Uber charges 25% less for UberExpressPOOL (i.e.

MPs-based OSMS) than for UberPOOL (i.e. a regular D2D-based OSMS). Therefore, when evaluating the effect of MPs introduction on passenger convenience, it is better to include the fare in the analysis.

6.4 Simulation Analysis Method

The static analysis shows that the introduction of MPs shortens the VKT and, reduces the average travel time of passengers more in MPs-based OSMS than in D2D-based OSMS if the number of shared passengers exceeds a certain number. However, the static analysis has the above-mentioned limitations, thus further analysis in a more realistic setting is needed. In addition, several configurations such as the locations of MPs, the number of vehicles, and vehicle capacity, should be adjusted to create conditions under which the average travel time of passengers can be reduced. Among the combinations of these configurations, I want to determine conditions that improve operational efficiency and passenger convenience. Therefore, I perform agent-based simulation analysis.

6.4.1 Simulator Configuration

The configuration of the simulator is shown in Figure 6.4. Passengers and vehicles are treated as agents, and the simulator represents the traffic conditions of the day. It consists of network data, passenger models, and vehicle models. The network data consist of nodes and links. Nodes are intersections and links are roads connecting nodes. The passenger model is used to calculate the utility (convenience) of trips [1].

[1] In the future, I plan to incorporate the choice model of transportation modes or D2D- and MPs-based OSMS

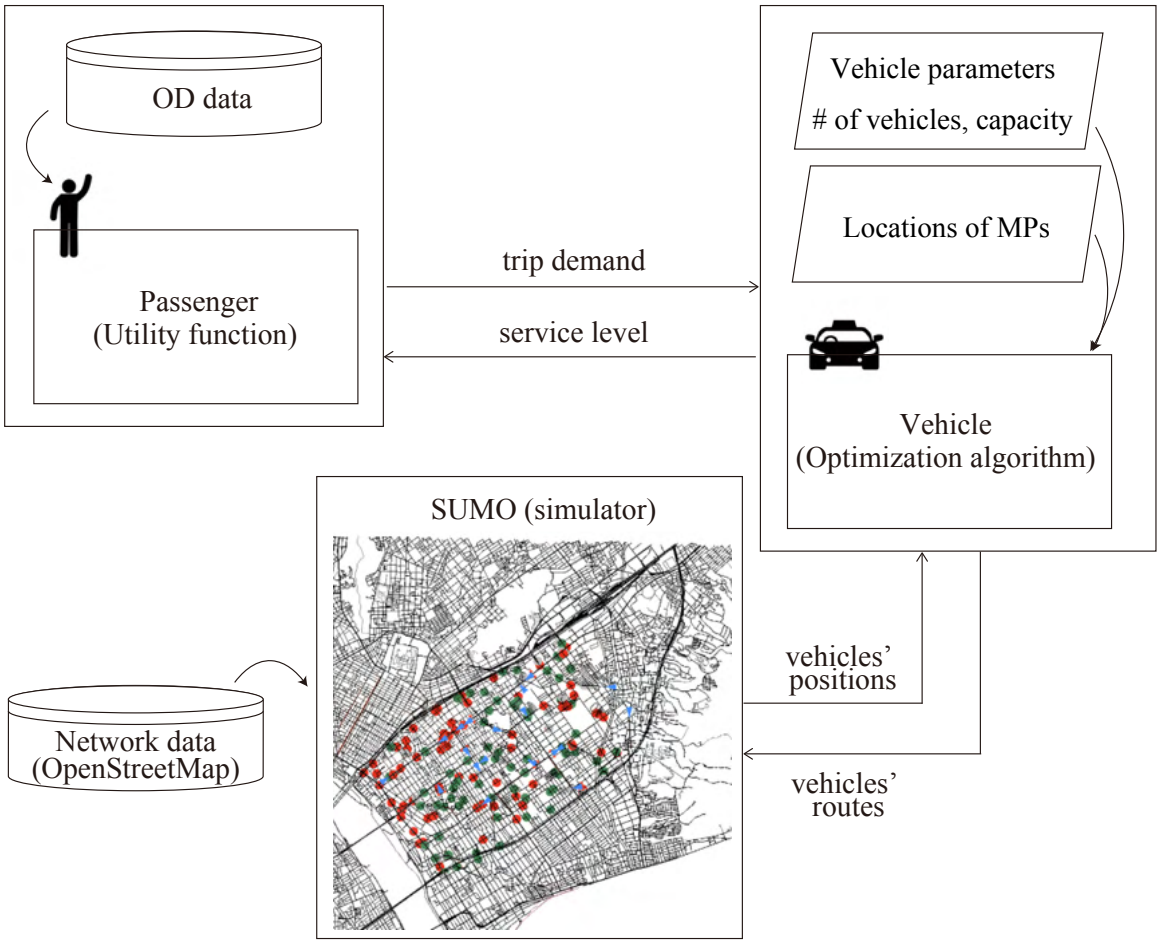

Figure 6.4: Configuration of our simulator.

The utility calculation method is described in Section 6.5. The vehicle movement is simulated using the traffic simulator Simulation of Urban Mobility (SUMO) [81].

6.4.2 Allocation Method

The vehicle agent moves in accordance with the optimized route by using the successive best insertion method proposed by Noda et al. [101]. This algorithm is adopted in SAVS (Smart Access Vehicle Service) [102], which is one of the OSMS provided in Japanese cities. Although many optimization algorithms have been pro-

posed, such as [103], the object of this study is not to validate optimization algorithms. Moreover, this algorithm leads to a quasi-optimum, and I believe that the tendency of the simulation is not different from that of using an algorithm that leads to a fully optimal solution.

The centralized system has information on the current demand and the location of vehicles and performs vehicle allocation and route optimization each time a demand generates, based on the following constraints. An illustration of the successive best insertion method is shown in Figure 6.5.

- The vehicle v that accepts the new demand d does not change the order of pick-up and drop-off of the already accepted demand $d' \in D_v$ but inserts the pick-up and drop-off of the new demand.
- Each demand has a time constraint for pick-up and drop-off, and vehicles are allocated to satisfy the time constraint. When a new demand is received, the vehicle shall be allocated so that the time constraints of the existing demand are not exceeded.
- The allocation of vehicles v is determined in such a way that for each new demand d accepted, the travel time of the new demand $t_{travel}^{d,v}$ and the total delay time for the existing demand $t_{delay}^{d',v}$ are minimized (Eq. 6.7).

$$\arg\min_{v} \quad t_{travel}^{d,v} + \sum_{d' \in D_v} t_{delay}^{d',v} \tag{6.7}$$

Note that for t_{travel} and t_{delay}, the travel time is obtained by dividing the Manhattan distance between two points in the pick-up and drop-off sequence by the vehicle speed.

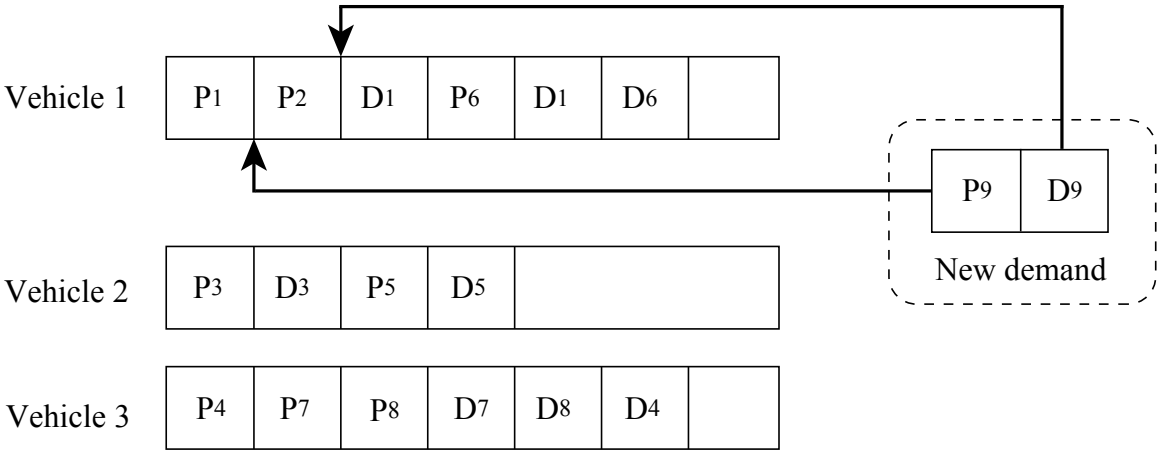

Figure 6.5: Illustration of the successive best insertion method for real-time OSMS.

Each demand has a time constraint for pick-up and drop-off, and the time constraint is calculated at the time the demand is generated. In D2D-based OSMS, a time constraint is set for drop-off so that it is not faster to travel on foot. In MPs-based OSMS, it is assumed that passengers are picked up and dropped off at MPs. Moreover, as a pick-up time constraint, the vehicle does not arrive at an MP before passengers arrive at that MP. The constraint on the drop-off time is the same as in D2D-based OSMS.

In addition, the selection of MPs also affects operational efficiency and passenger convenience. For example, in the case shown in Figure 6.6, if the nearest MP is used, the passenger would take route (a) every time. However, depending on the location of the vehicle, it may be better to use route (b) even though it may require a longer walk. Therefore, in MPs-based OSMS, when a demand is generated, four MPs around the origin or destination are searched, and the successive best insertion method is used to optimize the allocation for each of the 16 route patterns (4×4). The pattern with the lowest cost among the 16 patterns is selected. This MP selection is expected to improve vehicle operating efficiency and passenger convenience. A comparison of the

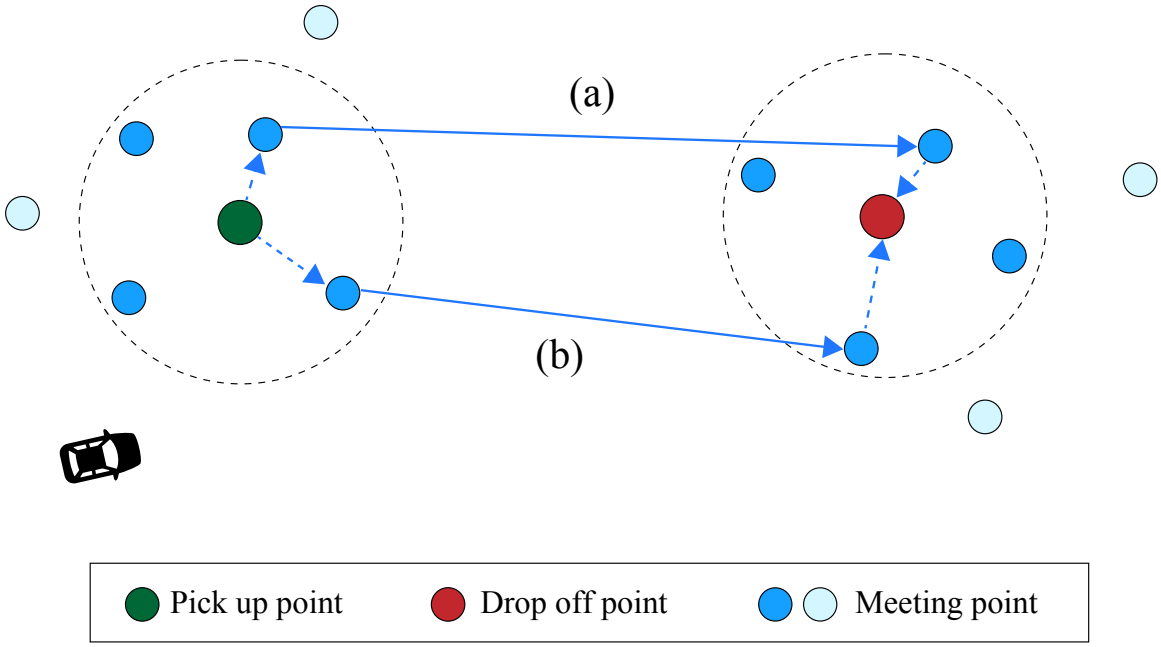

Figure 6.6: Illustration of MP selection.

case with the closest MP and the case with MP selection is mentioned in Section 6.5.

6.4.3 Simulation Flow

The simulation flow is as follows.

1. Input service configurations such as the locations of MPs, the number of vehicles, and vehicle capacity.
2. A passenger requests a trip (a demand) following the OD data representing the passenger's origin, destination, and departure time.
3. The current vehicle location is obtained from SUMO, and the vehicle allocation is optimized.
4. The vehicle agent moves on SUMO following the optimized route.
5. Steps 2 to 4 are repeated until all passenger demands have been attended to.

6. Return various indices related to operational efficiency and passenger convenience.

6.5 Simulation Analysis Settings and Results

I examine the effects of MPs introduction on operational efficiency and passenger convenience using real maps and demand data. I explain the actual data, service configurations, and the results.

6.5.1 Data

I focus on the area south of central station (Shizuoka Station), Shizuoka City, shown in gray in Figure 6.7 [2]. Figure 8.9 shows the road network in the service area, consisting of 4,045 nodes and 9,257 links. The average link length is 43.8 [m]. The area is 3 [km] long and 4 [km] wide. The edge colors in Figure 8.9 correspond OpenStreetMap way tags.

I use the Person Trip Survey (a kind of Household Travel Survey) conducted in 2012 as source data to generate passenger demands. The survey asked citizens to respond to a questionnaire, which included their characteristics (e.g., age and gender), the purpose of travel, places of origin and destination, time of travel, and travel mode. The origin and destination points were aggregated by the zones shown in Figure 6.7. I select travels by public transportation (bus, taxi) and/or private cars as potential candidates of OSMS users. I also omit trips within the same zone and trips of less than 1 [km] travel distance.

[2] In this area, the local government and some companies have frequently conducted demonstration tests of new mobility services such as OSMS and MaaS (Mobility as a Service).

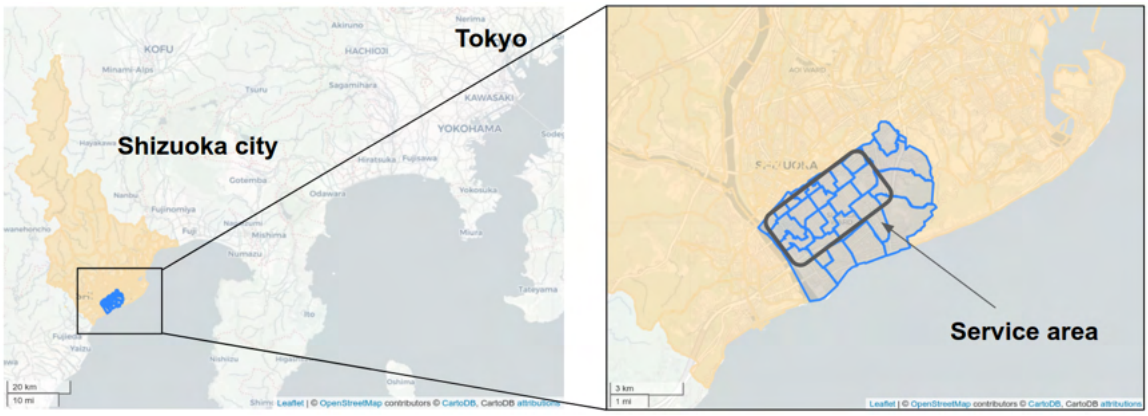

Figure 6.7: Map of Shizuoka City. The service area is highlighted in the gray square. The zones delimited by the blue line are the aggregation zones used in the Person Trip Survey.

From the Survey, the most frequently traveled hour was 4 P.M. The total number of demands at 4 P.M. is 2,038. Figure 6.9 shows the distributions of origin (a) and destination (b) at 4 P.M. The color intensity indicates the number of origins and destinations within a 200 [m] mesh; the mesh with the highest concentration of origins is located at the central station. The same mesh is also a highly concentrated area on the destination map. Another highly concentrated mesh in the destination map is located southeast of the station, which is a shopping mall zone.

To verify the result of the static analysis, I perform simulations with varying the numbers of demands. The static analysis indicates that the average travel time of passengers is shorter in MPs-based OSMS than in D2D-based OSMS when the demand exceeds a certain level. I define the number of minutes of starting the travel for each demand by uniformly sampling between 0~59 because the Person Trip Survey does not record the start time of the travel in minutes. Then, from the 2,038 demands at 4 P.M., I randomly sample 50, 100, 200, 500, and 1,000 demands. To eliminate randomness, the demand data were generated by sampling each demand number 100

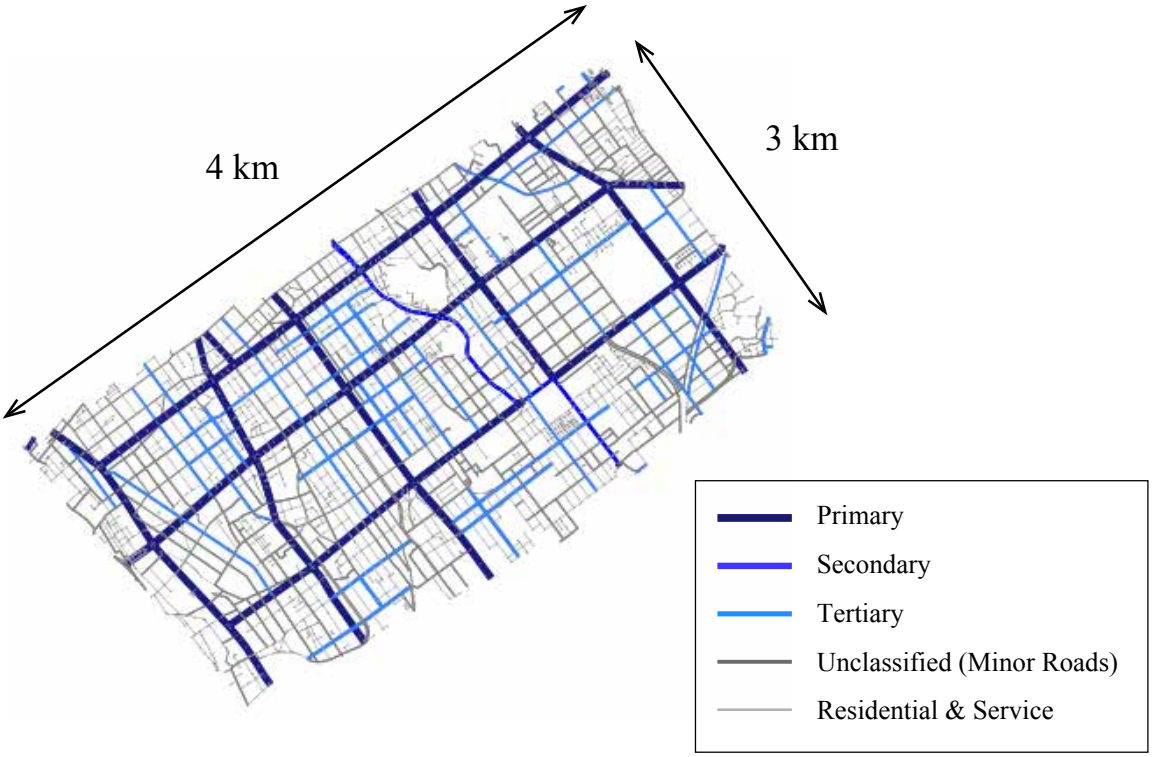

Figure 6.8: Network and road types (Source: OpenStreetMap).

times. Note that the demand for travel by taxi, bus, and private cars for elderly persons aged 65 and over at 4:00 p.m. is approximately 500.

6.5.2 Settings

To demonstrate the effects of MP in real-world scenarios, I need to carefully select the parameters of MPs and OSMS. Especially, the locations of MPs, the number of vehicles, and vehicle capacity are three key parameters reflecting the real features of the OSMS with MPs.

Locations of MPs depend on two parameters: the average interval between MPs and the categories of road edges where MPs are located. For the average interval, I use 200 [m] and 400 [m] in the experiments. The value 400 [m] reflects a setting

(a) Origin (b) Destination

Figure 6.9: Origin and destination distributions of peak time (4 P.M.) demand.

similar to typical bus services with stops spaced 300 to 500 [m] apart. The value 200 [m] is the case that OSMS with MPs provide more convenient services than the bus services. I suppose that shorter MP intervals will reduce the cost of walking for passengers. For the categories of road edges, I choose only "primary," "secondary," and "tertiary" edges in OpenStreetMap data, excluding residential and minor edges, because frequent traffic on such minor roads tends to cause accidents. It has also been reported that on-demand services often travel on residential roads [84]. Finally, I determine the MPs as follows: Collect midpoints of the primary/secondary/tertiary edges and choose a subset of them as MPs with their intervals greater than 200 [m] and 400 [m]. Figure 6.10 shows MP locations. The number of MPs for 200 [m] and 400 [m] intervals is 175 and 77, respectively.

I find the minimum fleet sizes that avoid any rejections. In other words, find the minimum number of vehicles needed to ensure that travels of all demands are faster than walking. Since the actual minimum number of vehicles depends on the number of demands and the size of the area, I perform 100 simulations for different combinations of the number of vehicles and other parameters and determine the minimum number.

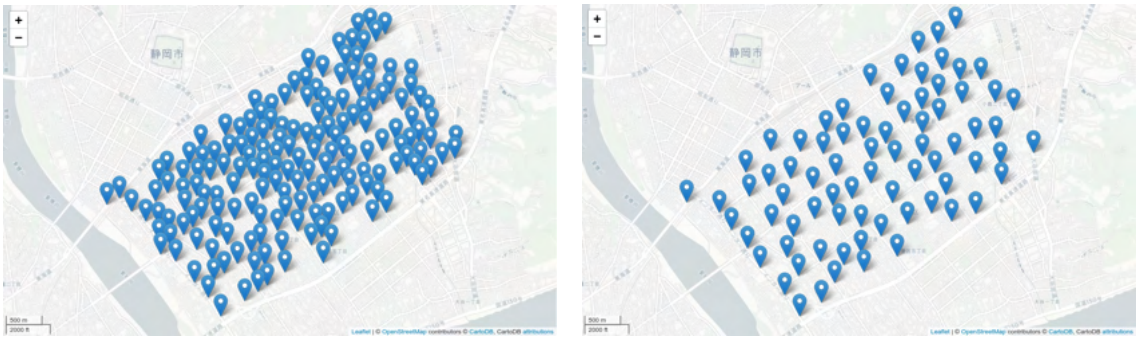

(a) 200 m (b) 400 m

Figure 6.10: Locations of MPs.

Vehicle capacity affects operational efficiency and passenger convenience. It can be assumed that the VKT and, by extension, the the travel time of passengers is reduced by picking up and dropping off passengers at the same MP because D2D detours are avoided. The reduction will be greater as more passengers are picked up and dropped off at the same MP. Larger vehicle capacity will improve the possibility of accepting more passengers at the same MP. In the experiment, 1, 2, 4, and 8 vehicle capacities are tested. A vehicle capacity of 1 assumes an operation of a regular taxi in which passengers don't share their trip. A vehicle capacity of 2 or 4 indicates the number of passengers that can be accommodated in a regular taxi vehicle. A capacity of 8 assumes the case of a minibus.

The parameters in the simulation, along with other parameters are shown in Table 6.1. The stop time for pick-up and drop-off is 15 [s], regardless of the number of passengers, and the acceleration/deceleration time uses the default value of SUMO. And the initial locations of all vehicles are Shizuoka Station.

Table 6.1: Simulation parameters.

Parameter	Value
Number of demands (1 hour)	50, 100, 200, 500, 1000
MP location interval	200, 400 [m]
Vehicle capacity	1, 2, 4, 8 passengers
Stop time for boarding and alighting	15 [s]
Maximum speed of the vehicle	60 [km/h]
Walking speed	3 [km/h]

6.5.3 Results

The number of vehicles affects operational efficiency and passenger convenience. The number of vehicles required for each demand pattern is shown in Table 6.2. This table shows that the vehicle capacity has the largest impact on the number of vehicles, followed by MPs introduction. The number of vehicles in D2D-based OSMS is reduced by increasing the vehicle capacity from 1 to 2 and from 2 to 4. When demand is low, there is no difference between vehicle capacities of 4 and 8, but when demand is high (1000 demands), there is a difference. The results also show that as the number of demands increases, the reduction in the number of vehicles due to the introduction of MPs becomes more significant.

Here, I discuss the results of D2D- and MPs-based OSMS with the adjusted number of vehicles required for each service (Case 1) and the results of MPs-based OSMS

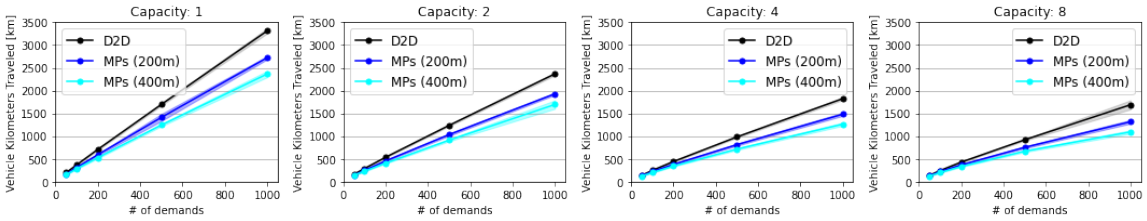

(a) Case 1: adjusted number of vehicles

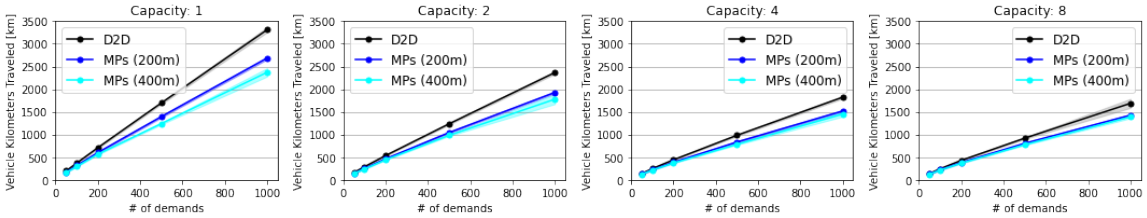

(b) Case 2: same number of vehicles

Figure 6.11: Total vehicle kilometers traveled (VKT).

with the same number of vehicles as in D2D-based OSMS (Case 2) (Number of vehicles of D2D-based OSMS in Table 6.2).

VKT

Figure 6.11 shows the VKT for each vehicle capacity and demand. The solid line indicates the mean value of 100 simulations, and the width indicates the standard deviation. Since the number of vehicles required is reduced by capacity expansion and the MPs introduction, the VKT is also reduced.The VKT reduction in Case 2 is smaller than in Case 1 because the number of vehicles is the same. However, even when the number of vehicles is the same, the MPs introduction can reduce the VKT.

The larger vehicle capacity and MPs intervals mean that more passengers can be picked up and dropped off at a single MP, leading to fewer detours than in D2D-based OSMS, which is thought to reduce the VKT. In addition, fewer stops due to pick-up

and drop-off reduce the demand processing time, allowing for more efficient operation with fewer vehicles. The VKT is also reduced when the vehicle capacity is 1, i.e., when MPs are introduced in a normal taxi operation. This is because passengers walk part of the way between ODs, and since the detour is reduced by passengers are picked up and dropped off at the MPs.

Travel time of passengers

Figure 6.12 shows the average travel time of passengers. This figures show that in Case 1, the travel time is longer in MPs-based OSMS than in D2D-based OSMS, even when the number of demands is increased. On the other hand, in Case 2, the travel time is shorter in MPs-based OSMS than in D2D-based OSMS when the number of demands is increased. Note that from Welch's test, it was statistically found that MPs-based OSMS has shorter travel time of passengers than D2D-based OSMS when the number of demands is greater than 100 for capacity 1, and when the number of demands is greater than 200 for capacities 2, 4, and 8.

Figure 6.13 and Figure 6.14 show the on-boarding and waiting time, respectively. Incidentally, the walking time is approximately 6 [min] when the MPs interval is 200 [m] and approximately 10 [min] when MPs interval is 400 [m] for all conditions. Figure 6.13 shows that as vehicle capacity increases, the on-boarding time increases. This is due to the increase in the number of shared passengers. However, the introduction of MPs reduces the on-boarding compared with D2D-based OSMS for all conditions. In addition, Figure 6.14 shows that the introduction of MPs reduces waiting time. However, the walking time to use MPs is greater than the reduction in on-boarding and waiting time, increasing the travel time in Case1. On the other hand, in Case 2, the MPs introduction significantly reduces the waiting time compared to

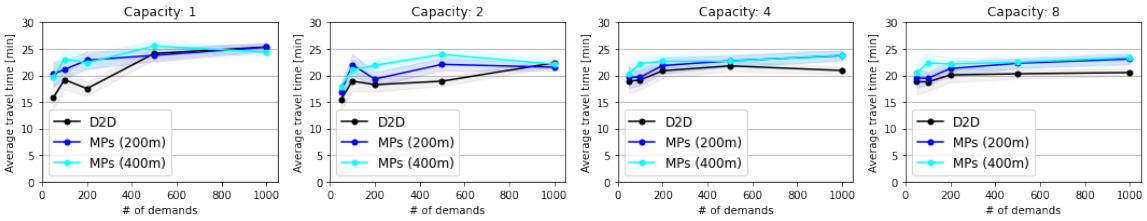

(a) Case 1: adjusted number of vehicles

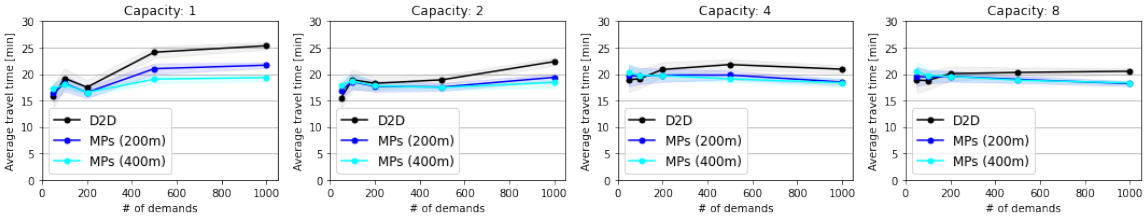

(b) Case 2: same number of vehicles

Figure 6.12: Average travel time of passengers.

Case 1, resulting in a shorter travel time than D2D-based OSMS.

Figure 6.15 shows the average number of pick-up passengers at an MP. For a vehicle capacity of 1, the number of pick-up passengers per MP is 1, even for an MPs-based OSMS. As the vehicle capacity is increased, the average number of passengers per MP increases. The larger the MP interval, the larger the number of pick-up passengers per MP. This is because the larger the MP interval, the fewer the number of MPs, and thus, the greater the probability of passengers being concentrated into a single MP. This tendency is stronger when the number of demand is larger. In Case 2, the number of vehicles in MPs-based OSMS is larger than in Case 1, so the average number of passengers per MP is smaller, but this trend is consistent. Figure 6.14(b) shows that the waiting time in MPs-based OSMS decreases as the number of demands increases when vehicle capacities of 4 or 8. This is because the average number of pick-up passengers per MP increases as the demand increases. The introduction of MPs

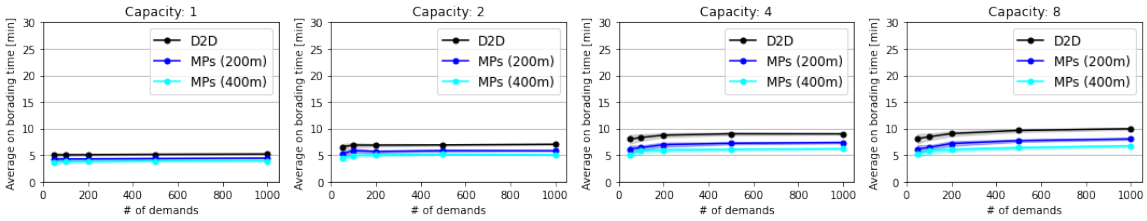

(a) Case 1: adjusted number of vehicles

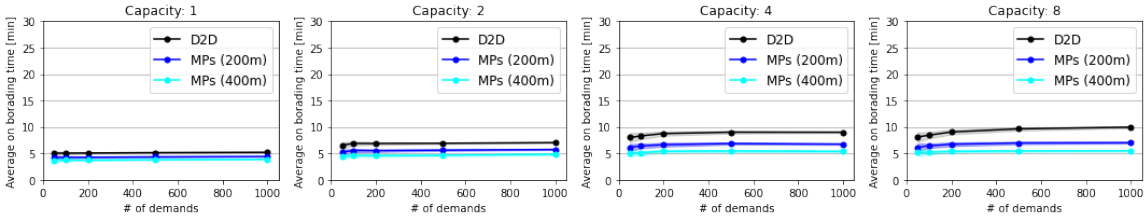

(b) Case 2: same number of vehicles

Figure 6.13: Average on-boarding time.

allows passengers to board a vehicle and alight at the same MP, even if the number of passengers increases, thus reducing the number of detours and the time spent waiting for other passengers. The reduction in VKT also shows that the introduction of MPs reduces the number of detours, allowing demand to be processed more quickly, thus reducing the waiting time. Therefore, the average travel time of passengers is shorter in MPs-based OSMS than in D2D-based OSMS when the demand is increased.

Illustrative results

For a more intuitive understanding, I focus on a certain OD set to explain the effects of introducing MPs. Based on the results for the 1000 demands, the number of vehicles is 48, and the vehicle capacity is 8, I focus on the five ODs moving from east to west, as shown in Figure 8.11. Figure 8.11 shows the trajectory of the vehicle for these five ODs.

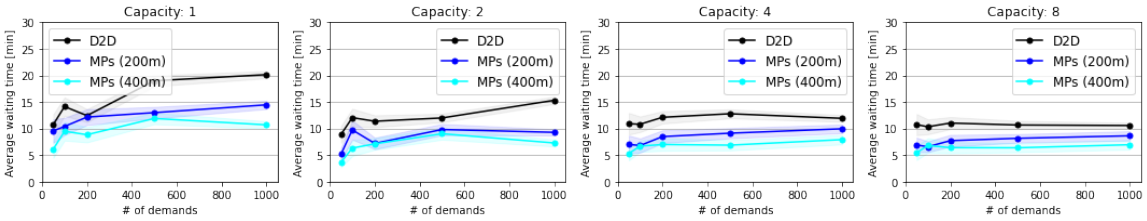

(a) Case 1: adjusted number of vehicles

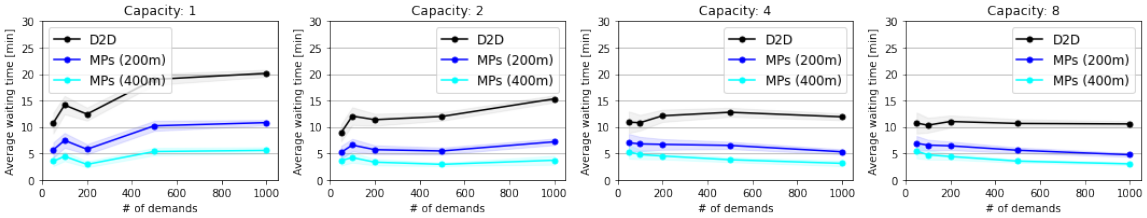

(b) Case 2: same number of vehicles

Figure 6.14: Average waiting time.

I can see that in the D2D- and MPs-based (200 [m]) cases, the demand is handled by three vehicles, Whereas, in the MPs-based (400 [m]) case, it is handled by one vehicle. In the D2D-based case, the vehicles detour to process other demands as well. The dispatch and routing are optimized under a time constraint such that the travel time between the pick-up and drop-off points is shorter than the time required for walking. In the MPs-based case, the time constraint is tighter than in the D2D-based case because the distance between the pick-up and drop-off points is shorter. Therefore, the routing optimization is performed to minimize the number of detours in the MPs-based case. This can be clearly seen in Figure 8.11.

Table 6.3 shows the results for this sample OD. As shown in Figure 8.11, the introduction of MPs significantly reduces the VKT. The effect is further improved by increasing the MPs intervals, i.e., by aggregating more passengers to a single MP. The travel time is 68% of D2D at 200 [m] intervals and almost the same at 400 [m]

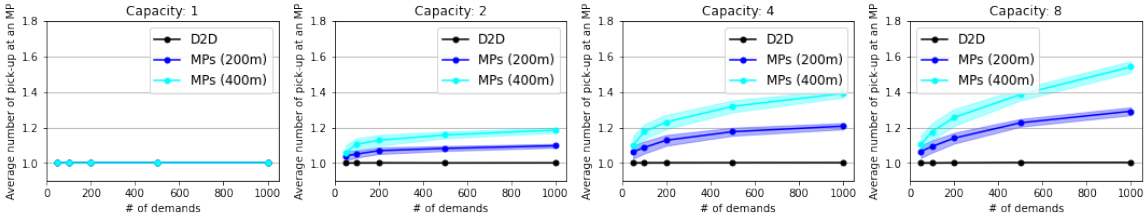

(a) Case 1: adjusted number of vehicles

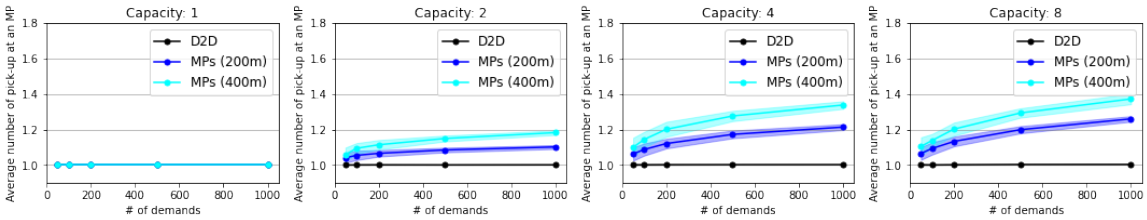

(b) Case 2: same number of vehicles

Figure 6.15: Average number of pick-up passengers at an MP.

intervals. Note that the results for this sample represent the most effective example of aggregation, so the improvement in VKT is large, while the reduction in travel time is small.

Summary of results

The introduction of MPs reduce the number of vehicles required to maintain a certain level of service quality. If the number of vehicles is reduced in response to the introduction of MPs, the travel time of passengers will increase, but only by a maximum of 5 [min]. The static analysis results that the introduction of MPs into OSMS shortens the VKT and reduces the average travel time of passenger in MPs-based OSMS more than in D2D-based service if the number of demands are above a certain number, are also verified by simulation analysis. Although not conducted in our experiment, if the number of demand is further increased, the travel time by

(a) D2D (b) MPs (200 m) (c) MPs (400 m)

Figure 6.16: Examples of D2D-based and MPs-based OSMS routes. The green circle indicates the origin and the red circle indicates the destination. The gray circles indicate the pick-up/drop-off points of the demand handled by the vehicle in addition to the five ODs. The light blue markers are MPs. The black solid lines indicate vehicle trajectories and the dotted lines indicate passenger walkways.

MPs-based OSMS is expected to be more shorter than that by D2D-based OSMS.

Czioska et al. stated that the introduction of MPs increases passenger travel time, but this is a result of using the minimum required number of vehicles for D2D- and MPs-based OSMS, respectively. I have conducted a similar experiment, with the same results as Czioska et al., as shown in Case 1. In addition, unlike Fielbaum et al., I simply compare travel times in D2D- and MPs-based OSMS under no demand rejection conditions.

According to the result in this study, the introducing MPs can reduce not only the efficiency of vehicle operation but also the travel time of passengers if the number of vehicles required for D2D-based OSMS is sufficient to prevent a constraint (i.e., it is not faster to walk) and if the number of demands is above a certain level. Furthermore, the introduction of MPs is effective in improving operational efficiency and travel time not only for shared services such as OSMS but also for conventional one-vehicle, one-passenger services such as a taxi and on-demand mobility services.

6.5.4 Further Evaluation

The introduction of MPs may reduce travel time, but only if passengers are willing to walk. Walking is probably more inconvenient for passengers; so it is difficult to argue that simply shortening travel time will improve passenger convenience. Therefore, I evaluate passenger convenience using a generalized cost. The generalized cost is an index that changes the advantages and disadvantages of travel, such as travel time, into monetary values.

As the same process described in Chapter 2, I estimate the travel mode choice model with a different definition of the utility function. Unlike Chapter 2, travel time is divided into on-boarding time, walking time, and waiting time. The estimated parameters are listed in Table 6.4. From the estimated parameters, I find, for example, that a transportation mode that requires a longer on-boarding time is less likely to be chosen. $\bar{\rho}^2$ is the pseudo-determination coefficient, which indicates the fitness of the model, and 0.2 or higher indicates that the model is valid [104].

I define the generalized cost for a trip other than fare, GC w/o fare, as the following Eq. 6.8. This represents the monetary equivalent of the utility of travel, consisting of on-boarding time, waiting time, and walking time.

$$
\begin{aligned}
GC \text{ w/o fare} = -\frac{1}{\beta_{\text{Fare}}}(& \\
\beta_{\text{On\_boarding\_time}} \times x_{\text{On\_boarding\_time}} & \\
+\beta_{\text{Walking\_time}} \times x_{\text{Walking\_time}} & \\
+\beta_{\text{Waiting\_time}} \times x_{\text{Waiting\_time}}) &
\end{aligned}
\tag{6.8}
$$

Based on the above, I obtain the generalized cost in the D2D-based and MP-based

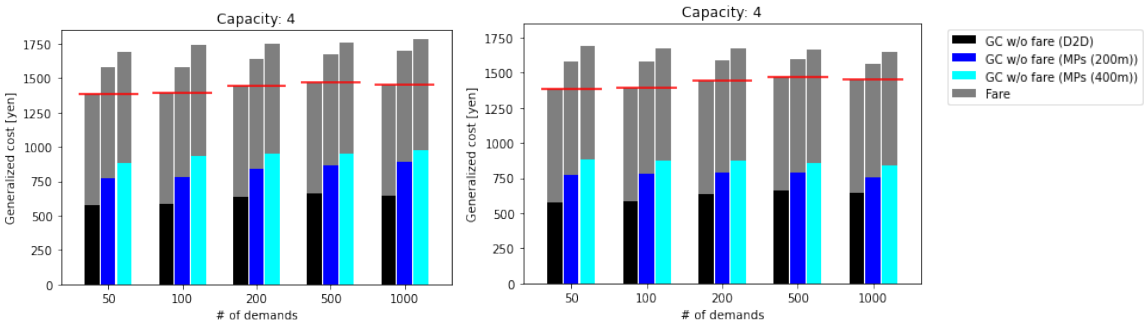

(a) Case 1: adjusted number of vehicles (b) Case 2: same number of vehicles

Figure 6.17: Generalized cost calculated using the Nested logit model parameters (Vehicle capacity is 4).

OSMS. Figure 6.17 shows the average generalized cost for a vehicle capacity of four passengers. The generalized cost comprised *GC* w/o fare and fare for taxi services. The taxi fare calculation is 420 [yen] up to 1.052 [km], and 80 [yen] is added for every 233 [m] beyond that. This taxi fare calculation is based on Tokyo area [105].

For example, in Case 1, the generalized cost of D2D-based OSMS is 31% (200 [m]) and 42% (400 [m]) less than that of MPs-based OSMS for a vehicle capacity of four passengers and 1000 demands [3]. On the other hand, in Case 2, the generalized cost for a D2D-based OSMS is 14% (200 [m]) and 25% (400 [m]) less than that of MPs-based OSMS for a vehicle capacity of four passengers and 1000 demands. In the case of a conventional taxi-like operation with a predetermined number of vehicles or drivers, the same convenience as in D2D-based OSMS can be achieved at a lower discount rate than in Case 1.

[3]Case 1 can be viewed as a type of work in which drivers work when they want to work, such as Uber. Uber offers its OSMS, UberPOOL, at half the price of its regular on-demand service, UberX, and its MPs-based OSMS, UberExpressPOOL is reportedly offered at a further 25% off. Our results indicate that the discount rate is excessive.

6.5.5 Effects of MP selection

I have confirmed that the introduction of MPs reduces travel time when the number of vehicles is approximately the same as the number of vehicles in D2D-based OSMS (Case 2) and when the number of demands is above a certain level. Here, I discuss the effect of the MP selection on the vehicle allocation algorithm. As described in Section 6.4.2, when a new demand is generated, MPs at four locations around the origin and destination of that demand are listed. The MPs combination that minimizes the cost is determined. At this time, there is a possibility that passengers may be asked to walk to a slightly more distant MP depending on the situation.

To verify the difference between dynamic MP selection and simply assigning the closest MP, I perform simulations for 1000 demands with the same number of vehicles as for D2D-based OSMS. The MPs intervals is 200 [m]. Vehicle capacity is 4 and 8.

Figure 6.18 shows the VKT, passenger travel time, walking time, and waiting time for D2D- and MPs-based OSMS when using the closest MP and MP-based OSMS with dynamic MP selection. Figure 6.18(a) shows that the case with MP selection reduces the VKT more than that without the MP selection. Note that simply using the nearest MP increases the travel time, whereas MP selection reduces the travel time, as shown in Figure 6.18(b). These results show that the travel time can be reduced by introducing MPs only when an MP is dynamically determined. On the other hand, since MPs are determined according to the situation, the closest MP is not always selected, increasing the walking time. This means that there is a tradeoff between walking time and vehicle operating efficiency or the travel time of passengers.

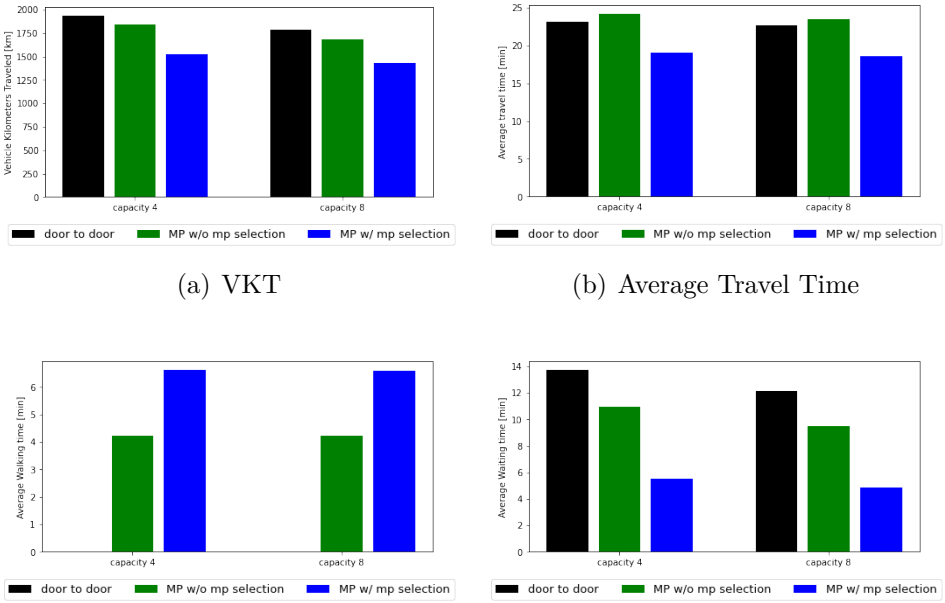

(a) VKT

(b) Average Travel Time

(c) Average walking time

(d) Average waiting time

Figure 6.18: Effects of MP selection.

6.6 Conclusion

I analyzed the benefits of introducing MPs into OSMS in terms of operational efficiency and passenger convenience, especially travel time. Previous studies have shown that the introduction of MPs into OSMS can improve operational efficiency. However, the benefits in terms of passenger convenience have not been sufficiently investigated. The static analysis and the simulation analysis using actual maps and demands show that the introduction of MPs shortens the VKT and, if the number of demands exceed a certain number and the number of vehicles is equivalent to D2D-based OSMS, reduces the average travel time of passengers compared with D2D-based OSMS.

Some limitations of this study must be addressed. The first is to optimize the location of the MPs. In this study, MPs were placed at equal intervals on major

roads, but adjusting the location of MPs based on the spatial distribution of demand can be expected to further improve operational efficiency and passenger convenience. In addition, this study was limited to an investigation of one-hour demand. Analysis for longer periods, including peak and off-peak periods, is required for a more detailed understanding of the advantages and disadvantages of MP-based OSMS.

One interesting future issue will be how to encourage passengers to use MPs. Based on the simulation analysis, there are tradeoffs between the number of vehicles, VKT, passenger travel time, and walking time. To better understand these tradeoffs, a topic to study is the use of multi-objective optimization in the vehicle allocation algorithm to optimize all indicators simultaneously. Once the tradeoffs are known, it is possible to determine how much of a fee discount is best for both the service provider and the passenger.

Another important topic is how to integrate various types of mobility services. The service design could be based on demand, for instance, D2D-based OSMS could be used when demand is low and MP-based OSMS could be used when demand is high. Recently, on-demand services have become popular; however, despite their convenience, on-demand services have negative effects, such as congestion. Therefore, OSMS has been developed, and MPs-based services, which are the subject of this study, are being considered. There is a sense that the time is reversing from on-demand to conventional fixed-route transport. Railways and buses are the largest sharing services. The development and research of tools to support service design based on demand and regional characteristics, such as the extent to which services should be on-demand and the extent to which they should be fixed, will also be an issue in the future.

Table 6.2: Number of vehicles.

		Number of demands				
Capacity	Type	50	100	200	500	1000
1	D2D	6	10	20	40	77
	MPs (200m)	5	9	16	37	70
	MPs (400m)	5	8	15	32	64
2	D2D	5	8	15	34	61
	MPs (200m)	5	7	14	29	56
	MPs (400m)	5	7	12	25	50
4	D2D	4	7	12	26	50
	MPs (200m)	4	7	11	23	41
	MPs (400m)	4	6	10	21	36
8	D2D	4	7	12	26	48
	MPs (200m)	4	7	11	22	38
	MPs (400m)	4	6	10	20	32

Table 6.3: Results of sample OD.

	D2D	MPs (200 [m])	MPs (400 [m])
Number of vehicles that handle the sample OD	4	3	1
Total VKT [km]	16.8	9.1	3.5
Average travel Time [min]	22.1	15.2	21.5
Average on-boarding Time [min]	10.3	7.5	6.8
Average waiting Time [min]	11.8	2.2	4.4
Average walking Time [min]	0	5.6	10.2

Table 6.4: Estimated parameters of the travel mode choice model.

	estimated parameters	t-value
$\beta_{\text{On\_boarding\_time}}$	-23.90	-1.99
$\beta_{\text{Walking\_time}}$	-32.89	-4.17
$\beta_{\text{Waiting\_time}}$	-13.65	-2.61
β_{Fare}	-0.59	-2.79
$\bar{\rho}^2$	0.25	

Chapter 7

Crowd Movement Simulation Analysis and Optimization: A Review

7.1 Introduction

Crowding can sometimes lead to accidents that kill or injure hundreds of people, so countermeasures are needed. Crowding is especially likely to occur during evacuations from disasters and large-scale events when many people move in the same place at the same time. Under crowded conditions, people are squeezed, which may lead to accidents. Crowding accidents have been reported in various parts of the world, including a fireworks display in Akashi City and a pilgrimage to Mecca in Saudi Arabia [106, 107]. Therefore, it is necessary to move crowds safely and efficiently.

"Spatial design" and "crowd control" can mitigate crowd congestion. Spatial design refers to determining the placement of exits and the width of routes to facilitate

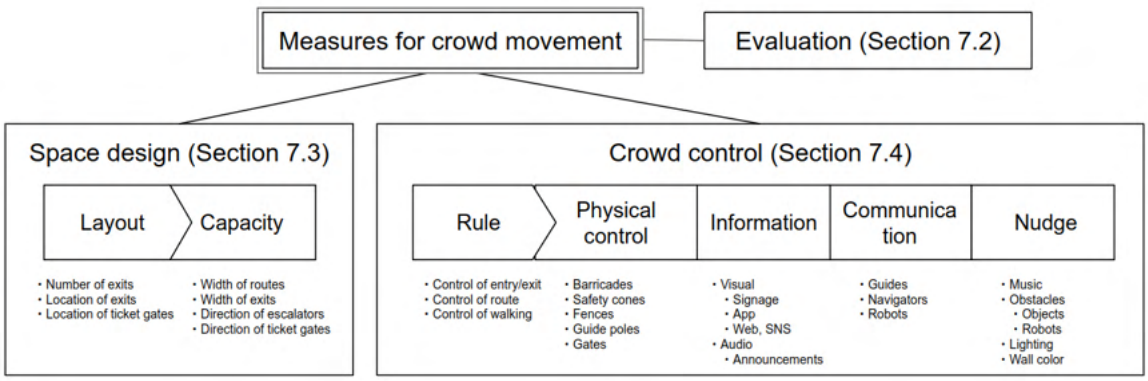

Figure 7.1: Classification of crowd control approach

crowd movement. On the other hand, crowd control is the direct intervention and manipulation of crowd movement by information presentation, guidance, etc.

Simulation can be a powerful tool for evaluating spatial design and crowd control. Testing crowd movement in response to various exit arrangements and guidance methods requires measurements at public events or gathering people for experiments, both of which are costly. Therefore, simulation, which can be repeated on a computer, is suitable for this purpose. There are two approaches to representing crowd movement: a macro approach that applies fluid dynamics to model crowd movement as a fluid or gas, and a micro approach that focuses on the movement of individual pedestrians and models the interactions among pedestrians and between pedestrians and the environment.

Simulation of crowd movement is an area that has been actively studied since the 1990s and has already been systematized. Interested readers are referred to the survey papers [108, 109, 110]. As with simulations, there has also been extensive research on the measurement of crowd movement. Measurement methods include manual, Wi-Fi, RFID, Bluetooth, cameras, LiDAR, and GPS. For a review of measurement methods,

please refer to the literature [111]. In addition, analytical methods for interpreting crowd status from measurement data have also been studied. For example, analytical methods can extract information such as the location of individual pedestrians, crowd density, and movement patterns. For more information on analytical methods, please refer to the literature [112, 113].

On the other hand, methods and findings on spatial design and crowd control using crowd simulation are not well organized. For example, a survey of studies on the measurement, analysis, prediction, and control decisions of crowd movement up to 2016 is reported [114]. A survey of studies using optimization for the problem of crowd evacuation has also been reported [115]. However, it is noted that in these papers, optimization is often applied to pedestrian models, with few studies targeting spatial design and control.

Since 2018, several survey papers on spatial design and crowd control studies have been reported. In 2018, survey about guidance methods using signs, guidance personnel, smartphones, robots, etc. [110]; in 2020, the optimization of evacuation routes and the optimization of allocation to evacuation centers[116]; and in addition to the optimization of guidance methods and evacuation routes, the design of buildings and the installation of obstacles are also reported [117]. However, all of these are focused on crowd movement at the time of evacuation.

The purpose of this chapter is to systematize the research on spatial design and crowd control and to summarize the current findings. The knowledge of spatial design and crowd control is distributed among artificial intelligence, information processing, transportation engineering, civil engineering, architecture, physics, and so on. In this study, I summarize the research trend of spatial design and crowd control from

the viewpoint of crowd simulation and its optimization. This paper will also cover research on crowd movement not only during evacuation but also during events and in daily life. The expected readers are not only researchers in related fields who are interested in crowd movement but also event organizers and facility managers who need to realize safe and efficient crowd movement.

In this chapter, I cover papers retrieved from ScienceDirect using the keywords "crowd control," "pedestrian control," "crowd guidance," "pedestrian guidance," "crowd management," and "pedestrian management". Relevant research has been published in Safety Science, Transportation Research Part C, Physica A, Applied Mathematical Modelling, Simulation Modeling Practice and Theory, Fire Safety Journal, etc., and the survey covers a wide range of fields including informatics, civil engineering, and physics.

In this chapter, detailed methods of spatial design and crowd control are organized as shown in Figure 8.2. Spatial design is to determine the layout, such as the arrangement of exits, that facilitates the movement of crowds and to determine the capacity of the space for movement, such as the width of the path. On the other hand, crowd control is to intervene in crowd movement through physical control, information presentation, guidance, and nudges so that the crowd follows rules such as the time to start moving and the route to move. Physical control is a method of controlling movement by means of guardrails and gates, and information presentation is a method of informing people of information such as movement routes and congestion by means of signs and applications. Guidance can be provided by a guide who remains motionless in a fixed position or by a guide who moves with the crowd. In particular, the latter type of guide is called a navigator in this paper. In behavioral

economics, nudging, which is a method to promote behavioral change by working on people's unconsciousness, has been attracting attention in recent years. In the field of crowd movement, it has become clear that the speed of pedestrians can be controlled unconsciously by using music, light, and obstacles. The results of this research are described below. Although the characteristics of crowd movement can be distinguished into the one-directional flow, counter-flow, inflow to exit, etc.[118], and the target movement characteristics differ among studies, this paper does not classify studies by movement characteristics but only describes them.

This chapter is organized as follows. The purpose of spatial design and crowd control is to move crowds efficiently and safely. In order to establish a common understanding of this purpose, evaluation indices for crowd movement are first described in Section 7.2. In this chapter, the evaluation indices are organized in terms of efficiency and safety. Next, spatial design is discussed in Section 7.3, and crowd control is discussed in Section 7.4. Section 7.5 discusses future research directions, and Section 7.6 concludes.

7.2 Evaluation of Crowd Movement

Efficiency and safety are generally used as evaluation indices for crowd movement. Some studies have quantified the stress of inefficient movement [119]. However, it is difficult to measure the psychological stress felt by pedestrians themselves. When evaluating comfort such as stress and ease of walking, it is necessary to conduct a questionnaire survey. In this paper, I focus on measurable efficiency and safety indices.

In Table 7.1, I show the indicators for evaluating crowd movement and the papers

that use these indicators. Note that I also include cases in which efficiency and safety metrics are used as constraints in determining spatial design and crowd control. From Figure 7.1, I can see that many studies use travel time as an evaluation index among the efficiency measures. Most of these studies are concerned with evacuation. On the other hand, there are studies that evaluate not only efficiency but also safety during events and daily travel [120, 3]. This section clarifies the definition of each evaluation indicator.

7.2.1 Efficiency

Travel Time

Travel time is often used to evaluate the efficiency of crowd movement. If travel time can be measured for each pedestrian, total travel time or average travel time is used. On the other hand, when only fixed-point observation is available, the completion time, which is the time it takes for all the pedestrians to complete their movement, is used. In addition, the number of people who have completed their movement at each time may be visualized and evaluated. For example, when comparing multiple crowd control methods, visualization of the number of people who have completed or not completed a move at each time, as in Figure 7.2, allows comparison of not only the final movement completion time but also the temporal transition.

Travel Distance

Travel distance is also used as a measure of the efficiency of crowd movement. While travel time varies depending on congestion, travel distance is viewed purely as a cost of travel.

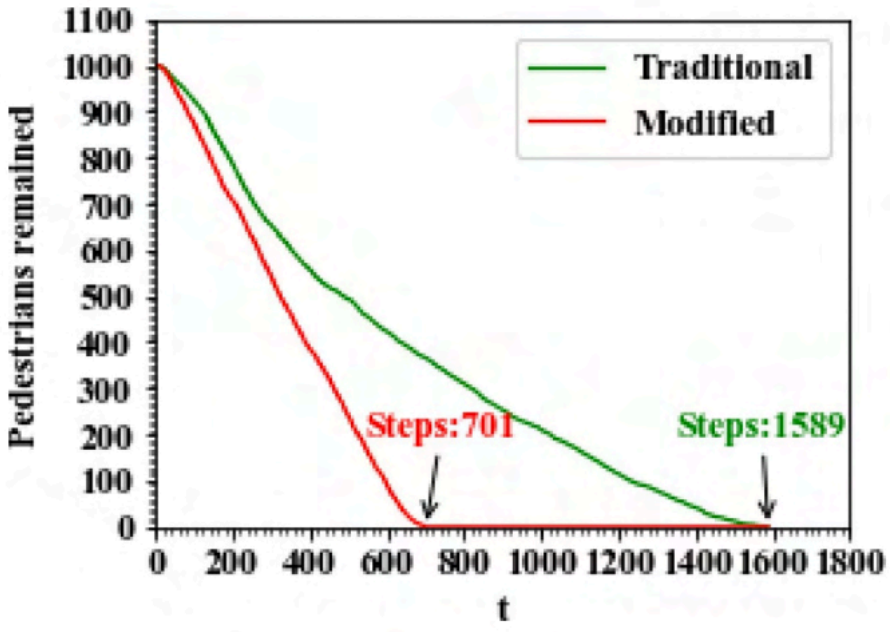

Figure 7.2: The number of pedestrians remained against time [1]

Flow and velocity

Flow rate and velocity are also often used to evaluate efficiency. The flow rate is also called the flow coefficient. Flow rate, velocity, and density are often used as indicators of traffic flow characteristics in traffic engineering. These three indices have the relationship "flow=velocity×density". In many cases, two of the three indices (e.g., density and flow rate) are used as axes in the figure, as shown in Figure 7.3. Such a diagram is called a "basic diagram. From the basic diagram, a rough indication of the maximum flow rate can be seen, which can be used as an indicator of the desired flow rate.

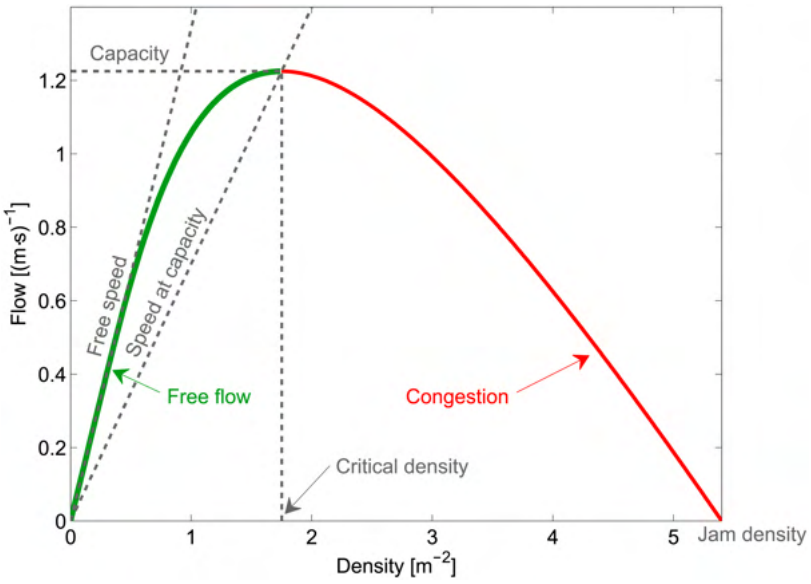

Figure 7.3: Fundamental diagram. Flow-density representation [2]

7.2.2 Safety

Congestion degree

Congestion degree is used as a measure of safety to account for the hazards of crowding. Typically, crowd density is used as a measure of crowding. The number of pedestrians for a given area is often used as the density [120, 148]. Alternatively, there is the local density method, which calculates the spatial distribution of the crowd with respect to a certain location [129, 149]. For comparison of spatial design and crowd control, there are two methods: graphical representation of the density at a given range or location at a given time, as in Figure 7.4, or visualization of the density over the whole range, or the average or maximum density at a given time, as in Figure 7.5.

Densities should be small but can be tolerated up to a certain degree. Therefore, a threshold value is used to evaluate the safety of the community. For example, Lopez-

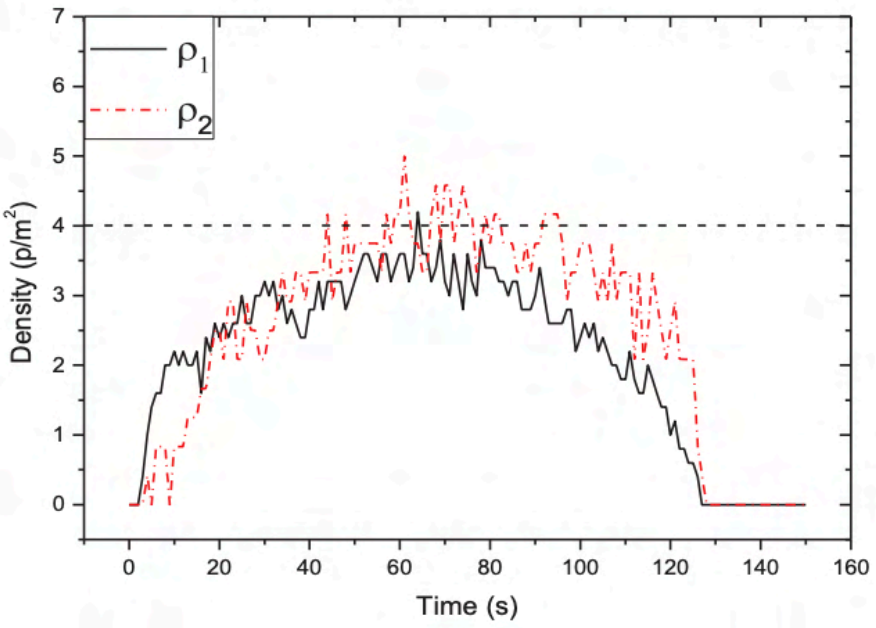

Figure 7.4: The density against time [3]

Carmona et al. define the density at which the flow rate decreases as a threshold value using a basic diagram, and assume that safety becomes low when the density exceeds the threshold value [148]. In addition, the Level of Service (LOS) defined by Fruin is used as a criterion to evaluate safety based on the density of pedestrians [150]. The LOS is divided into six levels as shown in Table 7.2. Levels A to C are defined as stable flow, D as near unstable flow, E as unstable flow, and F as dangerous flow. Crowding accidents are more likely to occur from level E, and level F has a very high probability of causing fatalities and injuries.

Some studies have used the degree of pedestrian body overlap as a measure of congestion other than density [7].

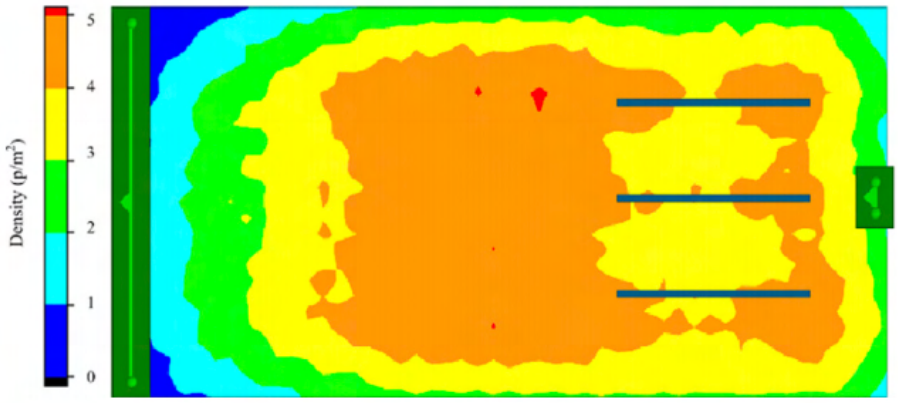

Figure 7.5: Visualization of crowd density [3]

Other

In addition to congestion, there are other indicators to assess crowd safety. For example, Qiao et al. evaluated safety based on the degree of change in the direction of travel when guardrails are installed in a subway corridor[146] Lu et al. used the risk of fire as an evaluation index [65]. In addition, some studies have evaluated the number of people infected by COVID-19 in recent years [147].

7.3 Space Design

Spatial design refers to the design of buildings to facilitate the movement of crowds. Before the development of simulation technology, the design was conducted in accordance with "specification rules" stipulated in the Building Standard Law. These specifications included specific numbers for the number of entrances and exits, path widths, and so on, and following the specifications had the advantage of facilitating design. However, the specific specifications in the specification rule limited the degree of freedom of design. Therefore, based on the idea that free design is possible as

long as the building meets performance requirements such as safety and efficiency in the event of an evacuation, "performance specifications" were introduced to evaluate the quality of design based on performance. The calculation method of performance is described in the Building Standard Law, and the walking time required to reach the exit of a room and the time required to pass through the exit can be calculated based on the area of the room and the distance of the route. Currently, simulation technology has been developed to evaluate performance with higher accuracy, and the use of simulation is increasing [151].

This paper reports a paper that studies spatial design in terms of layout, such as the number and arrangement of exits, and the capacity of spaces that can be traveled, such as routes and exits. The object of spatial design is mainly rooms in a building or an entire building. The classification of space design and related papers are shown in Table 7.3. Layout and capacity studies are described in turn.

7.3.1 Layout

At exits, turnstiles, and ticket booths, flow rates are smaller and congestion is more likely to occur. Therefore, research is being conducted to determine their optimal number and location.

Increasing the number of exits makes crowd movement more efficient, but for the same number of exits, the location of the exits affects the travel time. It has been reported that when a single exit is placed in a room, it is desirable to place the exit in the corner of the room. When exits are placed in the center of a room, the force is received from three directions, whereas when exits are placed in the corners of a room, the force is received from only two directions, resulting in less repulsive force

between pedestrians and more efficient movement. In addition, when multiple exits are installed in a single room, it is desirable to install them in such a way that the exits are as discrete as possible [125]. On the other hand, it is considered desirable for the exits in multiple rooms to be in the same position in the rooms facing each other across the corridor [124]. It should also be noted that placing exits at the corners of rooms is counterproductive since congestion is more likely to occur at the final exit, as shown in Figure 7.6 (below). In such a case, placing the exit in the middle of the room, as in the case of Figure 7.6 (above), and avoiding too large a flow rate will prevent congestion from occurring at the final exit.

Unlike the case of exits, ticket gates (or ticket booths) are generally located in the same position to some extent. Ticket gates tend to be bottlenecks because of the time required to cut the ticket when passing through the ticket gate. According to the literature [143, 5], a way to alleviate congestion is to install ticket gates in a recessed position. Consider the case where the ticket gates are installed "parallel, convex, or concave" to the crowd walking from bottom to top, as shown in Figure 7.7. When the ticket gates are parallel or convex, most pedestrians tend to use them from the outside. On the other hand, if the ticket gates are concave, pedestrians will first use the inner ticket gate, which has a short travel distance. Therefore, it has been reported that the use of the inner turnstiles also increases, and crowds are dispersed to all the turnstiles, thereby reducing congestion.

7.3.2 Capacity

Once the layout, including the number and location of exits, is determined, it is necessary to design the capacity of the route to the exit and the capacity of the

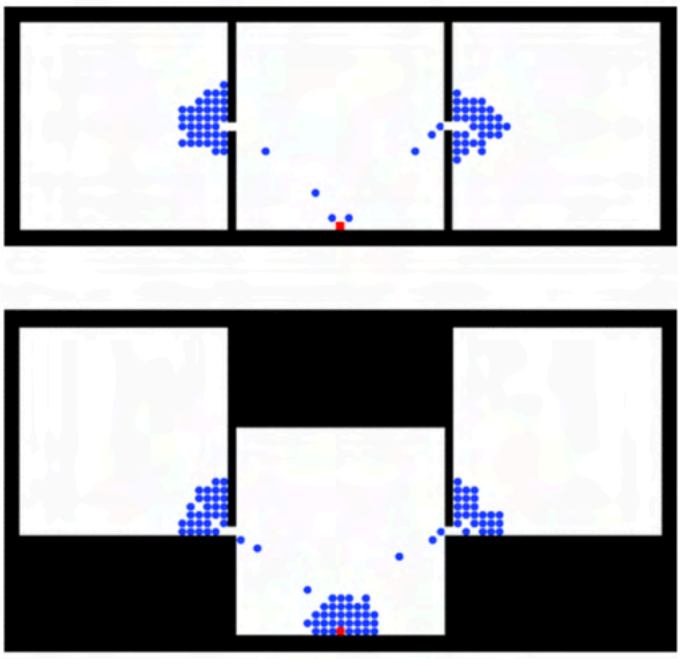

Figure 7.6: The difference between the location of the exits and the crowd movement. (Top) Exit in the middle of the room (Bottom) Exit in the corner of the room. Blue points indicate pedestrians and a red point indicates the final exit. [4]

exit. As for the connection method of the route, it is included in the problem of determining the capacity of the route, which is determined by whether or not the capacity of the route is set to zero.

Increasing the capacity of a route reduces congestion and shortens travel time. However, increasing the capacity also increases the installation cost, so it is necessary to design an appropriate route capacity. For this reason, designing a route capacity

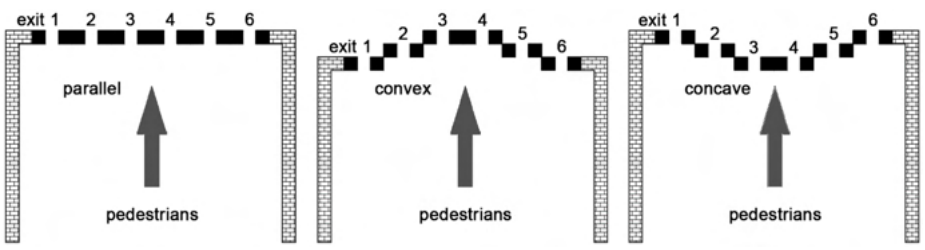

Figure 7.7: Difference in the location of ticket gate and crowd density [5]

within the installation budget is considered [132, 126], and designing using LOS, which is an index of safety against congestion as described in Table 7.2.

It has also been found that eliminating restrictions on the direction of travel of turnstiles and escalators during emergencies can increase the path capacity and contribute to shorter evacuation times [120, 136]. Therefore, it is necessary to design the escalator in advance so that the direction of travel can be manipulated quickly in an emergency.

If the exit width is small, the exit will become a bottleneck and congestion will occur, so the exit width must be designed appropriately. It is a matter of course, but by increasing the exit width above a certain level, congestion near the exit can be eased and travel time can be shortened. However, it is necessary to keep in mind that the width of the exit, especially the main exit, has a large impact on travel time [123].

The layout and capacity design have been described above. In spatial design, before constructing a moving space such as a building or a road, various design plans are simulated in advance to consider design plans that allow crowds to move safely and efficiently. When there are many design alternatives and not all of them can be considered, optimization methods are used to conduct the search. Meta-heuristics algorithms such as tabu search and genetic algorithms are often used [132, 124, 1].

7.4 Crowd Control

Crowd control is the intervention in crowd movement through physical control, information presentation, guidance, and nudging so that the crowd follows rules such as the time to start moving and the route to travel. The methods of crowd measure-

ment, analysis, and modeling and simulation [152, **?**] are classified using the level of pedestrian behavior defined by Hoogendoorn et al. . Hoogendoorn et al. classified pedestrian behavior into three levels as shown in Table 7.4 [12]. When a pedestrian moves, he/she makes decisions in order from the top of the three levels. This paper also classifies crowd control methods in terms of the pedestrian's level of action, as shown in Table 7.5. In the original definition, the strategic level includes activity selection, but I do not treat activity selection in the strategic level because the target activity of crowd movement in this paper is uniquely determined, such as evacuation or returning home from an event.

In the real world, crowd control is needed for various purposes, such as movement during the evacuation, movement during large-scale events such as sports and music events with tens of thousands of people, and movement inside train stations. There are also multiple locations to be controlled, such as a single route, a portion of an indoor area, or the entire building of a skyscraper or stadium. The scale of such crowd control is also distinguished based on the level of pedestrian activity. For example, if I want to control movement along a route, only walking at the Operational level is controlled because pedestrians have already made a decision at the Tactical level. On the other hand, if I want to control the exit from the stadium, the start time of movement at the Strategic level, the path at the Tactical level, and the walk at the Operational level can all be controlled. This combination of action levels to be controlled allows us to distinguish the scale of crowd movement targeted by crowd control. In this paper, I do not strictly categorize the crowd movement but use this as a reference when selecting a control method depending on the target of control.

7.4.1 Strategic Level

Controls the start time of the crowd's movement. The movement start time is also called pre-movement time. There are still few studies and demonstrations on the control of pre-movement time. For this reason, only case study results are presented here, rather than general findings from rule studies. Physical controls include limiting the number of people at the entrance/exit gates and, in the case of a stadium, distributing the start time of movement by block. Information could be presented by audio announcements, and guidance could be provided by onsite staff.

Rule

Staggering the start time of a move is expected to reduce congestion and improve the efficiency and safety of the move. A rule determines who starts moving and when.

Simulation analysis for evacuation and return home from the stadium confirms that the dispersion of travel start times contributes to the reduction of travel time when there are multiple exits and routes. In a study targeting evacuation, optimization of both evacuation exits and evacuation start times indicated that it is better to start evacuation immediately for those close to the exit and after a short wait for those far away [128]

On the other hand, research has also reported that, depending on the situation, it is better for everyone to start moving at the same time rather than spreading out the time to start moving [6]. Figure 7.8 shows the results of a simulation with different dispersion of movement start times for a scenario in which the participants move from the upper left and right rooms to the exit of the lower room. When everyone starts moving at the same time, congestion is created in the middle room, but the

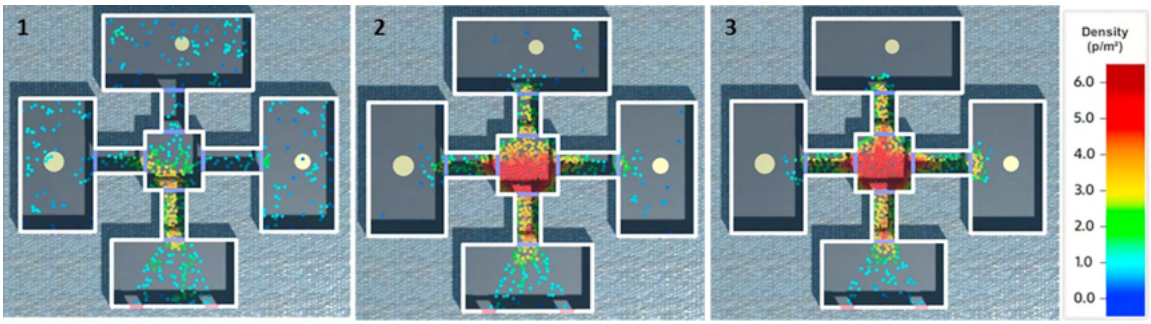

Figure 7.8: Relationship between the dispersion of the pre-evacuation time and crowd density [6]

average travel time is the smallest. This is because the physical pressure caused by the congestion does not delay the evacuation of the entire building unless it reaches a level that causes an accident, and the delay in the start of movement caused by the dispersion of movement start times is greater.

Assuming evacuation from a fire in a high-rise building, an evacuation method in which the time to start evacuation is divided by floor is also considered. This method is called "sequential evacuation," in which the fire-stricken floor and the floor immediately above it are evacuated first, and the other floors are evacuated later. Although sequential evacuation does not necessarily shorten the evacuation time, simulation analysis has shown that it avoids congestion caused by merging at the staircase [164, 165].

7.4.2 Tactical Level

Tactical level crowd control controls the movement paths of the crowd and the choice of exits to use. In the real world, physical control using barricades and guide poles, or nudges that change the color of walls or the brightness of rooms to guide people, are considered. In addition, many studies have verified the effectiveness using

simulations. It has been found that the appropriate selection of travel routes and exits by pedestrians is effective in preventing crowd accidents and improving travel efficiency by dispersing the flow of pedestrians and reducing congestion. This section presents specific methods and findings of Tactical level crowd control.

Rule

Since congestion occurs when each individual pedestrian takes the shortest path, managers need to set rules for pedestrian movement. By setting a rule that pedestrians coordinate with each other, localized congestion can be reduced and the travel time of the entire crowd can be shortened [155, 166]. For example, it has been confirmed that when evacuating, pedestrians cooperate with each other and use not only the shortest route but also multiple routes, congestion is dispersed and evacuation is safe and efficient [135]. It has also been shown that in the event of a fire in a building, safe evacuation can be achieved by using the A* algorithm to optimize the assignment of evacuation routes and having the safest detour route selected [130].

Since some pedestrians do not follow the presented rules in the real world, it is necessary to consider pedestrian decision-making. By adding pedestrian models of pedestrians who do not follow the rules to the simulation, the effectiveness of crowd control can be confirmed by assuming a crowd that is close to reality [148, 156]. For example, some studies have conducted experiments by mixing pedestrian models that take into account the anxiety and frustration of pedestrians expected during evacuations to verify the effectiveness of crowd control in an environment with pedestrians who choose irrational routes [65].

In crowd movement, there is a trade-off between efficiency and safety, and multi-objective optimization is used to simultaneously optimize the conflicting objectives.

Using the multi-objective optimization method NSGA-II [167], evacuation route optimization has been conducted with the objective function of evacuation time and crowd density [153] for evacuation from a stadium, or evacuation time and disaster risk [154] for evacuation in urban areas. The optimization of evacuation routes is carried out using the objective function.

Information

In order to present information to pedestrians, signs need to be placed in appropriate locations. By varying the number and position of signs, information can be conveyed more efficiently, and pedestrians can move smoothly [133]. For example, by using particle swarm optimization to optimize the position and angle of signs to maximize their visibility, the speed of finding exits can be improved, and people can evacuate efficiently without getting lost [131].

It is also necessary to be able to present information in small groups since presenting information by signs may cause the entire crowd to change course and congestion may not be dispersed. For example, by providing information on congestion to some people in the waiting line for a theme park attraction via an app, it is possible to disperse the congestion by having them change their purpose to an empty attraction [157].

Guidance

Static physical control and information presentation may not be sufficient to deal with temporary congestion during events. Therefore, situation-specific control by guides or navigators is necessary. In a study of stadium entry, it was reported that the opening and closing of entrances are controlled by guides and that the travel

time can be shortened by optimizing the interval between opening and closing using reinforcement learning [158].

A control method using navigators is also being considered that takes advantage of the property of pedestrians to follow other pedestrians around them. Due to the nature of pedestrians, if one pedestrian moves in the wrong direction, the surrounding pedestrians also tend to move in the wrong direction. Therefore, by placing navigators in appropriate positions, people around them can evacuate efficiently without getting lost [159, 139, 110]. In addition, in a study targeting indoor evacuation, the placement of navigators in densely populated areas improves the speed of finding exits and reduces evacuation time [160].

7.4.3 Operational Level

Operational level crowd control controls the walking behavior of pedestrians as they move toward a destination or transit point. Physical controls such as guardrails and fences force pedestrians to follow them, and nudges guide pedestrians while leaving them free to make choices with obstacles, music, and so on. The risk of accidents is extremely high in environments where crowds of pedestrians frequently change their walking speed to avoid contact with others or to overtake. Therefore, crowd control is needed to unify walking speeds. In addition, recently, due to the influence of Covid-19, more and more studies have been conducted to investigate the distance between pedestrians to prevent the spread of infectious diseases [147, 120].

Rule

Rules that regulate speed and distance between pedestrians are considered. Experiments on movement near exits have shown that high walking speeds cause congestion at exits and reduce overall evacuation efficiency. Such a phenomenon is called "faster-is-slower," and it is recommended to reduce walking speed near exits [168, 120]. In a similar experiment, Zou et al. proposed a rule that gives priority to evacuate slow walkers such as critically ill patients. By applying the rule, they succeeded in reducing the evacuation completion time from 1589 seconds to 701 seconds [140]. Recently, Hernandez et al. have verified the rules for walking in a store to prevent the spread of infectious diseases using simulations. They concluded that if the spread of infectious diseases is to be reduced by more than 90%, the maximum number of people in a store should be 20 and the distance between pedestrians should be maintained at least 1 m [147].

Control

Physical control methods such as guardrails and fences have been considered as a means of reducing walking speed variability. In an environment where walking speeds are uneven, the risk of collisions increases due to the frequent occurrence of pedestrians overtaking. The installation of guardrails not only organizes the line of pedestrians but also adjusts the width of the road to a length where overtaking is not possible. Several experiments have been conducted with guardrails and have shown that they are safer than when no guardrails were used [146, 3].

Nudge

Walking behavior is greatly influenced by human visual information, and control methods using obstacles are being considered. Obstacles can be densely avoided by using people's avoidance behavior, and are effective as a means of reducing the risk of accidents caused by congestion. One effective method of installing obstacles is to place them in the center of the path in the direction of pedestrian movement. Crowd collisions are a problem in corridors where people flow in both directions, and it has been shown that placing an obstacle in the center can help to avoid collisions because it divides the flow of the crowd [129]. Experiments placing an obstacle in the center before the exit have shown similar effects. Another method of placement near the exit is to place obstacles at both ends of the exit, as shown in Figure 7.9(a). The redder the color of the figure, the more it is involved in crowd congestion. The reason why there is less red in (a) than in (b) is thought to be because the congestion near the exit has been separated by the obstacle [7, 163]. Other experiments include an experiment that reduces the evacuation time of pedestrians by adjusting the location [121, 161] and the shape of obstacles and the pedestrian speed adjustment using moving obstacles [162].

In an environment where music is playing, auditory information, in addition to visual information, also influences walking behavior [145]. Therefore, music-based control is considered. Walking speed is faster when listening to active music and slower when listening to relaxing music, and walking speed is said to be related to BPM (Beats Per Minute), which represents the speed of a song [169, 170]. Experiments using music with a high BPM in high-density environments have shown that more people walked faster than normal, making it more dangerous than when no music was

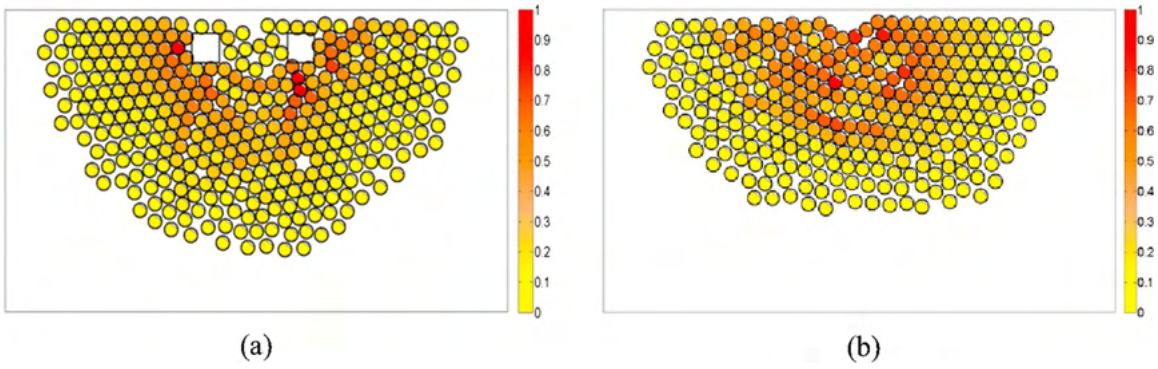

Figure 7.9: Relationship between existence of the object and crowd density [7]

playing [145].

7.5 Challenges and Approaches

I have organized and described our research on spatial design and crowd control. In this section, I extract issues from the current problems and describe approaches to solve them. A summary of the problems, challenges, and approaches is shown in Figure 7.10.

7.5.1 Challenges

The current issues and challenges of crowd control for spatial design and each pedestrian's level of activity are described.

Space design

Because most spatial design studies currently assume simple environments, it is necessary to verify the design in more complex and extensive spaces, assuming actual facilities such as buildings and stadiums.

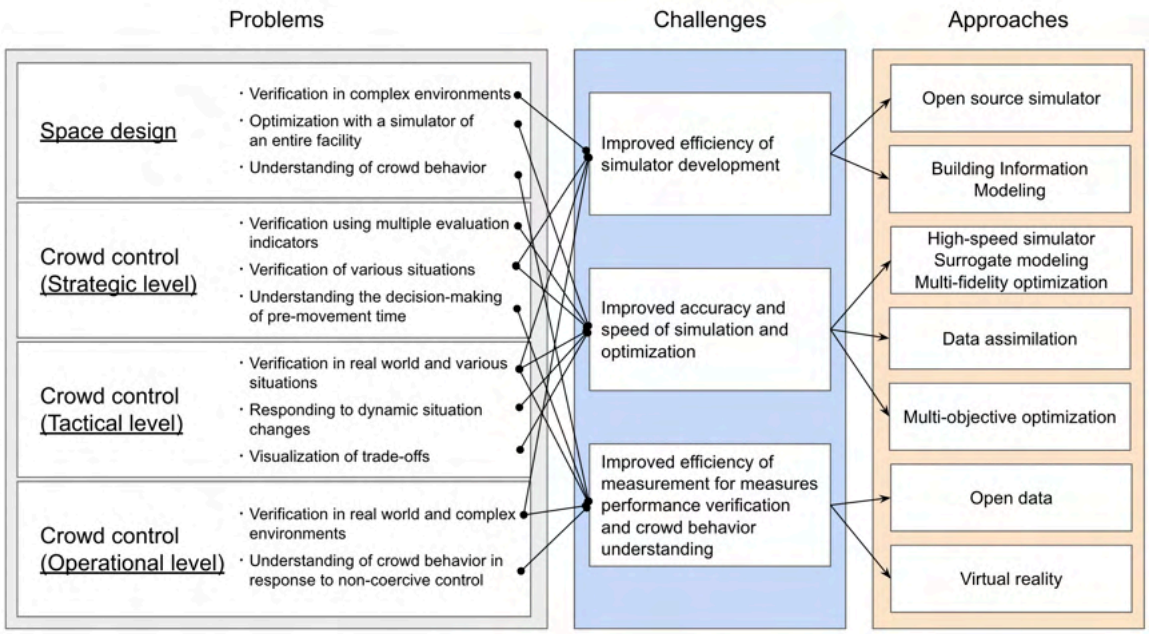

Figure 7.10: Future research direction

In addition, as mentioned in Section 7.3, placing exits at the corners of rooms sometimes reduced the efficiency of movement when considering movement from multiple rooms. Thus, partial optimization and total optimization may differ, and verification using a simulator that simulates the entire facility is necessary.

Furthermore, pedestrian movement is known to be affected by lighting [171], store space [55], landscape [172], and the number of intersections [54], in addition to the placement of exits and the width of routes. It is known to be affected by the number of intersections. Therefore, future spatial design should incorporate these factors as well, and an understanding of crowd behavior for various factors is necessary.

I consider the issues that need to be addressed to solve the problems described above. First, a simulator that imitates an actual facility is necessary to design a complex and extensive space that simulates an actual facility. However, since the development of a simulator is technically and time-consuming, most designs are done

using the calculation formulas prescribed by the laws and regulations described in Section 7.3, and in practice, there are few examples of designs done using simulators. Therefore, I believe that efforts should be made to improve the efficiency of simulator development in the future.

In addition, optimization using a simulator that simulates the entire facility is computationally expensive. This is because a simulation run for an entire facility takes longer than a simulation run for a simple environment, and many more simulation runs are required to optimize the simulation. Therefore, it is necessary to increase the speed of simulation and reduce the computational cost of optimization calculations.

Understanding crowd behavior requires the measurement of actual crowd behavior. However, crowd-prone situations such as evacuations and events are not common. Therefore, it is difficult to generate benefits commensurate with the cost of installing and maintaining measurement equipment, making it impractical to install such equipment. It is also costly to conduct experiments with a large number of people. Therefore, it is necessary to consider ways to reduce the cost of crowd measurement for understanding behavior.

Strategic level

As shown in Table 7.5, the progress of crowd control research differs among the pedestrian action levels, especially for the Strategic level, i.e., the control of movement start time, which has been less studied. The reasons may be that delaying the start of movement for evacuation is not realistic and has not been discussed in the past, and that data collection and modeling studies are less advanced than at other levels and have not yet reached the stage where control is a subject of research [152].

The first priority for control at the strategic level is to clarify its effectiveness.

For this purpose, it is necessary to evaluate not only efficiency but also safety. In previous studies, when efficiency is the only evaluation index, it is better to move all at the same time without distributing the start time of movement. I believe that the effectiveness of movement start time control will be revealed by verifying the results using multiple evaluation indices.

In the current study, there are only a few situations that can be assumed, and it is not clear under what circumstances it is better to disperse or not to disperse. Therefore, verification of various situations is also needed.

In addition, it is important to understand the factors involved in selecting the start time of pedestrian movement in order to provide effective guidance and control in real-world situations. In evacuations, individual perceptions of danger, distance from the source of the disaster, and distance from the exit have been found to influence the start time of movement [173, 174]. However, in the case of sporting and musical events, the factors involved in the choice of travel start time are not clear. In addition, it is necessary to model the relationship between multiple factors and choices in order to conduct simulations.

In order to solve the problems described above, the following issues need to be addressed: (1) increasing the accuracy of simulations to evaluate not only efficiency but also safety using multiple evaluation indices, (2) developing simulators that can handle various situations and increasing the speed of simulations for comprehensive simulations, and (3) understanding the behavior at the time of travel start. and more efficient crowd measurement to understand the behavior at the start time of migration.

Tactical level

Tactical level control has been studied up to optimization in a simulation environment that reproduces actual evacuation and events. However, few studies have verified the effectiveness of optimized control in the real world. The reason for this is thought to be the high cost of measurement and control and the difficulty of conducting demonstration experiments due to the large scale of the experimental target, such as an entire city or building.

While research has progressed to the point where the results of the research can be verified in the real world, it is also necessary to verify the effectiveness of control in various environments and situations. Therefore, I believe that the effectiveness of control methods will be revealed by preparing unified experimental data and simulators.

In addition, for effective control in the real world, it is important to control according to the ever-changing crowding conditions. At sporting events and music events, where crowd control is required, there is a risk of sudden changes in crowd conditions and accidents. Therefore, control that can respond to dynamic situation changes is required.

Furthermore, real-world crowd control must consider both efficiency and safety, which are trade-offs. Many existing studies often evaluate and optimize either efficiency or safety to reduce the search space due to the high computational cost of simulation, making it difficult to determine the effectiveness of control. Optimizing multiple indicators simultaneously requires visualization of trade-off information.

Issues to be addressed to solve the problems described above include: more efficient verification of the effectiveness of measures, and the development of simulators

that can handle various situations, faster optimization for dynamic control, and faster simulation for simultaneous optimization of multiple indicators.

Operational level

Operational level control has been studied from the simulation environment to the point where it is implemented in the real world. However, the environments used are often partial, and it has not been verified whether the control is effective for the entire environment. It has also not been verified that the control results assumed in simulations are the same as those in the real world. In order to achieve this, it is necessary to conduct control experiments during actual evacuations and events, which is currently difficult due to the high cost of control and measurement as well as the Tactical level.

In particular, the environments used in operational level research are simple environments such as one-way streets or square rooms. In actual environments In actual environments, there are multi-way streets and rooms that are a combination of two large and two small rooms. When crowd control is used for more complex environments, control for complex environments is necessary.

Walking behavior is changed by crowd control. Control also influences human psychology. However, measurement devices such as cameras and GPS have not been able to formulate the relationship between crowd control and psychological changes in walking behavior. Examples include music and rhythm. In order to realize effective crowd control, it is important to formulate changes in human psychology, and it is required to measure information that may be related to psychology.

To solve the problems described above, it is necessary to verify how effective the measures are in actual evacuations and events, and to measure various factors to

understand unknown behaviors.

7.5.2 Approaches

Based on the current research, I identified the following issues to be addressed in the future: more efficient simulator development, faster and more accurate simulation and optimization, and more efficient measurement for verifying the effectiveness of measures and understanding behavior. In this paper, as an approach to solving these issues, I have developed a number of simulation and optimization methods, such as open source simulators, building information modeling, simulation approximation and multi-fidelity optimization using fast simulators and proxy models, as shown in Figure 7.10. Simulation and optimization acceleration techniques such as fast simulators, building information modeling, simulation approximation by fast simulators and surrogate models, multi-fidelity optimization, prediction using real-time data by data assimilation, multi-objective optimization, open data, and virtual reality. Each approach is described.

Open source simulator

While simulators can represent realistic phenomena with high accuracy, they are expensive to develop. In recent years, commercial simulators and open-source simulators have been developed, and by using these simulators, the cost of developing a simulator from scratch can be avoided.

Commercial simulators include SimTread [175] by A&A, Viswalk [176] by PTV, LEGION [177] by Bentley, and buildingEXODUS [178] developed by the Fire Safety Engineering Group at the University of Greenwich. CrowdWalk[1] [**?**] is an open-source

[1]https://github.com/crest-cassia/CrowdWalk

crowd simulator. Other open-source crowd simulators include the traffic simulators SUMO[2] [81] and MATSim[3], or the general-purpose multi-agent simulator, NetLogo[4], for crowd simulation. Open source simulators are available on GitHub and new features can be added. It is expected that the diversification of functions will increase the number of users, who will then add more functions to the simulator, creating a virtuous cycle.

Building Information Modeling

Open-source simulators make it easy to run simulations, but the maps needed to run the simulations must be created by the users themselves, depending on the scenario they are targeting. In recent years, Building Information Modeling (BIM) has become a popular process for managing information about facilities, in which the corridors, walls, etc. that make up a facility are defined as objects, and attribute information such as shape, material, and assembly process is assigned to them. Since the model of the facility is converted into 3D data, the map data of the facility can be easily imported into the simulator. This allows an efficient cycle of building the simulator from the map, optimizing the spatial design using simulation, modifying the map, and inputting the data into the simulator again, as shown in Figure 7.11. The commercial simulator LEGION has the ability to build a simulator from BIM data [179]. If similar functions can be realized in open source simulators in the future, I can expect accelerated research in spatial design and crowd control. In addition, point cloud data obtained by LiDAR is increasingly being used to construct BIM data [180].

[2]https://github.com/eclipse/sumo
[3]https://github.com/matsim-org
[4]https://github.com/NetLogo/NetLogo

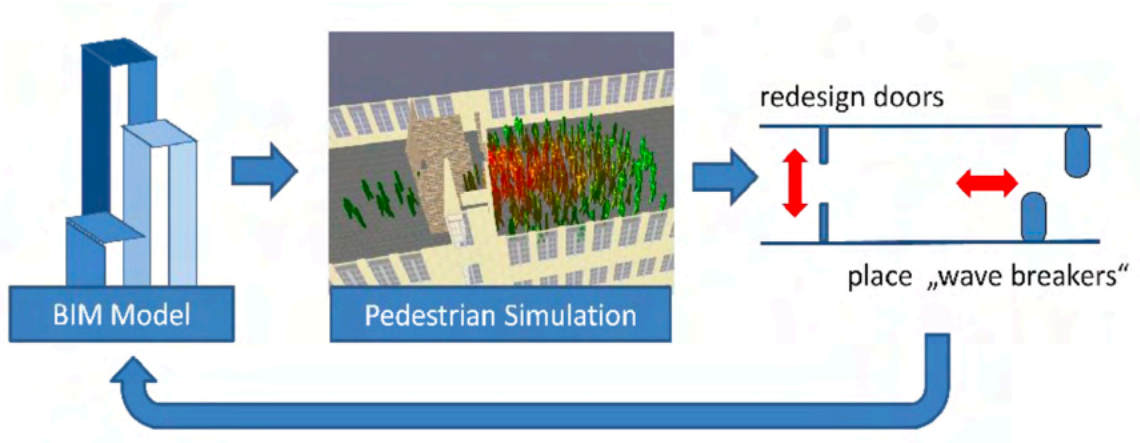

Figure 7.11: Simulation using BIM cited by[8]

Processing of point cloud data, such as that measured by LiDAR, is also developing in the field of artificial intelligence, and the automation of LiDAR measurement of facility spaces, processing of point cloud data, and creation of BIM data will be important research topics in the future to promote efficiency in simulator development.

Accelerated simulation and optimization techniques

Many of the studies presented in this paper use multi-agent simulation, in which each pedestrian is considered as an agent. However, the computational time of multi-agent simulation increases as the number of agents increases, making it impractical for large-scale experiments involving tens of thousands of people or for optimization problems that require repetitive calculations due to its high computational cost. Therefore, it is necessary to consider methods to speed up simulation and reduce the computational cost of optimization. Research to speed up simulation has proposed a one-dimensional pedestrian model with simplified computation and a method to approximate the output of simulation with a surrogate model or machine learning [181, **?**]. On the other hand, methods to reduce the computational cost of optimiza-

tion have rarely been studied in the field of crowding, and research is being conducted in the field of structural optimization, such as windmill and automobile design. For example, multi-fidelity optimization, which combines simulations of multiple accuracy levels, is used in the optimization of the shape design of windmill blades [182]. The fidelity is the fidelity of a simulation or model. Simulations with high fidelity are more accurate and computationally expensive because they closely reproduce the real world, such as 3D models. multi-fidelity optimization reduces the number of runs of high-fidelity simulations by performing global search in low-fidelity simulations, thereby successfully reducing the computational cost.

In the future, I believe that structural optimization techniques can be applied to the field of crowding, where speeding up simulation and optimization is a challenge.

Prediction using data assimilation

Accurate prediction of swarm migration requires real-world observations and precise swarm simulations. In reality, however, only partial observation data are available, and crowd simulations are computationally demanding, making real-time prediction difficult. Therefore, data assimilation, which combines partial observation data and numerical simulation to predict large-scale phenomena, is attracting attention as a means of crowd forecasting.

Data assimilation is a technique that has been used to predict natural phenomena such as weather and oceanographic information. Because it is difficult to obtain observation data of natural phenomena for the entire real world, partial observation data are fed to simulations for forecasting. Although conventional observational data for communities are not as large as those for natural phenomena, they are now being used for communities as well, thanks to improvements in measurement equipment

and computational performance. Shigenaka et al. have successfully reproduced event crowds with high accuracy by assimilating measured data from crowd simulations to observed data from cameras and GPS [183].

The prediction method is based on the assumption that the uncertainty increases as the period of time increases. The longer the time period, the greater the uncertainty of the forecasting method. This is due to the nature of the forecast target, the lack of observational data, and the fineness of the simulation. While observational data and simulation performance can be improved to some extent with the development of technology, the nature of the forecast target requires improvement in the method itself. In the meteorological field, ensemble forecasting methods that take into account uncertainties have been developed in recent years, and the errors estimated from forecasts can be used to support long-term forecasts. If ensemble forecasting methods can be developed in the field of crowding, long-term forecasts can be expected.

Multi-objective Optimization

In this paper, efficiency and safety are the two indicators used to evaluate herd movement. The weight given to either indicator varies depending on the magnitude of risk, but both are important indicators. Since there is a trade-off relationship between the two indicators, it is important to visualize the trade-off by using multi-objective optimization, which optimizes multiple indicators simultaneously, to determine spatial design and crowd control.

Current studies of multi-objective optimization for crowding are limited to a couple of objective functions, with the efficiency and safety of crowding as the objective functions for optimization. However, to apply crowd control in the real world as something acceptable to all pedestrians, it is necessary to consider the perspective

of the pedestrian in addition to the event manager. If I extend the perspective to each individual pedestrian and consider that each has a different objective function, the number of objective functions will ultimately number in the hundreds or tens of thousands. This is a very challenging task compared to existing multi-objective optimization.

It has already been pointed out in the field of multi-objective optimization that convergence to a Pareto solution becomes more difficult as the number of objective functions increases, and that it becomes more difficult to approximate and visualize high-dimensional trade-off surfaces. The most direct way to solve this problem is to increase the number of simulation trials, and speeding up the simulation process is an important issue. Approaches to solving this problem are described above. Another approach is to reduce the number of objective functions; a method called objective reduction has been proposed to handle correlated objective functions together, and I believe it can be applied to swarm optimization problems. Future research should focus on problem formulation and multi-objective optimization algorithms that take into account a greater variety of objective functions.

Open data

Real-world data on crowd movement is necessary to improve the accuracy of simulations and to verify the effectiveness of measures that assume real-world conditions. However, the cost of measuring crowd movement and the small number of situations in which crowd movement occurs make it difficult to collect such data. Therefore, it is important to openly collect data on crowd movement and to promote more active research on modeling and simulation of pedestrian behavior. Currently, some crowd trajectory data are open. For example, trajectory datasets have been organized in a

survey paper on trajectory prediction [184].

However, most of the crowd movement data that are currently open are for movements that do not change the path or exit point of movement. Therefore, these data can be used for modeling and simulation at the Operational level, but not at the Tactical or Strategic level. For the Tactical level, data measuring pedestrian path selection in a crowd environment are openly available [61, 185].

On the other hand, at the strategic level, for example, the dataset of evacuation from a movie theater is used to model the choice of evacuation start time in the document [186], but it has not been made public. In the future, more advanced behavioral-level data should be made publicly available, which would further promote the study. On the other hand, it is necessary to consider the issue of privacy.

Virtual reality

Although spatial design and crowd control have been evaluated using simulations, it is still necessary to verify the effectiveness of these methods on actual crowds and pedestrians. However, the cost of gathering people makes it difficult to test on real crowds. In addition, data on crowd movement is needed to enhance the model. One possible solution is to conduct experiments using virtual reality. Recently, virtual reality has been applied to verify the effectiveness of guidance using signs and tactile devices, and to collect data on exit selection during evacuation [187, 131, 9].

Virtual reality spaces are often created in Unity 3D [188, 189, 9, 190]. In the future, the development of simulators, the representation of virtual reality spaces using Unity 3D, and the creation of a flow of subject experiments using virtual reality spaces will lead to more efficient evaluation of space design and crowd control, as well as data collection on crowd movement.

Figure 7.12: Collection of route choice behavior data using VR environment cited by [9]

7.6 Conclusion

Designing a space where crowds can move easily and intervening with them to control their movement are necessary to move them safely and efficiently, but these methods are not well organized at present. Therefore, this paper summarizes previous studies on spatial design and crowd control. First, the evaluation indices of crowd movement are summarized from the viewpoints of safety and efficiency. Then, the current findings on spatial design are summarized, and crowd control methods are categorized and explained at the level of pedestrian behavior. The problems of the previous studies are summarized, and the approaches to solve them are presented.

Table 7.1: Evaluation indices of crowd movement

Evaluation Indices			Papers
Efficiency	Travel time	Max travel time	[121, 122, 123, 124, 125] [65, 126, 3, 127]
		Total/average travel time	[128, 129, 130, 131, 132] [6, 120, 133, 134]
		Distribution of the number of pedestrians remained	[135, 122, 136, 137, 7, 1] [3, 138, 64, 139, 140]
	Travel distance	Total/average travel distance	[131, 141, 142]
	Velocity/Flow	Velocity	[129, 143, 137, 144, 145]
		Flow	[129, 145]
Safety	Congestion degree	Density	[129, 120, 5, 3, 145]
		Overlap degree	[7]
	Other	Change of direction	[146]
		Disaster risk	[130, 65]
		Number of infected people	[147]

Table 7.2: Level of Service (LOS)

	Density [peds/m^2]		
	Walkway	Stairs	Queue
A	<0.31	<0.54	<0.83
B	0.31 - 0.43	0.54 - 0.72	0.83 - 1.08
C	0.43 - 0.72	0.72 - 1.08	1.08 - 1.54
D	0.72 - 1.08	1.08 - 1.54	1.54 - 3.59
E	1.08 - 2.17	1.54 - 2.69	3.59 - 5.38
F	>2.17	>2.69	>5.38

Table 7.3: Classification of crowd movement space design

Design object		Papers
Layout	Location of exits	[4, 124, 125]
	Location of ticket gates	[143, 5]
Capacity	Width of routes	[132, 1, 126]
	Direction of turnstiles and escalators	[120, 136]
	Width of exits	[123]

Table 7.4: Classification of pedestrian behavior level

Behavior level	Definition
Strategic Level	Decision-making before starting a travel, selecting the time to start moving or the activity.
Tactical Level	After the selection at the strategic level, select the route and the exit (door) to go through.
Operational Level	Walking while avoiding others and obstacles on the route selected at Tactical level

Table 7.5: Classification of crowd control

Control objects			Papers
Strategic Level	Rule	Pre-movement time	[128, 6, **?**]
Tactical Level	Rule	Route	[130, 153, 154, 148, 65] [155, 156, 138]
	Information	Signage	[131, 133]
		App	[157]
	Guidance	Guides	[158]
		Navigator	[159, 160, 139, 110]
Operational Level	Rule	Walking velocity	[120, 140]
		Distance between pedestrians	[147]
	Physical control	Guardrails	[146, 3]
	Nudge	Music	[145]
		Obstacles	[129, 121, 161, 162, 7, 163]

Chapter 8

Multi-objective Deep Reinforcement Learning for Crowd Movement

8.1 Introduction

Overcrowding is particularly likely to occur during evacuation from a disaster or a large-scale event when many people move simultaneously in the same place, which can cause crowd stamping and lead to serious accidents that cause hundreds of casualties. These accidents have been reported in several areas of the world [191, 106]. Therefore, evacuation policymakers and event managers must safely guide crowds. However, each pedestrian in a crowd wants to move quickly. Because movement safety and efficiency are often in conflict in crowd movement, both indicators must be considered when determining crowd guidance.

The guidance of the crowd to appropriate routes is effective in preventing crowd

accidents and improving movement efficiency by dispersing the crowd flow and reducing congestion. Most studies use pathfinding algorithms to find the shortest path or safest path [192, 166, 156, 193]. Additionally, the information presented by the signs can guide the crowd to the appropriate route. Therefore, some studies have optimized the position and angle of the sign to adjust its visibility and maximize the effectiveness of the information [133, 131, 194].

Multi-objective optimization and dynamic response are the current research issues in crowd route guidance. First, most studies have focused only on movement efficiency. Besides, not only movement efficiency (short travel time and distance) but also safety (less congestion) is an important indicator. If one focuses only on efficiency, safety may be compromised. Both efficiency and safety must be considered simultaneously to develop an effective crowd guidance strategy. Second, based on awareness of the problem, some studies on crowd route optimization using multi-objective optimization to optimize multiple indicators simultaneously have been conducted [195, 142, 141, 196, 134]. However, most studies have assumed a static environment. During evacuations and events, the number of pedestrians in the crowd tends to be unknown in advance, and the state of the crowd changes from moment to moment. Therefore, optimized guidance assuming static conditions may not be effective. Thus, establishing guidance strategies that can adapt to dynamic state changes is imperative. In other words, sequential decision-making is required according to the situation.

Reinforcement learning (RL) can solve the current research issues in crowd route guidance optimization. RL is an approach used to solve sequential decision-making problems. RL learns a function (strategy or policy) that maps the optimal action for a

state. Recent advances in RL have helped solve problems in robot control and games such as Atari and Go [197]. Multi-objective reinforcement learning (MORL) is also being studied to address real-world problems with multiple and possibly contradictory objectives. [198]. In recent years, research on multi-objective deep RL (MODRL), which uses deep learning to address problems with high dimensionality and complex state spaces, has been progressing.

The optimal action for a state can be learned by RL, thus dynamically enabling the decision of a guidance route according to the crowd state. Moreover, MORL can be used to learn multiple strategies that consider multiple indicators (e.g., travel time, travel distance, and congestion degree). Furthermore, MODRL can accommodate complex state changes in crowd movements using deep learning. RL involves repeated trial-and-error learning in a computer simulation environment. Crowd movement is represented by multi-agent simulations that treat pedestrians as agents and have them interact with each other.

In this chapter, I attempt to apply MODRL to a multi-objective dynamic crowd route guidance problem. I consider the application of Pareto-DQN (PDQN) [199] among MODRL. PDQN can learn multiple Pareto strategies during the learning process. PDQN has undergone testing for how well it performs in-game problems, but its effectiveness in complex real-world problems has not been fully established. To apply PDQN to real problems, it is necessary to adjust a parameter of PDQN and to improve action selection criteria. The parameter affects the approximation of the Pareto solution. Additionally, action selection criteria that determine which actions are chosen during the learning process also affect which solutions PDQN can acquire. If the selection of actions during learning is biased, a variety of solutions

may not be acquired. Therefore, I experimentally show the difference in performance by parameters and introduce new action selection criteria.

I construct an environment in which crowd guidance can be learned by RL using a multi-agent crowd simulator. Then, I evaluate the improved version of PDQN on the toy problem, which is commonly used to evaluate MODRL, and the crowd guidance problem. The experimental results show that the performance varies greatly depending on the parameter of the PDQN and that Pareto strategies can be obtained for real problems by adjusting the parameter. I also clarify the advantages and disadvantages of several action selection criteria, including the introduced action selection criterion.

My contributions are summarized as follows:

1. I propose to adjust the parameter of PDQN and improve the action selection criteria during learning.

2. I create an environment where RL can be performed on a multi-agent crowd simulation.

3. I demonstrate that the improved PDQN can search for good strategies compared to the original PDQN and can obtain better strategies than simplified strategies on the crowd route guidance optimization problem.

The remainder of this chapter is organized as follows. Section 8.2 reviews related work on crowd guidance optimization and MODRL. Section 8.3 introduces the PDQN and preliminaries. Section 8.4 describes the improved version of PDQN, and Section 8.5 describes experiments on a toy problem, Section 8.6 describes experiments on the crowd route guidance problem, and finally Section 8.7 summarizes this study with future work.

8.2 Crowd Guidance Optimization

The state of the crowd and the environment changes from moment to moment during evacuations and events, and guidance assuming static conditions may not be effective. Therefore, it is important to establish a guidance strategy to adapt to dynamic environmental changes. In addition, trade-offs exist between efficiency and safety indicators of crowd movement, such as travel time, travel distance, and congestion degree, which need to be optimized simultaneously using multi-objective optimization methods.

Huang et al. dynamically optimized the position of the guidance information sign and the direction of the guidance route using genetic algorithm (GA) [194]. The goal is to minimize the flow rate and high congestion time on the route. However, because these indices are added together to form a single objective function, it is not a multi-objective optimization. GA is one method of evolutionary computation (EC). The EC algorithms are a kind of promising global optimization tool that has not only been widely applied for solving traditional optimization problems but also have emerged in booming research for solving complex optimization problems in recent years [200]. One of the complex optimization problems is the multi-objective optimization problem, and evolutionary multi-objective optimization (EMO), a multi-objective version of EC, has been studied as a solution method for this problem. For example, a more convergent EMO algorithm has been proposed [201], or various EMO algorithms for real-world problems, such as Job-Shop Scheduling [202], supply chain management [203], and a vehicle routing problem under Covid-19 situations [204], are being proposed.

EMO continues to be extended for various real-world problems, and several studies

have focused on crowd control [195, 142, 141, 205, 134]. Hu et al. have applied multi-objective Cartesian genetic programming, one of EMO algorithms, to dynamic and multi-objective optimization on a crowd control problem [120]. They used Cartesian genetic programming (CGP) to optimize a function that outputs an optimal control rule for movement speed using the current crowd density as an input. In addition, they used a multi-objective CGP to minimize the two objectives of travel time and high-congestion time. The results showed that both indices could be improved compared to no control or rule-based control. Although EMO has been applied to crowd management optimization, there are no studies dealing with the long-term effects of crowd control. For example, the effect of an optimized guidance strategy for the current state on the crowd movement one hour later is not considered.

RL is suitable because it enables a dynamic response by finding a function that outputs an optimal guidance strategy based on the current state at the current time. Furthermore, the guidance strategies learned using RL can also consider the future impact of the current guidance (action). Shimizu et al. used Advantaged Actor-critic, a deep RL (DRL) method, for the problem of deciding which routes to close to alleviate congestion when crowds move from multiple stations to a stadium [206]. Xue et al. also proposed a method for learning dynamic guidance based on Deep Q-Network (DQN), an RL method that uses neural networks [207]. They proposed a combined action-space DQN, in which the output layer nodes of a network are grouped according to the action dimension, and applied the method to the crowd guidance problem. However, in these studies, the objective function (reward) was only the travel time, and safety was not considered. To the best of our knowledge, no study has applied MORL or MODRL to crowd guidance problems.

8.3 Multi-objective Deep Reinforcement Learning

Decision-making problems that maximize long-term cumulative rewards have been studied in the fields of control theory and machine learning. Classically, optimal solutions are computed using dynamic programming (DP) such as value iteration (VI) and policy iteration (PI). However, these methods assume the known dynamics of the system. Because this is not a realistic assumption, various model-free methods have been proposed that can be applied even when the system dynamics are unknown. For example, Yang et al. extend λ-PI, which combines VI and PI, to a model-free method [208]. This extended method for finding optimal control strategies under the unknown dynamics of the system is called adaptive dynamic programming (ADP). Other extensions of ADP have been proposed for convergent and stable learning of nonlinear systems. For example, Yang et. al. considered the approximation error of the system [209] or relaxed the condition for convergence by efficiently collecting data using experience reply [210]. These methods are model-free, guarantee convergence, and account for system approximation errors, but they do not mention the applicability to complex systems such as crowd movement. If the system is very complex, DRL, which is an approach to approximate the dynamics of the system with a neural network while collecting data during the learning process, would be more practical. In addition, these control theory-oriented methods are not yet fully extended to multi-objective optimization. From this point of view, MODRL is suitable for solving real-world sequential decision-making problems.

In general, MODRLs are classified as single- and multi-policy methods [211]. The single-policy method is effective when the decision-maker's preferences are known and do not change. The scalarization function transforms multiple objective functions

into a single objective, and the optimal policy is obtained using a single-objective RL method based on the weight vector that represents the decision-maker's preferences. However, when the decision-maker's preferences are unknown or changeable, the multi-policy method, which aims to learn Pareto-front of policies, is suitable. In complex real-world problems, it is desirable to present multiple strategies to decision-makers, to help them decide on a good strategy. Therefore, in this study, I focus on a multi-policy method.

The multi-policy method is divided into outer- and inner-loop methods. The outer-loop method calculates multiple policies by repeatedly generating weight vectors and performing single-objective optimization. In contrast, the inner-loop method is designed to learn several policies at once. One of the outer-loop methods is deep optimistic linear support learning (DOL), proposed by Mossalam et al. [212]. This method combines the generation of weight vectors using optimistic linear support (OLS) with single-objective optimization using DQN. OLS is a weight determination method that efficiently determines Pareto front [213]. Mossalam et al. showed that the reuse of neural network parameters reduces the computational cost of single-objective optimization. However, because DOL repeatedly generates weight vectors and performs single-objective optimization, the overall computation time increases in proportion to the number of times the weights are updated if single-objective optimization is time-consuming. Another drawback of DOL is that it assumes a linear scalarization function; hence, it cannot solve for non-convex regions in Pareto-front.

Chen et al. proposed a method combining a multi-policy soft actor-critic (MP-SAC) and multi-objective CMA-ES (MO-CMA-ES) [214] to avoid iteratively computing scalarized single-objective optimizations. This method consists of two steps.

First, multiple weight vectors are generated, and a linear scalarized single-objective optimization problem is solved in parallel with each weight vector. For the parallel part, MP-SAC, an extension of soft actor-critic is used to parallel computation. Next, the optimal solution for each weight vector is further updated using MO-CMA-ES. The parallel computation reduces the computation time. It is also reported that even if linear scalarization is used, non-convex solutions can be searched for by updating with MO-CMA-ES in the second step. However, prior knowledge of the problem is required to prepare an appropriate set of weight vectors because this method requires the generation of multiple weight vectors in advance. If appropriate weight vectors cannot be set, they must be exhaustively generated. Exhaustive computation is time-consuming, even if parallel processing is possible because optimization is performed for each weight.

In existing outer-loop methods, the overall computation time increases in proportion to the number of times the weights are updated if single-objective optimization takes time. Therefore, I focus on the inner-loop methods. Pareto-Q is a typical inner-loop method that extends the Q-learning framework to multi-objective problems [215]. Furthermore, PDQN, a method that introduces neural networks, has been proposed to apply the Pareto-Q framework to high-dimensional and complex problems [199]. PDQN can acquire the Pareto front through learning without defining the weight vectors. Therefore, in this study, I consider the application of PDQN to the crowd route guidance problem.

8.4 Preliminaries

Before describing PDQN, I first describe the general RL formulation, Q-learning and DQN. Pareto-Q, the predecessor of PDQN, is then explained, and PDQN is described.

8.4.1 Reinforcement Learning

RL learns strategies through interaction with the environment. The environment is modeled as a Markov decision process. Let $S = \{s_1, \cdots, s_N\}$ be the state space and $A = \{a_1, \cdots, a_M\}$ be the action space. An action a is performed in state s, and according to the state transition probability $T(s'|s, a)$, it transits to the next state s' and receives an immediate reward $R(s, a)$. The goal of reinforcement learning is to find a strategy (policy) $\pi(a|s)$ that maximizes the cumulative sum of the rewards. The expected value of the sum of discounted rewards when an action a is taken in state s is called the Q-value and is denoted by $Q(s, a)$. The action is taken according to policy π,

8.4.2 Q-learning and DQN

Q-learning is a method of learning to take action with the highest Q-value among the possible actions in each state. The Q-value is estimated by repeating the action and is updated using Eq. (8.1)

$$\begin{aligned} Q(s,a) &\leftarrow Q(s,a) \\ &+ \alpha(R(s,a) + \gamma \max_{a' \in A} Q(s',a') - Q(s,a)) \end{aligned} \tag{8.1}$$

, where $\alpha \in [0, 1]$ denotes the learning rate. In addtion, $\gamma \in [0, 1]$ is the discount rate used to discount future rewards. The ε-greedy policy is often used during learning. Actions are selected randomly with a probability of ε and with a probability of $1 - \varepsilon$ to maximize the Q-value. Approximating the Q-value is equivalent to obtaining the optimal policy because the Q-value is the criterion for action selection.

DQN approximates the Q-values with a neural network. In DQN, transitions $\{s, a, r, s'\}$ $(r = R(s, a))$ obtained from interactions with the environment are aggregated in Replay buffer D, and during training, the transition information is randomly sampled to create mini-batches. This is called experience replay. The experienced data stored in Reply buffer is used to learn the parameters θ of the Q-network. The loss function is expressed by Eq (8.2).

$$L(\theta) = \mathbb{E}_{\{s,a,r,s'\}\sim D}[(r + \gamma \max_{a' \in A} Q(s', a'; \theta^-) - Q(s, a; \theta))^2] \tag{8.2}$$

,

where θ^- is the parameter of the Target Network, which has the same structure as the Q-network but with the parameter of a few steps earlier.

8.4.3 Pareto-Q

Pareto-Q extends the Q-learning framework to multi-objective problems. In MORL, the immediate rewards are multi-dimensional. In addition, the cumulative sum of the final rewards may not be superior or inferior. Therefore, there are multiple optimal policies, in other words, there are multiple Q values to be estimated. Thus, the Q-learning framework cannot be simply applied.

The Q-values obtained afterward vary depending on the policy. Therefore, in Pareto-Q, the set of Q-values is expressed by the following equation:

$$Q_{set}(s,a) = \bar{R}(s,a) + \gamma ND_t(s,a) \tag{8.3}$$

, where $\bar{R}$ represents the average immediate reward, which is updated by the following equation:

$$\bar{R}(s,a) = \bar{R}(s,a) + \frac{R(s,a) - \bar{R}(s,a)}{n(s,a)} \tag{8.4}$$

, where $n(s,a)$ is the number of times that action a is selected in state s. In addition, ND_t is the set of non-dominated solutions for the Q-value of the next state, represented by the following equation:

$$ND_t(s,a) = ND(\cup_{a' \in A} Q_{set}(s',a')) \tag{8.5}$$

, where ND denotes the operation for removing dominated solutions.

Pareto-Q uses Hypervolume as an indicator to evaluate the entire set of Q-values as a criterion for action selection, while the Q-learning strategy selects the action with the largest Q-value, as shown in Figure 8.1. Hypervolume represents the area or volume of the region in the objective function space that is dominated by the solution set.

8.4.4 Pareto-DQN

PDQN introduces neural networks to apply the Pareto-Q framework to high-dimensional and complex problems. The immediate reward $\bar{R}$ and the set of non-dominated solutions ND_t of the Q-values of the next state are approximated by a

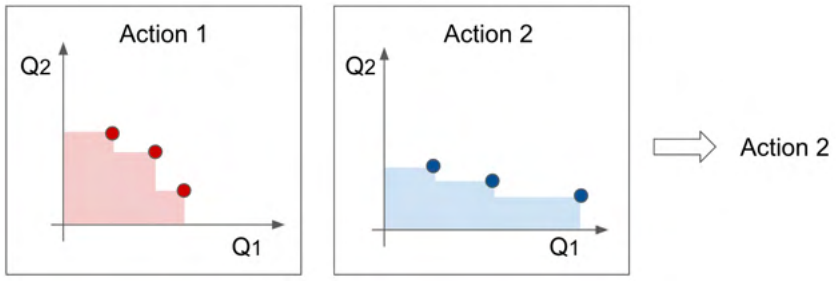

Figure 8.1: Hypervolume-based action selection

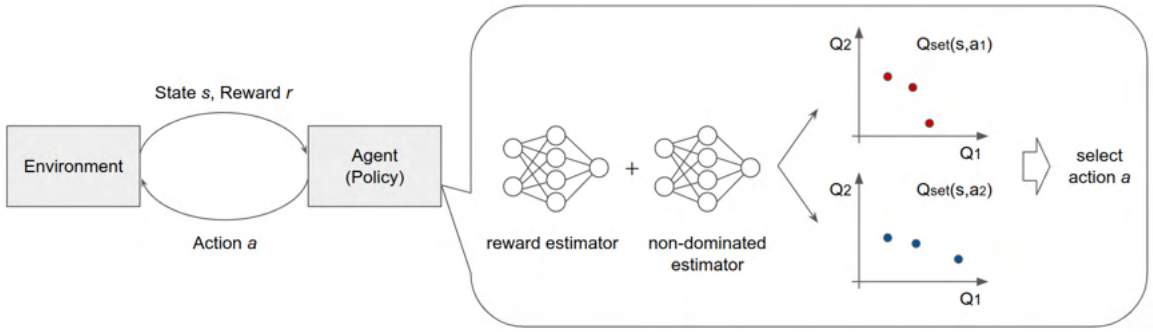

Figure 8.2: Agent-environment interactions in Pareto-DQN

neural network, respectively. The former is called a reward estimator, and the latter is a non-dominated estimator. A graphical overview and an outline of PDQN are given in Figure 8.2 and Algorithm 1.

For the reward estimator, the inputs are states and actions, and the outputs are rewards. If the number of objective functions is d, the reward is a d-dimensional vector. However, if the non-dominated estimator also assumes that the input is the state and action and the output is the non-dominated solution set, a problem arises in which the dimension of the output cannot be fixed. This is because the number of Pareto solution sets for a Q-value depends on state and action.

Therefore, in addition to the state and action, $d-1$-dimensional Q values are

used as an input. Subsequently, the dth Q-value is output. This fixes the number of output dimensions of the network. When selecting actions, the $d-1$-dimensional values are sampled in the $d-1$-dimensional objective function space, the dth value is output using a non-dominated estimator, and these are concatenated to form the d-dimensional value. The average immediate reward $\bar{R}$ output by the reward estimator is added to these values to compute $Q_{set}(s,a)$ (Eq. (3)). Sampling in $d-1$ dimension is performed p times so that the sample points are evenly distributed in the solution space, and the Q-value is computed at each sampling point to obtain $Q_{set}(s,a)$. In this way, $Q_{set}(s,a)$ for each action is estimated and, as in Pareto-Q, the action with the largest Hypervolume is selected. I refer to PDQN with Hypervolume-based action selection as HV-PDQN.

Once the Pareto front is known, the user selects the preferred policy and expects to reach the solution obtained by that policy. To do this, a tracking policy method is used in the evaluation phase in Pareto-Q and PDQN. First, Pareto Q-values for each action are estimated initially, and non-dominated solutions are extracted. Subsequently, the target solution is selected. The action that contains the Q-value closest to the target solution is selected. Subtract the immediate reward earned from the target value and set a new target value. Subsequently, it transitions to the next state and selects an action that contains a Q-value close to the new target. The desired solution is obtained by repeating this process.

8.5 Improvements of Pareto-DQN

PDQN can learn multiple Pareto strategies during the learning process. PDQN has undergone testing for how well it performs in-game problems, but its effectiveness

in complex real-world problems has not been fully established. To apply PDQN to real problems, I propose to adjust the number of sample points p and improve action selection criteria. This chapter describes our hypotheses for the number of samples and the new action selection criteria.

The number of samples corresponds to the number of Q-values when estimating Q_{set} using the neural networks. Therefore, a small number of samples is considered to be a poor approximation of the true Pareto solution. The number of true Pareto solutions in real problems is unknown, so it is difficult to set the appropriate number. Because the difference in the reward obtained in one step is the difference in the Pareto solution, I require sufficient samples to represent the difference. I assume that the number of samples should be set so that the sample interval is smaller than the reward value obtained in one step.

Next, I mention the action selection criteria. The strategies that can be acquired by PDQN rely on the action selection criteria that determine which actions are chosen during the learning process. Therefore, I focus on the action selection criteria and introduce new action selection criterion to obtain a variety of strategies (policies). Presenting a variety of strategies can assist decision-makers to balance the multiple conflicting objectives (safety and efficiency in the case of crowd movement). HV-PDQN may be biased in selecting actions during learning and may not find diverse solutions. First, the problems with HV-PDQN are explained, and the other action selection methods are described.

Hypervolume is the area of the solution set in the multi-objective space with respect to the reference point. Therefore, solutions farther away from the reference point have a greater impact on the Hypervolume. However, each solution is equally

important in multi-objective optimization problems, and it is problematic if distant solutions have a large impact on the goodness of the solution set. This also depends on the setting of the reference points [216]. Therefore, HV-PDQN is more likely to select actions involving distant solutions. This will result in the selection of only similar actions and may not find diverse solutions. In addition, the value of Hypervolume changes depending on the reference point setting; therefore, tuning the reference point is necessary to obtain a good strategy.

In this study, I introduce two selection criteria: Cardinality (CA) and Pareto-relation (PO). Both criteria were used as action selection criteria in the case of Pareto-Q [215]. First, as in Algorithm 2, $Q_{set}(s, a)$ is calculated for each action a, from which dominated solutions are omitted to form the set of non-dominated solutions $NDQs$. The number of solutions for each action in $NDQs$ is calculated, and the action that contains the most solutions is selected, as shown in Figure 8.3. PDQN with this action selection criterion is called CA-PDQN. I also consider a method that omits completely dominated actions that do not contain any solutions in $NDQs$ and randomly select from the other actions. PDQN with this action selection criterion is called PO-PDQN. In the case of PO-PDQN, replace line 9 of Algorithm 2 with line 10. The CA-PDQN and PO-PDQN are thought to be able to select diverse actions better than HV because they select actions that contain many non-dominated solutions.

8.6 Experiment: Deep Sea Treasure

In the experiments, I evaluate the improved version of PDQN on the toy problem, which is commonly used to evaluate MODRL, and the crowd guidance problem. I select the deep sea treasure (DST) [10] as the toy problem. The DST is a benchmark

problem for MORL. This section describes the DST settings and results.

8.6.1 Settings

A ship searches for treasure in the environment, as shown in Figure 8.4(a). The numbers in the cells represent the treasure value. There are two objective functions in this problem. The first is the treasure value. The second is the number of steps to obtain a treasure. A trade-off exists between these two objectives. The number of steps should be higher to increase the treasure value, while the treasure value should be lower to decrease the number of steps. The rewards are treasure and steps. Note that the step number is multiplied by -1 to maximize both objective functions. True Pareto front is shown in Figure 8.4(b).

The state corresponds to the cell in which the ship is located. Because, there are $11 \times 10 = 110$ cells, the state is represented by 110-dimensional one-hot vectors. The actions are the top, left, bottom, and right; therefore, the action is represented by 4-dimensional one-hot vectors. The reward estimator has the state and action as inputs and a 2-dimensional reward as output. The non-dominated estimator has the state, action, and a Q-value for the first objective, treasure, as inputs and a Q-value for the step number as output. The reward and Q-values are normalized by $[0, 124]$ in the first objective (treasure) and $[0, 19]$ in the second objective (steps). The network structure is the same as that used in [199]. Alike [199], Adam is used to optimize the two networks, and the learning rates are set to 10^{-3} and 10^{-4}, respectively. Additionally, $\gamma = 1$. The decay rate of ε is set as 0.999. I set the number of samples to 10 because the number of true Pareto solutions is 10. The training is performed for 10000 episodes.

In this experiment, I verify whether CA-PDQN and PO-PDQN can obtain more diverse solutions than HV-PDQN. In addition, I verify whether the performance of HV-PDQN differs depending on the reference point setting. Therefore, I also test different reference points for HV-PDQN; $(-1, -2)$ and $(-2, -2)$. Hypervolume and inverted generational distance (IGD) [217] are used to evaluate the goodness of the acquired Pareto policies. IGD is used to assess the quality of approximations to the Pareto front. Note that for each solution of the Pareto front estimated by the learned network, I evaluate the obtained solution using the policy-tracking method described in Section 3.

8.6.2 Results

First, I describe the differences in the acquired Pareto solutions using the three action selection criteria. Table 8.1 lists the values of Hypervolume and IGD. According to these metrics, Pareto front approximations with higher Hypervolume or lower IGD are better. The results show that CA-PDQN and PO-PDQN are able to acquire more diverse solutions than HV-PDQN. Figure 8.5 shows the Pareto solution obtained using the learned policies. For example, HV-PDQN does not obtain a solution (24, -13), whereas CA-PDQN and PO-PDQN do. The deepest solution (124,-19) is not obtained using any of the action selection criteria. This is assumed to be the case because few such solutions are acquired during the learning process, and not many are included in the neural network training data. Presenting a variety of strategies can assist decision-makers to balance multiple conflicting objectives. From this point of view, CA- and PO-PDQN are more useful than HV-PDQN. The results are consistent with the original PDQN paper [215], which also reported that Pareto-Q with CA or PO

Table 8.1: Performance comparison of PDQN for each action selection criterion on the DST environment

	Hypervolume (↑)	IGD (↓)
HV-PDQN	2.713	0.079
CA-PDQN	2.717	0.047
PO-PDQN	2.717	0.052
True	3.122	0.0

achieved larger Hypervolume than with HV in DST problems.

Second, I discuss the difference in performance depending on the reference-point setting in HV-PDQN. In the DST problem, the value of the optimal cumulative reward is in the range [0,1] for Treasure and [-1,0] for the number of steps because of normalization. The original reference point is set as (-1,-2). Here, I consider the case in which the reference point is (-2,-2). The positions of the reference points and the solution space are shown in Figure 8.6(a). Hypervolume is the area of the solution set with respect to the reference point, indicating the goodness of the solution set. When the reference point is set to (-2,-2), the values in the horizontal axis direction, that is, the treasure values, are more likely to affect the Hypervolume than when the reference point is set to (-1,-2).

Figure 8.6(b) and (c) show the acquired Pareto solutions of HV-PDQN when the reference points are (-1,-2) and (-2,-2), respectively. A larger treasure solution (specifically (24,-13)) is obtained when the reference point is (-2,-2) compared to the case where the reference point is (-1,-2). However, a smaller treasure solution is no

longer obtained. Thus, even with HV-PDQN, it is possible to increase the variety of solutions by adjusting the reference points. However, this is only possible if the range of possible optimal policies is known in advance. It is difficult to adjust the reference points when dealing with real-world problems because the knowledge of the solution range acquired by optimal policies tends to be unknown. From this perspective, it is desirable to apply CA-PDQN and PO-PDQN, which are independent of the reference point.

8.7 Experiment: Crowd Guidance

Experiments on the toy problem showed that using CA and PO as action selection criteria for the PDQN is effective. In this section, I examine differences in the number of samples and the effectiveness of PDQN for real problems and evaluate the advantages and disadvantages of each action selection criterion. The crowd guidance problem is treated as a real problem. I first describe the crowd movement simulation, which represents the movement of a crowd using multi-agent simulation, and then discuss the experimental settings and results.

8.7.1 Crowd movement simulation

In this study, I target crowd movement in fireworks display festivals. The road network is illustrated in Figure 8.7(a). The pedestrians move from the event site to the station after the event. A train arrives at the station every ten minutes, and the train capacity is 1600 people. The route guidance information is projected onto a building at a junction, as shown in Figure 8.7(b).

I use a multi-agent pedestrian simulator called CrowdWalk [67] to reproduce crowd

movement. CrowdWalk represents the space in which pedestrians move as a network of links and nodes, and the social force model (SFM) is implemented to represent pedestrian movement on the links [218].

At a fireworks display on August 13, 2018, I set up LiDAR at the junction to measure pedestrians' movements. I detected the number of pedestrians from LiDAR point cloud data using a clustering-based tracking method [66].

An example of the measured pedestrians' trajectories using LiDAR is shown in Figure 8.8(a). Cameras were also installed at the station to count the number of pedestrians passing through, as shown in Figure 8.8(b). Using these camera data and LiDAR measurement data, the number of pedestrians at each time point who start moving from the event site was derived as shown in Figure 8.8(c). The number of pedestrians starting to move from the event site to the station peaks at approximately 8:40 p.m., when the fireworks display ends, and decreases from 10:00 p.m. when the food stalls close.

In the simulation, pedestrian agents are generated according to the number of pedestrians starting to move, as shown in Figure 8.8(c), and at the junction, the pedestrians select Route 1 or Route 2 according to the guidance. The walking behavior on the route follows SFM.

8.7.2 Settings

The problem is to learn the guidance at the junction that minimizes the travel distance and congestion degree of the crowd movement from a fireworks display site to a station. Note that I measure the crowd movement at this fireworks festival every year, and the routes in this problem setting are simplified versions of the actual routes.

The routes are divided into links at 50 [m] intervals, and the number of pedestrians on each link is defined as a state. Here, the routes can be delimited into 20 links. The action is route guidance at the junction. The interval between steps is 10 minutes. Specifically, the action determines the guided route during the next 10 minutes. I assume that I know the number of pedestrians who will start returning home in the next 10 [min]. The state is 22-dimensional, with the number of pedestrians on each of the 20 links, the number of pedestrians who will begin their return trip in the next 10 [min], and the time step. This action is two-dimensional because there are two routes.

There are two objective functions in this problem: the travel distance and congestion degree. A trade-off exists between the two objectives. The rewards are also the travel distance and the congestion degree. The travel distance is the total distance traveled by pedestrians arriving at the station at each step. The congestion degree is calculated as follows: I calculate the number of links with a density greater than 0.72 every 30 [s] within one step (10 [min]), and the sum of these numbers over 10 minutes is the congestion degree. Fruin's Level of Service, a criterion for evaluating safety based on crowd density, states that densities above 0.72 are unstable [150].

The reward estimator has the state and action as inputs and a 2-dimensional reward as output. The non-dominated estimator has the state, action, and a Q-value for the first objective, travel time, as inputs and a Q-value for the congestion degree as an output. The value of the optimal cumulative reward is normalized to the range [-1,0] for the travel time and [-1,0] for the congestion degree, and the reference point is set to (-2,-2). The non-dominated estimator structure is shown in Figure 8.9. Alike the experiment on DST, Adam is used to optimize the two networks. Additionally,

$\gamma = 1$. The decay rate of ε is set as 0.999. The training is performed for 10000 episodes.

Computing a single episode takes time when using a complex simulator such as a crowd simulator. I introduced two ideas to accelerate the learning process. The first is a learning rate schedule. The learning rate schedule is a predefined framework that adjusts the learning rate during training. It is difficult to converge if the learning rate is significantly high, and it may take time and lead to local solutions if the learning rate is significantly low. Therefore, it is considered efficient to reduce the learning rate as learning progresses. In this experiment, the learning rate is adjusted such that it starts at 1e-3 and is reduced to 1e-6 by multiplying each step by 0.9999. The start and final learning rates are set experimentally. The second is to reduce the fidelity of the simulation. There is a trade-off between simulation fidelity and computational cost. However, results that correlate with high fidelity can be output even with low-fidelity simulations. The same result has been reported for crowd simulations [219]. In our experiment, the number of pedestrians and route width are reduced by a factor of 10, resulting in an 8-fold speedup in the computation time.

In this experiment, I examine differences in the number of samples and the effectiveness of PDQN for the crowd guidance optimization problem and evaluate the advantages and disadvantages of each action selection criterion. When applied to DST, the number of samples is set to 10 in [199]. This is appropriate because the number of true Pareto solutions is 10. However, in a real-world problem, the number of true Pareto solutions is unknown. If the number of samples is too small, the distribution of Pareto solutions spread over the solution space may not be well represented. This may prevent the search from progressing. In particular, since CA is a criterion

for selecting actions based on the number of solutions, the solutions obtained by CA-PDQN may be highly dependent on the number of samples. One practical way to specify the number of samples is to consider the difference in the reward of Q1. Since the minimum reward obtained in a single step matches the minimum difference in the Pareto solution, I assume that the number of samples should be set so that the sample interval in Q1 is smaller than the reward value obtained in a single step. Therefore, I set the number of samples to 50 considering the variations in the reward for the travel distance (Q1). I also experimented with 10 samples as a lesser case and 100 samples as a greater case for comparison.

For comparison, simple guidance strategies are also verified. There are three strategies: a guide to Route 1 at all times (Route 1), a guide to Route 2 at all times (Route 2), and a strategy that switches between Route 1 and Route 2 every step (10 minutes) (Switch). I test whether PDQN can obtain superior Pareto solutions compared with simple guidance strategies and verify the applicability of PDQN for a real-world problem such as the crowd guidance optimization problem.

Experiments on DST show that CA- and PO-PDQN can obtain a greater variety of solutions than HV-PDQN, and the strategy obtained by HV-PDQN relies on the reference point. Therefore, I also verify whether the differences depending on each action selection criterion in the crowd route guidance problem are the same as those in the experiment with DST.

8.7.3 Results

I used AMD Ryzen Threadripper 3990X 64-Core Processor (2.9GHz) to conduct experiments and it took five days to run 10000 episodes. Figure 8.10 is the learning

curve of the non-domain estimator in training with 50 samples, showing convergence at 10000 episodes. It was also confirmed to converge within 10,000 episodes, whether the sample size was 10 or 100. In addition, there was no difference in computation time.

I present the results for different sample sizes. Figure 8.11 shows the distribution of the sum of rewards obtained during training when the number of samples is changed. I found that the trend of solutions obtained varies significantly depending on the number of samples. When the number of samples is smaller (10), the search proceeds to reduce the congestion degree and does not proceed in the direction of minimizing the distance. It is assumed that this is because the distribution of Pareto solutions in the solution space is not well learned. In the original proposal for Pareto-DQN [199], the action selection criterion is HV, and there is no statement regarding the number of samples, suggesting that the sample size is not sufficiently large. Therefore, in a real-world problem (in that paper, the traffic signal control problem), the Pareto front could not be learned well because it fell into local search, as shown in Figure 8.11(a). From this, it can be said that the number of samples has a significant impact on the search performance of PDQN, and it is better to set the number of samples large with considering one step reward.

When the number of samples is increased, the solutions obtained by HV-PDQN do not change significantly, but those obtained by CA-PDQN change significantly. In the case of CA-PDQN, the number of solutions for each action in NDQs is calculated, and the action that contains the most solutions is selected. Therefore, the possibility that an action (Action 2) that should be selected to search for a better solution is not selected and that another solution (Action 1) is selected increases if the number

of samples is significantly large, as shown in Figure 8.12 I assume that the search does not proceed to optimize Q2, but continues to improve Q1, resulting in the result shown in Figure 8.11(f).

Next, I discuss the Pareto solution obtained using the learned policies when the number of samples is set to 50. As shown in Figure 8.13, PDQN using any action selection criteria generally obtains better solutions than simple measures. The strategy "Route 1" guides Route 1 at the all-step, which minimizes the distance but increases the congestion degree. The strategy "Route 2" guides Route 2 at the all-step, which decreases the congestion degree but increases the distance. The strategy "Switch" changes the guided route between Route 1 and Route 2 at each step, in which the distance is not long, but does not decrease the congestion degree because it only switches guidance without considering the current state or future effects. On the other hand, PDQN can learn the optimal action (guidance) based on the current state taking future effects into account, regardless of the action selection criteria. Therefore, it can obtain a strategy that minimizes distance and congestion compared to simplified strategies. By adjusting the number of samples in this way, PDQN can be applied to realistic problems.

Figure 8.14 shows the simulated crowd movement with the "Switch" strategy and the strategy acquired by PDQN (as shown in Figure 8.13), which reduces the congestion degree and travel distance. This shows that the policy acquired by PDQN is more effective in reducing congestion.

Finally, I mention the differences depending on each action selection criterion. Table 8.2 lists the Hypervolume of the Pareto solution of the PDQN for each action selection criterion. This indicates that CA- and PO-PDQNs can acquire more Pareto

Table 8.2: Performance comparison of PDQN for each action selection criterion on the crowd route guidance problem

	Hypervolume (↑)
HV-PDQN	2.966
CA-PDQN	3.012
PO-PDQN	3.016

policies than HV-PDQNs. However, HV-PDQN has acquired policies that can reduce congestion, whereas CA- and PO-PDQN have acquired policies that can reduce travel distance, making it difficult to determine which action selection criterion is better.

HV-PDQN relies on the reference point settings as described in Section 5. CA-PDQN may fall into local search if the number of samples is significantly large. PO-PDQN has the best Hypervolume at evaluation but has worse solutions acquired during learning than HV- or CA-PDQN, as shown in Figure 8.11. PO is a criterion that randomly selects an action other than the completely dominant action at each step. Therefore, it is not possible to consistently select actions toward a specific optimal solution in all steps. Figure 8.13 shows the results of the evaluation. During the evaluation, actions are selected to aim at the Pareto front estimated by the network. Because the action is selected consistently during the evaluation, PO-PDQN can obtain good Pareto solutions similar to CA-PDQN, although PO-PDQN cannot acquire those during learning. An improvement in PO-PDQN is a method of consistent action selection from the middle of the learning process. Switching to consistent action selection (the same procedure as during evaluation) when learning has progressed to a specific degree and the Pareto solution can be estimated by the network may further

advance the search.

8.8 Conclusion

In this chapter, I proposed an improved version of PDQN and demonstrated its effectiveness in a real-world problem such as crowd route guidance strategy optimization. In previous studies, PDQN has not been successfully applied to real-world problems, and I addressed sample size and action selection criteria as reasons for this. I proposed the use of a sufficient number of samples and the introduction of a new action selection criterion and tested its effectiveness in the toy problem and the crowd guidance problem. The experimental results show that PDQN can learn better strategies than simple guidance methods for crowd guidance optimization problems by adjusting the number of samples. Additionally, I demonstrated that the search performance of HV-PDQN depends on the reference points, CA-PDQN depends on a large number of samples, and PO-PDQN is independent of these parameters. Further improvement can be expected by integrating consistent action selection into PO-PDQN.

The experiment in this study is limited to the verification of one scenario of crowd movement. In the future, it is imperative to verify whether the learned optimal strategies can be applied to other scenarios. When applying the guidance in practice, it is desirable to scalarize multi-objective rewards based on the decision-maker's preferences and then take the action that maximizes the scalarized reward or value. A method for estimating the decision-maker's preferences in multi-objective sequential decision-making using inverse RL has been proposed [220]. Combining the estimation of the decision-maker's preferences with Pareto front learning, as performed in

this study, allows the decision-maker to make the desired choice in a multi-objective problem.

Algorithm 1 PDQN

initialize reply buffer D

initialize reward estimator $\bar{R}$

initialize non-dominated estimator ND_t

initialize target non-dominated estimator $\hat{ND_t} = ND_t$

for episode=1 to M **do**

  while not terminal **do**

    sample points p from $\mathbb{R}^{d-1}$

    estimate $Q_{set}(s, a)$ by calculating $Q_{set}(s, a, p) = \bar{R}(s, a) + \gamma ND_t(s, a, p)$ for each sample point

    select action a using ϵ-greedy policy and based on $Q_{set}(s, a)$

    execute a in environment, observe state s', reward r, terminal t

    add transition (s, a, r, s', t) to D

    sample minibatch $(s_i, a_i, r_i, s'_i, t_i)$ from D

    sample points p_i from $\mathbb{R}^{d-1}$

    if not t_i **then**

      $y_i = ND(\cup_{a' \in A} Q_{set}(s'_i, a', p'_i))$

    else

      $y_i = r_i$

    end if

    update ND_t by performing gradient descent step on $(y_i - Q_{set}(s_i, a_i, p_i))^2$

    update $\bar{R}$ by performing gradient descent step on $(r_i - \bar{R}(s_i, a_i))^2$

    every C steps copy ND_t to $\hat{ND_t}$

  end while

end for

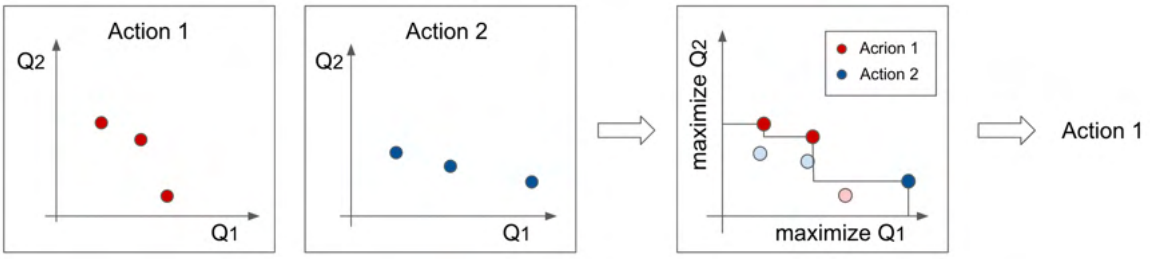

Figure 8.3: Cardinality-based action selection

Algorithm 2 Cardinality-based action selection

$Qs = \{\}$

for each action a in s **do**

  for each $\boldsymbol{Q}$ in $Q_{set}(s, a)$ **do**

    Append $[a, \boldsymbol{Q}]$ to Qs

  end for

end for

$NDQs \leftarrow ND(Qs)$

$n_a \leftarrow$ number of non-dominated solutions of action a in $NDQs$

$a \leftarrow \arg\max_{a \in A} n_a$ (A other than action $n_a = 0$)

($a \leftarrow$ random choice from A other than action $n_a = 0$)

return a

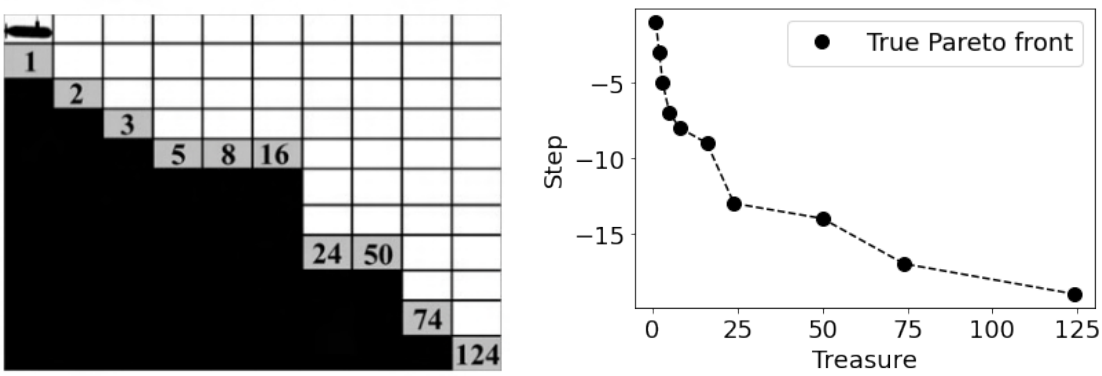

(a) Environment (b) True Pareto front of DST

Figure 8.4: Deep sea treasure [10]

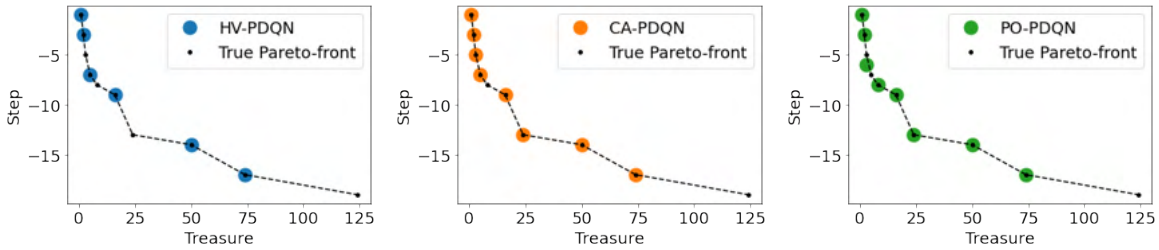

(a) HV-PDQN (b) CA-PDQN (c) PO-PDQN

Figure 8.5: Pareto solution obtained using policies learned by the PDQN for each action selection criterion on the DST environment

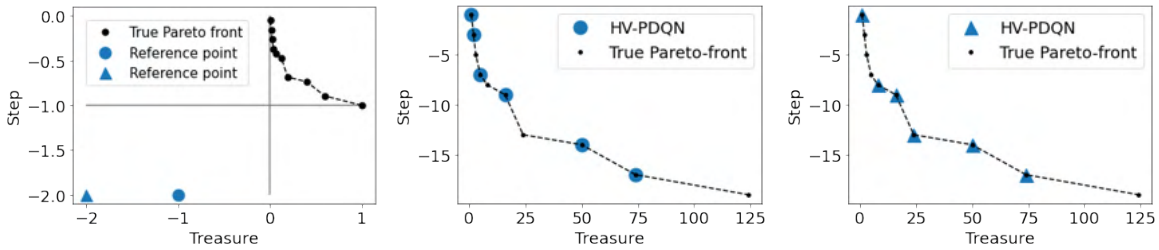

(a) reference points (b) (-1, -2) (c) (-2, -2)

Figure 8.6: The differences in Pareto solutions for different reference points in HV-PDQN

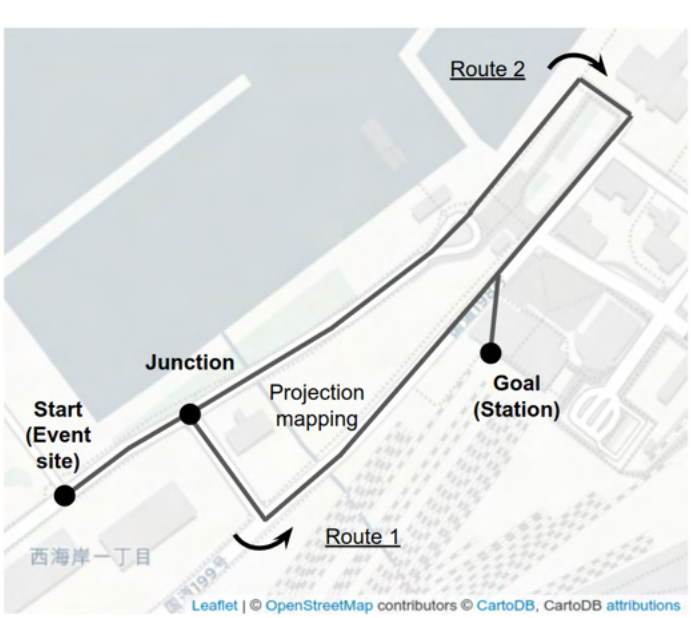

(a) Map

(b) Guidance with projection mapping

Figure 8.7: Fireworks display festival environment

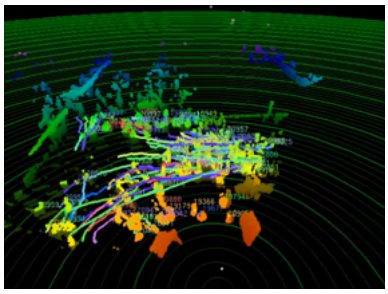

(a) LiDAR at the junction

(b) Camera tracking

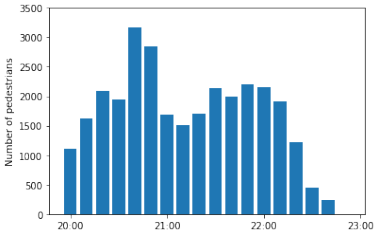

(c) The number of pedestrians starting to move

Figure 8.8: Measurement of crowd movement

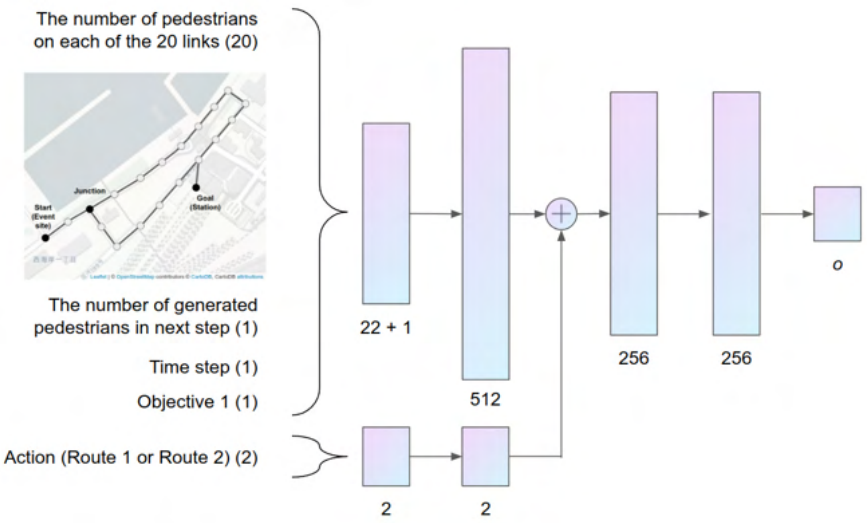

Figure 8.9: The non-dominated estimator ND_t architecture and inputs data

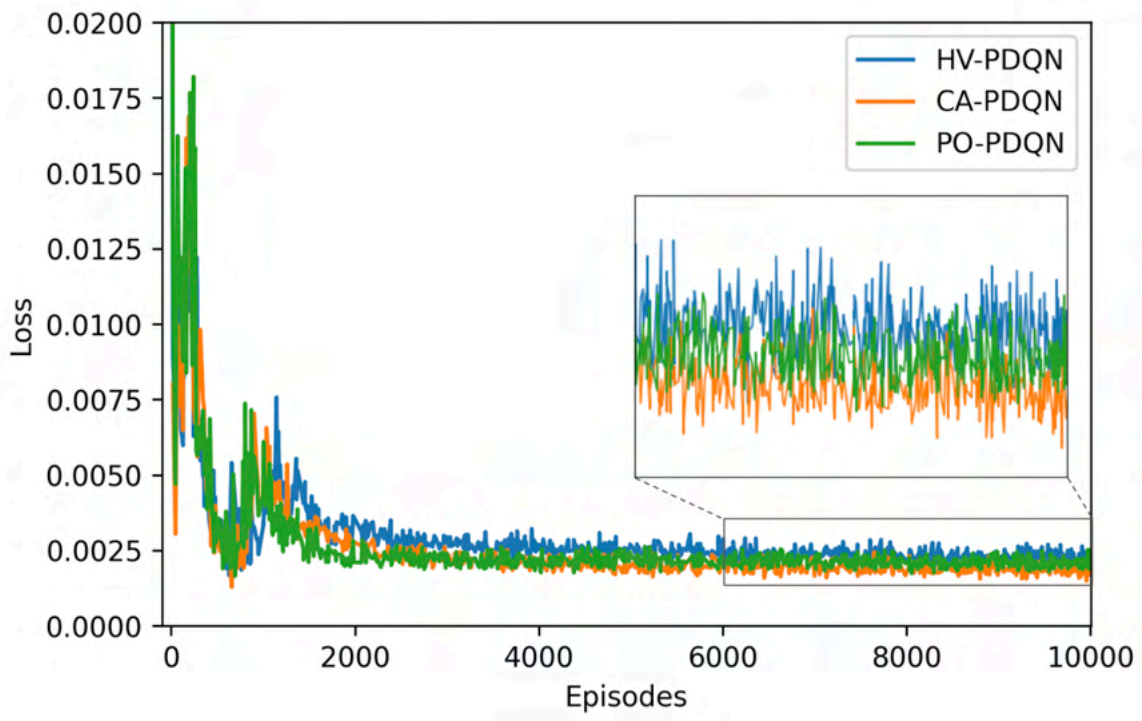

Figure 8.10: Learning curve of PDQN for each action selection criteria

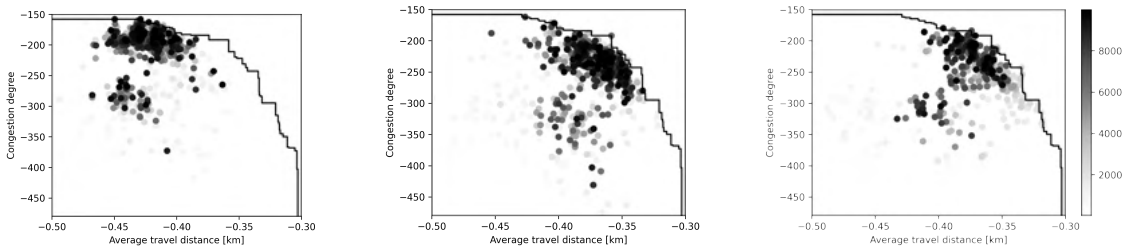

(a) HV-PDQN (10 samples) (b) HV-PDQN (50 samples) (c) HV-PDQN (100 samples)

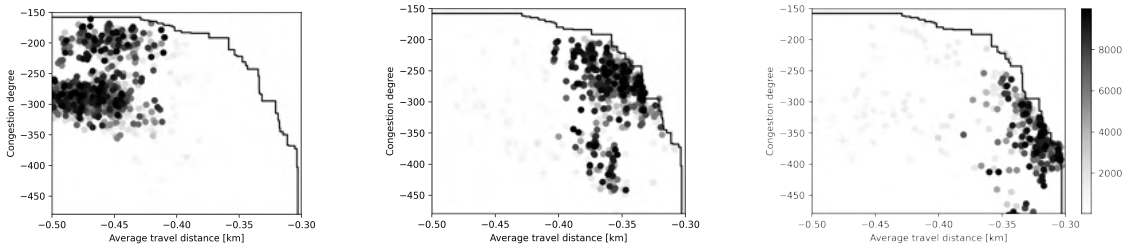

(d) CA-PDQN (10 samples) (e) CA-PDQN (50 samples) (f) CA-PDQN (100 samples)

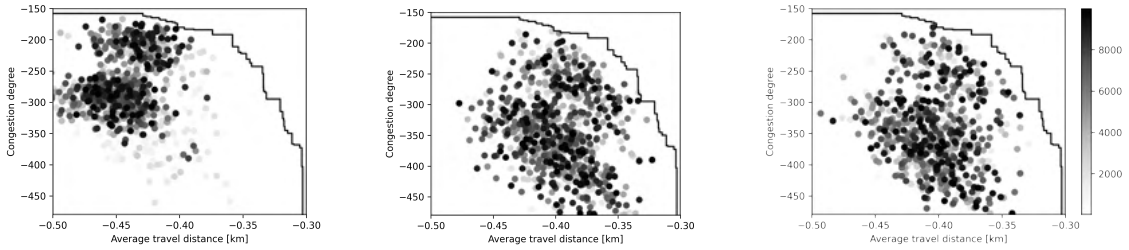

(g) PO-PDQN (10 samples) (h) PO-PDQN (50 samples) (i) PO-PDQN (100 samples)

Figure 8.11: Solution obtained during training. One point is the cumulative sum of rewards earned in one episode. The color becomes darker with each additional episode. The solid lines indicate the Pareto fronts of the solutions obtained in settings (a) through (i).

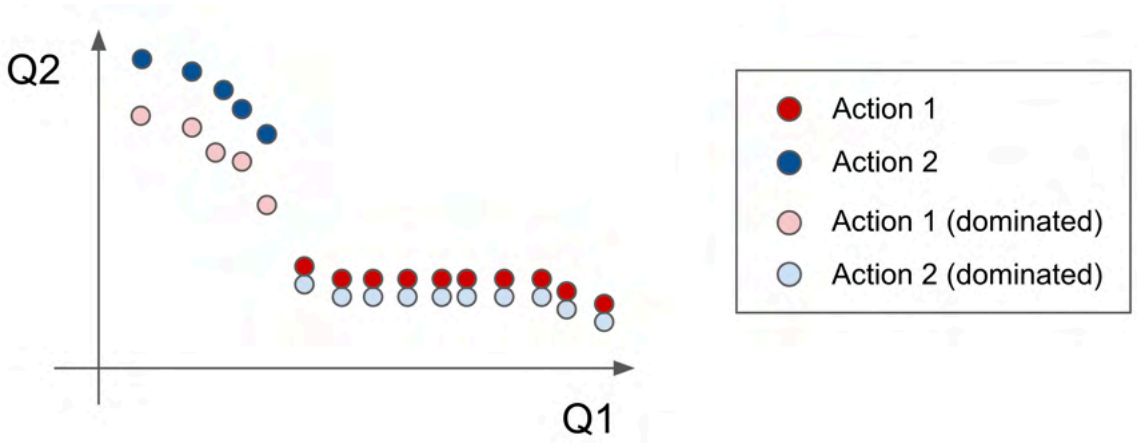

Figure 8.12: Examples of choosing actions that do not contribute to the search for a better solution.

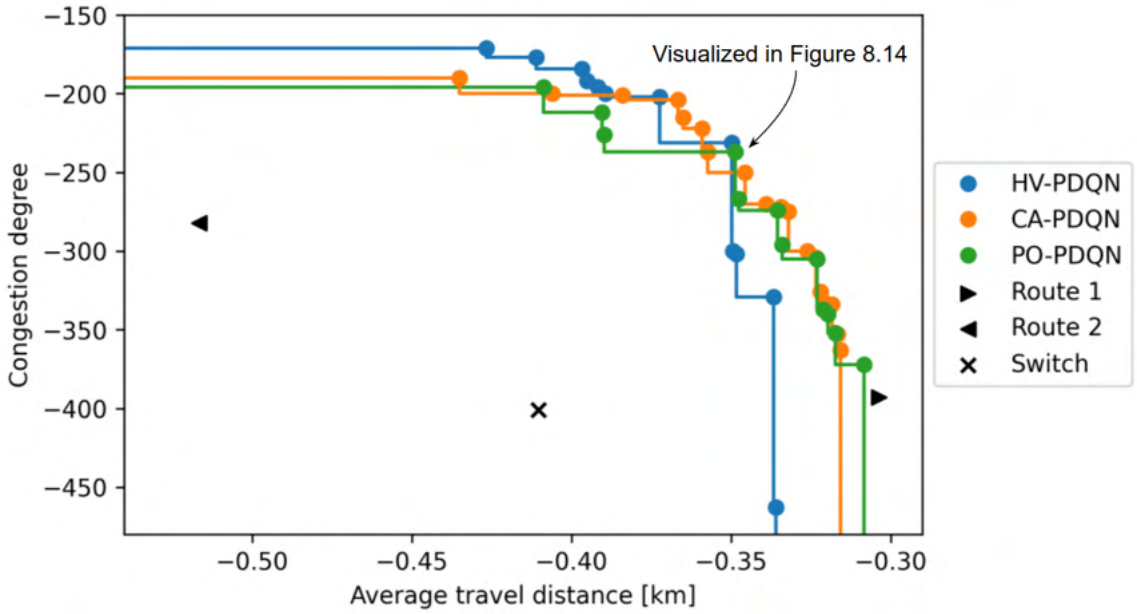

Figure 8.13: Pareto solution obtained using policies learned by the PDQN with sample size 50 for each action selection criterion on the crowd route guidance problem. One point is the result of one guidance policy, and it is the result of simulating until all pedestrians arrive at the station.

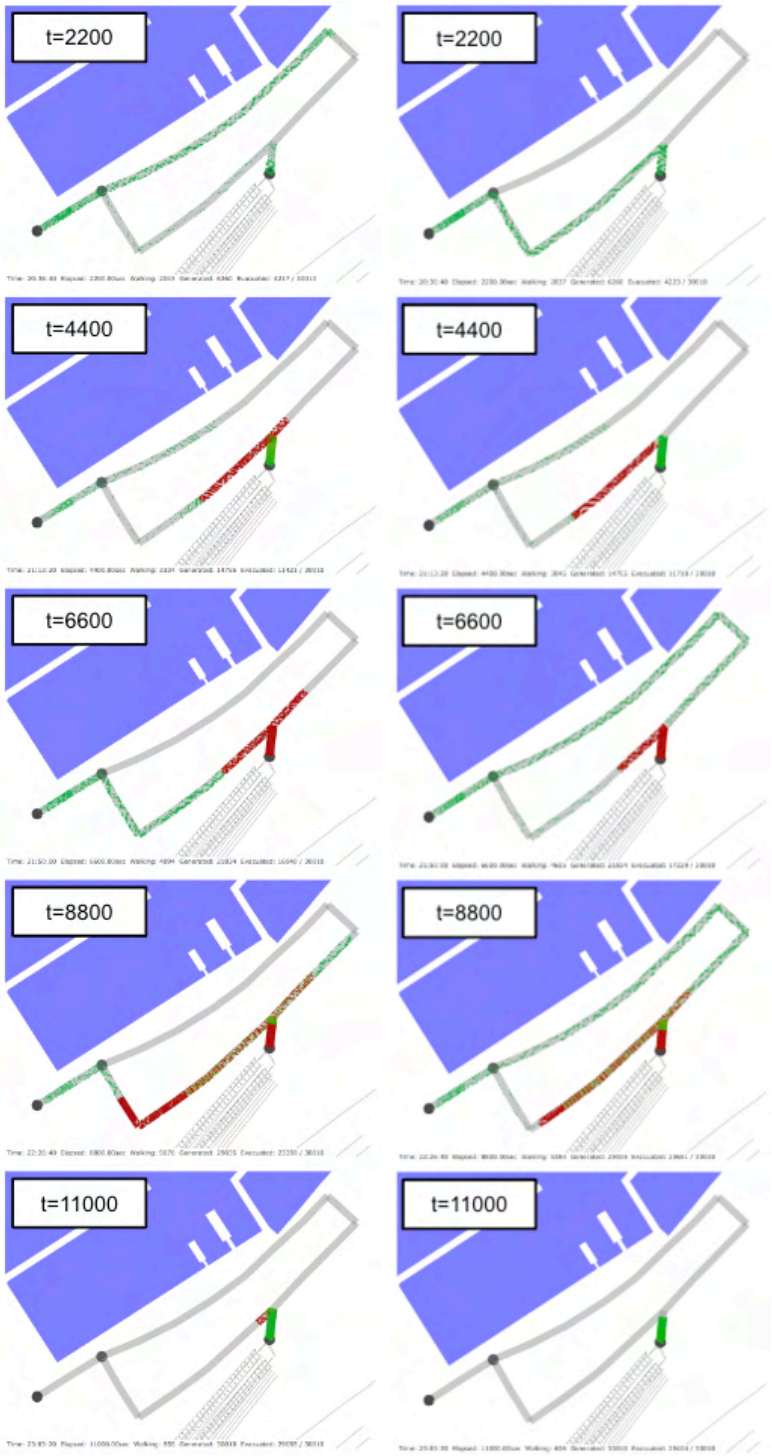

(a) Switch (b) PDQN

Figure 8.14: Simulated crowd movement. The dots represent pedestrians, and the color of the dots represents the pedestrian's speed. The speed decreases from green to red, and red means that the pedestrian is stationary at zero speed. That is, the red areas are under congestion. The guidance strategy acquired by PDQN is more effective in alleviating congestion.

Chapter 9

Conclusions

In this chapter, I summarize the discussions of this dissertation and mention the follow-up works.

9.1 Summary

In Chapter 2, I analyzed the usage history of apps and estimate a travel mode choice model for a Mobility as a Service (MaaS) demonstration experiment conducted in Shizuoka City in November 2019. In this demonstration experiment, the App. that enables users to search for routes combining railroads, local buses, and on-demand shared mobility service (OSMS), was developed. From the collected data, I analyzed the number of users of the MaaS app, user characteristics, trends in the number of searches, and the usage history of each travel mode. The nested logit model was used to represent the mode choice behavior and I identified the selection bias of OSMS in the MaaS demonstration.

In Chapter 3, I generalized and proposed a crowd simulation framework that is

consistent from actual crowd movement measurements to route choice model estimation and crowd simulator construction. I use discrete choice model (DCM) as the route choice model and social force model as the walking model. In experiments, I measured the crowd movements during the evacuation drill in the theater and the firework event in which tens of thousands of people moved, and proved that the crowd simulation incorporating the route choice model can reproduce the measured real large-scale crowd movement.

In Chapter 4, I considered the problem of learning DCM from a dataset that contains data that the selection result is unknown. Using a transportation mode choice dataset "swissmetro", I experimentally showed that positive and unlabeled learning, which is a method of semi-supervised learning, is also useful in choice modeling.

In Chapter 5, I presented a simulation analysis of the benefits that MaaS brings to users. The benefits to users of introducing OSMS in addition to railways and buses and increasing their transportation options were investigated in accordance with the setting of the MaaS demonstration experiment in Shizuoka. The results showed that the introduction of MaaS, or in other words OSMS, increases the benefits to users, but the provider loses profit when the number of users is small. If the number of users increases and the number of OSMS vehicles and fares are adjusted, the provider also archives benefits. However, since the share of railways and buses is reduced by the introduction of OSMS, coordination between the different operators of each mobility service is necessary.

In Chapter 6, I analyzed the benefits of introducing meeting points (MPs) into OSMS in terms of operational efficiency and passenger convenience, especially travel time. Previous studies have shown that the introduction of MPs into OSMS can im-

prove operational efficiency. However, the benefits in terms of passenger convenience have not been sufficiently investigated. The static analysis and the simulation analysis using actual maps and demands show that the introduction of MPs shortens the vehicle kilometers traveled and, if the number of demands exceed a certain number and the number of vehicles is equivalent to door-to-door (D2D)-based OSMS, reduces the average travel time of passengers compared with D2D-based OSMS.

In Chapter 7, I summarized previous studies on spatial design and crowd control. First, the evaluation indices of crowd movement are summarized from the viewpoints of safety and efficiency. Then, the current findings on spatial design are summarized, and crowd control methods are categorized and explained at the level of pedestrian behavior. The problems of the previous studies are summarized, and the approaches to solve them are presented.

In Chapter 8, I proposed an improved version of Pareto-Deep Q-Network (PDQN) and demonstrated its effectiveness in a real-world problem such as crowd route guidance strategy optimization. In previous studies, PDQN has not been successfully applied to real-world problems, and I addressed sample size and action selection criteria as reasons for this. I proposed the use of a sufficient number of samples and the introduction of a new action selection criterion and tested its effectiveness in the toy problem and the crowd guidance problem. The experimental results show that PDQN can learn better strategies than simple guidance methods for crowd guidance optimization problems by adjusting the number of samples.

9.2 Future Work

Future challenges for simulation-based management are to increase the accuracy of measurements, increase the accuracy of simulations, and increase the speed of simulations. Measurement accuracy is improving with the rise of deep learning and more accurate sensors. I believe that there are two approaches to improving the accuracy of simulation: model refinement and data assimilation. In this dissertation, some research was conducted using the approach of model refinement. On the other hand, data assimilation is also an important technique. Future work includes the establishment of a hybrid method in which statistical modeling is performed based on data, and then some of the parameters of the model are optimized by data assimilation in order to increase the accuracy of the simulation.

Simulation always takes a calculation cost, so it is not feasible to run simulations many times within the available time. Surrogate models are often used to speed up simulations. Approaches to replace agent-based simulation with deep learning have been studied [221]. However, there is a risk of black-boxing the simulation process when using deep learning methods. In addition, only the phenomena contained in the data used for training can be reproduced or predicted. In order to reproduce emergent phenomena, it is necessary to construct an agent-based simulator as before. Since there is a trade-off between accuracy and computational cost, it is desirable to construct a hybrid simulator that successfully combines the merits of both.

In the future, people's behavior will be further optimized by AI technologies such as recommendation systems. However, it should be noted that in a world with limited resources, the result of individual optimization may not always be system optimization.

Currently, services with personalized recommendation functions such as Netflix, Spotify (content distribution), YouTube, Instagram (SNS), and Amazon (e-commerce) are becoming popular. Content is unlimited, and social networking services are valuable for their large number of users. In addition, it is relatively easy to increase production volume in e-commerce. Therefore, the current mainstream recommendation systems focus only on increasing the number of users. In the future, personalized recommendations will extend to all aspects of life. This is a world in which optimal daily activities and scheduling will be recommended. Daily activities share limited resources, and resources (movement and action spaces such as roads and stores) cannot be easily increased, so if the number of users increases too much, there will be competition for resources.

While there has been a great deal of research in the field of transportation that considers not only individual optimization but also optimization of the entire system, in recent years there has been an increase in research on personalization and incentivization of individuals [222, 223]. On the other hand, in the field of recommendation systems, there has been an increase in research that considers not only the user's perspective, but also the perspectives of the company and the entire system, giving rise to the topic of multi-stakeholder recommendation [224, 225]. We believe that the transportation field, which has not considered individual heterogeneity, and the recommendation system field, which has not considered the perspective of the entire system, can complement each other. In the future, it is desirable to construct an advanced management system or socially-aware AI that achieves both individual and system optimization through cross-disciplinary research.

Bibliography

[1] Yapeng Li, Wei Cai, and Austin A Kana. Design of level of service on facilities for crowd evacuation using genetic algorithm optimization. *Safety Science*, 120:237–247, December 2019.

[2] Claudio Feliciani, Hisashi Murakami, and Katsuhiro Nishinari. A universal function for capacity of bidirectional pedestrian streams: Filling the gaps in the literature. *PloS one*, 13(12):e0208496, December 2018.

[3] Jinghong Wang, Bowei Jin, Jia Li, Fanghao Chen, Zhirong Wang, and Jinhua Sun. Method for guiding crowd evacuation at exit: The buffer zone. *Safety Science*, 118:88–95, October 2019.

[4] Takahiro Ezaki, Daichi Yanagisawa, and Katsuhiro Nishinari. Pedestrian flow through multiple bottlenecks. *Physical Review E*, 86(2):026118, August 2012.

[5] Weichen Liao, Xiaoping Zheng, Lisheng Cheng, Ying Zhao, Yuan Cheng, and Yafei Wang. Layout effects of multi-exit ticket-inspectors on pedestrian evacuation. *Safety Science*, 70:1–8, December 2014.

[6] Milad Haghani, Majid Sarvi, and Liam Scanlon. Simulating pre-evacuation

times using hazard-based duration models: Is waiting strategy more efficient than instant response? *Safety science*, 117:339–351, August 2019.

[7] Liang Li, Hong Liu, and Yanbin Han. Arch formation-based congestion alleviation for crowd evacuation. *Transportation Research Part C: Emerging Technologies*, 100:88–106, March 2019.

[8] Hermann Mayer, Wolfram Klein, Christian Frey, Simon Daum, Peter Kielar, and André Borrmann. Pedestrian simulation based on bim data. *Proceedings of the ASHRAE/IBPSA-USA Building Simulation Conference, Atlanta, GA*, 2014.

[9] Ruggiero Lovreglio, Achille Fonzone, and Luigi dell'Olio. A mixed logit model for predicting exit choice during building evacuations. *Transportation Research Part A: Policy and Practice*, 92:59–75, October 2016.

[10] P Vamplew, R Dazeley, A Berry, R Issabekov, and others. Empirical evaluation methods for multiobjective reinforcement learning algorithms. *Machine learning*, 2011.

[11] Md Sami Hasnine and Khandker Nurul Habib. Tour-based mode choice modelling as the core of an activity-based travel demand modelling framework: a review of state-of-the-art. *Transport Reviews*, 41(1):5–26, January 2021.

[12] S P Hoogendoorn and P H L Bovy. Pedestrian route-choice and activity scheduling theory and models. *Transportation Research Part B: Methodological*, 38(2):169–190, February 2004.

[13] Yafei Han, Christopher Zegras, Francisco Camara Pereira, and Moshe Ben-Akiva. A neural-embedded choice model: Tastenet-mnl modeling taste heterogeneity with flexibility and interpretability. February 2020.

[14] Donella H. Meadows et al. *The Limits to Growth; a Report for the Club of Rome's Project on the Predicament of Mankind*. New York :Universe Books, 1972.

[15] Nigel Gilbert and Klaus G. Troitzsc. *Simulation for the Social Scientist*. Open University Press, 1999.

[16] Michael Grieves. Digital twin: Manufacturing excellence through virtual factory replication. Technical report, 2015.

[17] David Jones, Chris Snider, Aydin Nassehi, Jason Yon, and Ben Hicks. Characterising the digital twin: A systematic literature review. *CIRP Journal of Manufacturing Science and Technology*, 29:36–52, May 2020.

[18] Werner Kritzinger, Matthias Karner, Georg Traar, Jan Henjes, and Wilfried Sihn. Digital twin in manufacturing: A categorical literature review and classification. *IFAC-PapersOnLine*, 51(11):1016–1022, January 2018.

[19] Gary White, Anna Zink, Lara Codecá, and Siobhán Clarke. A digital twin smart city for citizen feedback. *Cities*, 110:103064, March 2021.

[20] Taewoo Nam and Theresa A Pardo. Conceptualizing smart city with dimensions of technology, people, and institutions. In *Proceedings of the 12th Annual International Digital Government Research Conference: Digital Government*

Innovation in Challenging Times, dg.o '11, pages 282–291, New York, NY, USA, June 2011. Association for Computing Machinery.

[21] Rudolf Giffinger and Nataša Pichler-Milanović. *Smart cities: Ranking of European medium-sized cities*. Centre of Regional Science, Vienna University of Technology, 2007.

[22] A Downs. The law of peak-hour expressway congestion. *Traffic quarterly*, 16(3), July 1962.

[23] John Michael Thomson. *Great cities and their traffic*. Littlehampton Book Services, Worthing, England, January 1977.

[24] Marguerite Frank. The braess paradox. *Mathematical Programming. A Publication of the Mathematical Programming Society*, 20(1):283–302, December 1981.

[25] Michael G McNally. The four-step model. In A Hensher David and J Button Kenneth, editors, *Handbook of Transport Modelling*, volume 1, pages 35–53. Emerald Group Publishing Limited, January 2007.

[26] Kay W Axhausen and Tommy Gärling. Activity-based approaches to travel analysis: conceptual frameworks, models, and research problems. *Transport Reviews*, 12(4):323–341, October 1992.

[27] Sonja Heikkilä. Mobility as a service - a proposal for action for the public administration, case helsinki. MSc dissertation, Aalto University., 2014.

[28] Sampo Hietanen. "mobility as a Service"—The new transport model? Eurotransport, 12(2), 2–4, 2014.

[29] Wietse te Morsche, Lissy La Paix Puello, and Karst T Geurs. Potential uptake of adaptive transport services: An exploration of service attributes and attitudes. *Transport Policy*, 84:1–11, December 2019.

[30] Yang Liu, Prateek Bansal, Ricardo Daziano, and Samitha Samaranayake. A framework to integrate mode choice in the design of mobility-on-demand systems. *Transportation Research Part C: Emerging Technologies*, 105:648–665, August 2019.

[31] Valeria Caiati, Soora Rasouli, and Harry Timmermans. Bundling, pricing schemes and extra features preferences for mobility as a service: Sequential portfolio choice experiment. *Transportation Research Part A: Policy and Practice*, 131:123–148, January 2020.

[32] Melinda Matyas and Maria Kamargianni. The potential of mobility as a service bundles as a mobility management tool. *Transportation*, 46(5):1951–1968, October 2019.

[33] Melinda Matyas and Maria Kamargianni. Investigating heterogeneity in preferences for mobility-as-a-service plans through a latent class choice model. *Travel Behaviour and Society*, 23:143–156, April 2021.

[34] Chinh Q Ho, Corinne Mulley, and David A Hensher. Public preferences for mobility as a service: Insights from stated preference surveys. *Transportation Research Part A: Policy and Practice*, 131:70–90, January 2020.

[35] Melinda Matyas and Maria Kamargianni. Survey design for exploring demand for mobility as a service plans. *Transportation*, 46(5):1525–1558, October 2019.

[36] Anna-Maria Feneri, Soora Rasouli, and Harry J P Timmermans. Modeling the effect of mobility-as-a-service on mode choice decisions. *Transportation Letters*, 14(4):324–331, April 2022.

[37] Chinh Q Ho, David A Hensher, Corinne Mulley, and Yale Z Wong. Potential uptake and willingness-to-pay for mobility as a service (maas): A stated choice study. *Transportation Research Part A: Policy and Practice*, 117:302–318, November 2018.

[38] Daniel McFadden. Conditional logit analysis of qualitative choice behavior. 1973.

[39] Brian Sifringer, Virginie Lurkin, and Alexandre Alahi. Enhancing discrete choice models with representation learning. *Transportation Research Part B: Methodological*, 140:236–261, October 2020.

[40] H C W L Williams. On the formation of travel demand models and economic evaluation measures of user benefit. *Environment and Planning A*, 9(3):285–344, 1977.

[41] Daniel McFadden. Quantitative methods for analyzing travel behaviour of individuals: Some recent developments. Technical Report 474, 1977.

[42] Anne Durand, Lucas Harms, Sascha Hoogendoorn-Lanser, et al. Mobility-as-a-Service and changes in travel preferences and travel behaviour: a literature review. 2018.

[43] Lee Soomaroo and Virginia Murray. Disasters at mass gatherings: lessons from history. *PLoS currents*, 4:RRN1301, February 2012.

[44] G Keith Still. Crowd disasters. `https://www.gkstill.com/ExpertWitness/CrowdDisasters.html`.

[45] Guanghui Lu, Leiting Chen, and Weiping Luo. Real-time crowd simulation integrating potential fields and agent method. *ACM Transactions on Modeling and Computer Simulation*, 26(4):1–16, March 2016.

[46] Rahul Narain, Abhinav Golas, Sean Curtis, and Ming C Lin. Aggregate dynamics for dense crowd simulation. *ACM transactions on graphics*, 28(5):1–8, December 2009.

[47] V Blue and J Adler. Bi-directional emergent fundamental pedestrian flows from cellular automata microsimulation. *Transportation and traffic theory*, 14:235–254, 1999.

[48] Minoru Fukui and Yoshihiro Ishibashi. Self-organized phase transitions in cellular automaton models for pedestrians. *Journal of the Physical Society of Japan*, 68(8):2861–2863, August 1999.

[49] D Helbing and P Molnár. Social force model for pedestrian dynamics. *Physical review. E, Statistical physics, plasmas, fluids, and related interdisciplinary topics*, 51(5):4282–4286, May 1995.

[50] D Helbing, I Farkas, and T Vicsek. Simulating dynamical features of escape panic. *Nature*, 407(6803):487–490, September 2000.

[51] Jur van den Berg, Ming Lin, and Dinesh Manocha. Reciprocal velocity obstacles for real-time multi-agent navigation. In *2008 IEEE International Conference on Robotics and Automation*, pages 1928–1935, 2008.

[52] Miho Asano, Takamasa Iryo, and Masao Kuwahara. Microscopic pedestrian simulation model combined with a tactical model for route choice behaviour. *Transportation Research Part C: Emerging Technologies*, 18(6):842–855, December 2010.

[53] Armel Ulrich Kemloh Wagoum, Armin Seyfried, and Stefan Holl. Modeling the dynamic route choice of pedestrians to assess the criticality of building evacuation. *Advances in Complex Systems*, 15(07):1250029, October 2012.

[54] Asha Weinstein Agrawal, Marc Schlossberg, and Katja Irvin. How far, by which route and why? a spatial analysis of pedestrian preference. *Journal of urban design*, 13(1):81–98, February 2008.

[55] Zhan Guo and Becky P Y Loo. Pedestrian environment and route choice: evidence from new york city and hong kong. *Journal of Transport Geography*, 28:124–136, April 2013.

[56] Martin Stubenschrott, Christian Kogler, Thomas Matyus, and Stefan Seer. A dynamic pedestrian route choice model validated in a high density subway station. *Transportation Research Procedia*, 2:376–384, January 2014.

[57] Luca Crociani, Giuseppe Vizzari, Daichi Yanagisawa, Katsuhiro Nishinari and Stefania Bandini. Route choice in pedestrian simulation: Design and evaluation of a model based on empirical observations. *Intelligenza Artificiale*, 10(2):163–182, 2016.

[58] Weichen Liao, Armel U Kemloh Wagoum, and Nikolai W F Bode. Route choice in pedestrians: determinants for initial choices and revising decisions. *Journal*

of the Royal Society, Interface / the Royal Society, 14(127):20160684, February 2017.

[59] Giuseppe Vizzari, Luca Crociani, and Stefania Bandini. An agent-based model for plausible wayfinding in pedestrian simulation. *Engineering applications of artificial intelligence*, 87:103241, January 2020.

[60] Wenxi Liu, Rynson Lau, and Dinesh Manocha. Crowd simulation using discrete choice model. In *2012 IEEE Virtual Reality Workshops (VRW)*, pages 3–6, March 2012.

[61] Milad Haghani and Majid Sarvi. Following the crowd or avoiding it? empirical investigation of imitative behaviour in emergency escape of human crowds. *Animal behaviour*, 124:47–56, February 2017.

[62] Milad Haghani and Majid Sarvi. Imitative (herd) behaviour in direction decision-making hinders efficiency of crowd evacuation processes. *Safety science*, 114:49–60, April 2019.

[63] Yongxin Gao, Feng Chen, and Zijia Wang. Hybrid dynamic route planning model for pedestrian microscopic simulation at subway station. *Journal of Advanced Transportation*, 2019, April 2019.

[64] Xiaoxia Yang, Xiaoli Yang, Qianling Wang, Yuanlei Kang, and Fuquan Pan. Guide optimization in pedestrian emergency evacuation. *Applied mathematics and computation*, 365:124711, January 2020.

[65] X Lu, H Blanton, T Gifford, A Tucker, and N Olderman. Optimized guidance

for building fires considering occupants' route choices. *Physica A: Statistical Mechanics and its Applications*, 561:125247, January 2021.

[66] M. Onishi. Analysis and visualization of large-scale pedestrian flow in normal and disaster situations. *ITE Transactions on Media Technology and Applications*, 3(3):170–183, 2015.

[67] Tomohisa Yamashita, Takashi Okada, and Itsuki Noda. Implementation of simulation environment for exhaustive analysis of huge-scale pedestrian flow. *SICE Journal of Control, Measurement, and System Integration*, 6(2):137–146, March 2013.

[68] Yves Bentz and Dwight Merunka. Neural networks and the multinomial logit for brand choice modelling: a hybrid approach. *Journal of forecasting*, 19(3):177–200, April 2000.

[69] Harald Hruschka, Werner Fettes, Markus Probst, and Christian Mies. A flexible brand choice model based on neural net methodologya comparison to the linear utility multinomial logit model and its latent class extension. *OR Spectrum. Quantitative Approaches in Management*, 24(2):127–143, May 2002.

[70] Shenhao Wang, Baichuan Mo, and Jinhua Zhao. Deep neural networks for choice analysis: Architecture design with alternative-specific utility functions. *Transportation Research Part C: Emerging Technologies*, 112:234–251, March 2020.

[71] Melvin Wong and Bilal Farooq. Reslogit: A residual neural network logit model for data-driven choice modelling. *Transportation Research Part C: Emerging Technologies*, 126:103050, May 2021.

[72] Porter Jenkins, Ahmad Farag, J Stockton Jenkins, Huaxiu Yao, Suhang Wang, and Zhenhui Li. Neural utility functions. *Proceedings of the AAAI Conference on Artificial Intelligence*, 35(9):7917–7925, May 2021.

[73] S Van Cranenburgh, S Wang, A Vij, F Pereira, and J Walker. Choice modelling in the age of machine learning. January 2021.

[74] Charles Elkan and Keith Noto. Learning classifiers from only positive and unlabeled data. In *Proceedings of the 14th ACM SIGKDD international conference on Knowledge discovery and data mining*, KDD '08, pages 213–220, New York, NY, USA, August 2008. Association for Computing Machinery.

[75] Michel Bierlaire. Swissmetro. `https://transp-or.epfl.ch/documents/technicalReports/CS_SwissmetroDescription.pdf`, 2018.

[76] Peng Jing, Hanbin Hu, Fengping Zhan, Yuexia Chen, and Yuji Shi. Agent-based simulation of autonomous vehicles: A systematic literature review. *IEEE Access*, 8:79089–79103, 2020.

[77] Rick Wolbertus, Robert van den Hoed, Maarten Kroesen, and Caspar Chorus. Charging infrastructure roll-out strategies for large scale introduction of electric vehicles in urban areas: An agent-based simulation study. *Transportation Research Part A: Policy and Practice*, 148:262–285, June 2021.

[78] Marvin Klein, Lars Lüpke, and Markus Günther. Home charging and electric vehicle diffusion: Agent-based simulation using choice-based conjoint data. *Transportation Research Part D: Transport and Environment*, 88:102475, November 2020.

[79] Peraphan Jittrapirom, Valeria Caiati, A-M Feneri, et al. Mobility as a service: A critical review of definitions, assessments of schemes, and key challenges. *Urban Planning*, 2:13–25, 2017.

[80] Maria Kamargianni, Lampros Yfantis, Jakub Muscat, et al. Incorporating the mobility as a service concept into transport modelling and simulation frameworks. In *Transportation Research Board Annual Meeting*, 2019.

[81] Pablo Alvarez Lopez, Michael Behrisch, Laura Bieker-Walz, et al. Microscopic traffic simulation using sumo. In *The 21st IEEE International Conference on Intelligent Transportation Systems*. IEEE, 2018.

[82] Mirai share. `http://www.miraishare.co.jp/en/savs/`.

[83] Alejandro Tirachini. Ride-hailing, travel behaviour and sustainable mobility: an international review. *Transportation*, 47(4):2011–2047, August 2020.

[84] Sebastian Hörl, Felix Becker, and Kay W Axhausen. Simulation of price, customer behaviour and system impact for a cost-covering automated taxi system in zurich. *Transportation Research Part C: Emerging Technologies*, 123:102974, February 2021.

[85] Susan Shaheen and Adam Cohen. Shared ride services in north america: definitions, impacts, and the future of pooling. *Transport Reviews*, 39(4):427–442, 2019.

[86] Mohamed Jama Mohamed, Tom Rye, and Achille Fonzone. Uberpool services – approaches from transport operators and policymakers in london. *Transportation Research Procedia*, 48:2597–2607, 2020.

[87] Wenxiang Li, Ziyuan Pu, Ye Li, and Xuegang (Jeff) Ban. Characterization of ridesplitting based on observed data: A case study of chengdu, china. *Transportation Research Part C: Emerging Technologies*, 100:330–353, 2019.

[88] Yanshuo Sun and Lei Zhang. Potential of taxi-pooling to reduce vehicle miles traveled in washington, d.c. *Transportation research record*, 2672(8):775–784, 2018.

[89] Paul Czioska, Ronny Kutadinata, Aleksandar Trifunović, Stephan Winter, Monika Sester, and Bernhard Friedrich. Real-world meeting points for shared demand-responsive transportation systems. *Public Transport*, 11(2):341–377, 2019.

[90] Andy Ham. Dial-a-ride problem with meeting point feature known-as expresspool. *IEEE Access*, 9:86404–86411, 2021.

[91] Andres Fielbaum, Xiaoshan Bai, and Javier Alonso-Mora. On-demand ridesharing with optimized pick-up and drop-off walking locations. *Transportation Research Part C: Emerging Technologies*, 126:103061, 2021.

[92] Dough. Uber Pool vs Express Pool: What's the Difference? (July 14th, 2020), 2022. `https://www.ridesharingdriver.com/whats-uberpool-shared-ride-cheaper-than-other-uber-services/`, last accessed on 05/16/2022.

[93] Mitja Stiglic, Niels Agatz, Martin Savelsbergh, and Mirko Gradisar. The benefits of meeting points in ride-sharing systems. *Transportation Research Part B: Methodological*, 82:36–53, 2015.

[94] Paul Czioska, Aleksandar Trifunović, Sophie Dennisen, and Monika Sester. Location- and time-dependent meeting point recommendations for shared interurban rides. *Journal of location based services*, 11(3-4):181–203, 2017.

[95] Wenyi Chen, Martijn Mes, Marco Schutten, and Job Quint. A ride-sharing problem with meeting points and return restrictions. *Transportation Science*, 53(2):401–426, 2019.

[96] Ulrich Matchi Aïvodji, Sébastien Gambs, Marie-José Huguet, and Marc-Olivier Killijian. Meeting points in ridesharing: A privacy-preserving approach. *Transportation Research Part C: Emerging Technologies*, 72:239–253, 2016.

[97] Yue Zheng, Wenquan Li, Feng Qiu, and Heng Wei. The benefits of introducing meeting points into flex-route transit services. *Transportation Research Part C: Emerging Technologies*, 106:98–112, 2019.

[98] Krishna Murthy Gurumurthy and Kara M Kockelman. Dynamic ride-sharing impacts of greater trip demand and aggregation at stops in shared autonomous vehicle systems. *Transportation Research Part A: Policy and Practice*, 160:114–125, June 2022.

[99] Felix Zwick, Nico Kuehnel, Rolf Moeckel, and Kay W Axhausen. Agent-based simulation of city-wide autonomous ride-pooling and the impact on traffic noise. *Transportation Research Part D: Transport and Environment*, 90:102673, January 2021.

[100] H Levinson. Analyzing transit travel time performance. In Transportation Research Board of the National Academies, editor, *In Transportation Research Record: Journal of the Transportation Research Board*, 915, pages 1–6, 1983.

[101] Itsuki Noda, Masayuki Ohta, Kosuke Shinoda, et al. Evaluation of usability of dial-a-ride systems by social simulation. In *Multi-Agent-Based Simulation III. 4th International Workshop, MABS 2003 (LNAI-2927)*, pages 167–181, 2003.

[102] SAVS. `https://www.miraishare.co.jp/en/`.

[103] Javier Alonso-Mora, Samitha Samaranayake, Alex Wallar, Emilio Frazzoli, and Daniela Rus. On-demand high-capacity ride-sharing via dynamic trip-vehicle assignment. *Proceedings of the National Academy of Sciences of the United States of America*, 114(3):462–467, January 2017.

[104] D McFadden. Quantitative methods for analysing travel behaviour of individuals: some recent developments. *Behavioural travel modelling*, 1979.

[105] Tokyo Hire-Taxi Association. Rates Table, 2022. `https://www.taxi-tokyo.or.jp/english/call/pricelist.html`, last accessed on 05/16/2022.

[106] Lee Soomaroo and Virginia Murray. Disasters at mass gatherings: lessons from history. *PLoS currents*, 4:RRN1301, February 2012.

[107] G Keith Still. *Introduction to Crowd Science*. CRC Press/Taylor & Francis Group, 2014.

[108] George Sidiropoulos, Chairi Kiourt, and Lefteris Moussiades. Crowd simulation for crisis management: The outcomes of the last decade. *Machine Learning with Applications*, 2:100009, December 2020.

[109] Shanwen Yang, Tianrui Li, Xun Gong, Bo Peng, and Jie Hu. A review on crowd simulation and modeling. *Graphical models*, 111:101081, September 2020.

[110] M Zhou, H Dong, B Ning, and F Wang. Recent development in pedestrian and evacuation dynamics: Bibliographic analyses, collaboration patterns, and future directions. *IEEE Transactions on Computational Social Systems*, 5(4):1034–1048, December 2018.

[111] Adriana Draghici and Maarten Van Steen. A survey of techniques for automatically sensing the behavior of a crowd. *ACM Comput. Surv.*, 51(1):1–40, February 2018.

[112] Teng Li, Huan Chang, Meng Wang, Bingbing Ni, Richang Hong, and Shuicheng Yan. Crowded scene analysis: A survey. *IEEE Transactions on Circuits and Systems for Video Technology*, 25(3):367–386, March 2015.

[113] Beibei Zhan, Dorothy N Monekosso, Paolo Remagnino, Sergio A Velastin, and Li-Qun Xu. Crowd analysis: A survey. *Machine Vision and Applications*, 19(5):345–357, October 2008.

[114] Nanda Wijermans, Claudine Conrado, Maarten van Steen, Claudio Martella, and Jie Li. A landscape of crowd-management support: An integrative approach. *Safety science*, 86:142–164, July 2016.

[115] Hendrik Vermuyten, Jeroen Beliën, Liesje De Boeck, Genserik Reniers, and Tony Wauters. A review of optimisation models for pedestrian evacuation and design problems. *Safety Science*, 87:167–178, August 2016.

[116] A Kaveh, S M Javadi, and R Mahdipour Moghanni. Emergency management systems after disastrous earthquakes using optimization methods: A comprehensive review. *Advances in engineering software*, 149:102885, November 2020.

[117] Milad Haghani. Optimising crowd evacuations: Mathematical, architectural and behavioural approaches. *Safety science*, 128:104745, August 2020.

[118] Dorine C Duives, Winnie Daamen, and Serge P Hoogendoorn. State-of-the-art crowd motion simulation models. *Transportation Research Part C: Emerging Technologies*, 37:193–209, December 2013.

[119] Toshihiro Osaragi. Modeling of pedestrian behavior and its applications to spatial evaluation. In *Autonomous Agents and Multiagent Systems, International Joint Conference on*, volume 3, pages 836–843, 2004.

[120] Nan Hu, Jinghui Zhong, Joey Tianyi Zhou, Suiping Zhou, Wentong Cai, and Christopher Monterola. Guide them through: An automatic crowd control framework using multi-objective genetic programming. *Applied soft computing*, 66:90–103, May 2018.

[121] Emiliano Cristiani and Daniele Peri. Handling obstacles in pedestrian simulations: Models and optimization. *Applied Mathematical Modelling*, 45:285–302, May 2017.

[122] Hairong Dong, Xiang Gao, Tongxin Gao, Xubin Sun, and Qianling Wang. Crowd evacuation optimization by leader-follower model. *IFAC Proceedings Volumes*, 47(3):12116–12121, January 2014.

[123] Vi Ha and George Lykotrafitis. Agent-based modeling of a multi-room multi-floor building emergency evacuation. *Physica A: Statistical Mechanics and its Applications*, 391(8):2740–2751, April 2012.

[124] Nurulaqilla Khamis, Hazlina Selamat, Fatimah Sham Ismail, Omar Farouq

Lutfy, Mohamad Fadzli Haniff, and Ili Najaa Aimi Mohd Nordin. Optimized exit door locations for a safer emergency evacuation using crowd evacuation model and artificial bee colony optimization. *Chaos, Solitons & Fractals*, 131:109505, February 2020.

[125] Heba A Kurdi, Shiroq Al-Megren, Reham Althunyan, and Asma Almulifi. Effect of exit placement on evacuation plans. *European journal of operational research*, 269(2):749–759, September 2018.

[126] Lakshay Taneja and Nomesh B Bolia. Network redesign for efficient crowd flow and evacuation. *Applied mathematical modelling*, 53:251–266, January 2018.

[127] Marc Goerigk, Kaouthar Deghdak, and Philipp Heßler. A comprehensive evacuation planning model and genetic solution algorithm. *Transportation Research Part E: Logistics and Transportation Review*, 71:82–97, November 2014.

[128] Ahmed Abdelghany, Khaled Abdelghany, Hani Mahmassani, and Wael Alhalabi. Modeling framework for optimal evacuation of large-scale crowded pedestrian facilities. *European journal of operational research*, 237(3):1105–1118, September 2014.

[129] Siyuan Chen, Libi Fu, Jie Fang, and Panyun Yang. The effect of obstacle layouts on pedestrian flow in corridors: An experimental study. *Physica A: Statistical Mechanics and its Applications*, 534:122333, November 2019.

[130] Minji Choi and Seokho Chi. Optimal route selection model for fire evacuations based on hazard prediction data. *Simulation Modelling Practice and Theory*, 94:321–333, 2019.

[131] Rohit K Dubey, Wei Ping Khoo, Michal Gath Morad, Christoph Hölscher, and Mubbasir Kapadia. Autosign: A multi-criteria optimization approach to computer aided design of signage layouts in complex buildings. *Computers & graphics*, 88:13–23, May 2020.

[132] Lei Feng and Elise Miller-Hooks. A network optimization-based approach for crowd management in large public gatherings. *Transportation Research Part C: Emerging Technologies*, 42:182–199, May 2014.

[133] Zhe Zhang, Limin Jia, and Yong Qin. Optimal number and location planning of evacuation signage in public space. *Safety science*, 91:132–147, January 2017.

[134] Yuki Tanigaki, Yoshihiko Ozaki, Shusuke Shigenaka, and Masaki Onishi. Evolutionary multiobjective optimization for pedestrian route guidance with multiple scenarios. In *2020 IEEE Congress on Evolutionary Computation (CEC)*, pages 1–7, July 2020.

[135] Amy Wenxuan Ding. Implementing real-time grouping for fast egress in emergency. *Safety Science*, 49(10):1404–1411, December 2011.

[136] H U Ji-hua, Zhan Cheng-zhi, Cheng Zhi-feng, and Wang Bo. A research of pedestrian evacuation simulation for brt station based on fine grid method. *Procedia Engineering*, 52:137–144, January 2013.

[137] Vladislav Karbovskii, Oksana Severiukhina, Ivan Derevitskii, Daniil Voloshin, Alva Presbitero, and Michael Lees. The impact of different obstacles on crowd dynamics. *Journal of Computational Science*, 36:100893, September 2019.

[138] Sai-Keung Wong, Yu-Shuen Wang, Pao-Kun Tang, and Tsung-Yu Tsai. Optimized evacuation route based on crowd simulation. *Computational Visual Media*, 3(3):243–261, September 2017.

[139] Zhe Zhang and Limin Jia. Optimal guidance strategy for crowd evacuation with multiple exits: A hybrid multiscale modeling approach. *Applied Mathematical Modelling*, 90:488–504, February 2021.

[140] Baobao Zou, Chunxia Lu, and Yi Li. Simulation of a hospital evacuation including wheelchairs based on modified cellular automata. *Simulation Modelling Practice and Theory*, 99:102018, February 2020.

[141] Jialiang Kou, Shengwu Xiong, Zhixiang Fang, Xinlu Zong, and Zhong Chen. Multiobjective optimization of evacuation routes in stadium using superposed potential field network based aco. *Computational intelligence and neuroscience*, 2013:369016, June 2013.

[142] Zhixiang Fang, Xinlu Zong, Qingquan Li, Qiuping Li, and Shengwu Xiong. Hierarchical multi-objective evacuation routing in stadium using ant colony optimization approach. *Journal of Transport Geography*, 19(3):443–451, May 2011.

[143] Meiying Jiang, Qibing Jin, and Lisheng Cheng. Effects of ticket-checking failure on dynamics of pedestrians at multi-exit inspection points with various layouts. *International journal of environmental research and public health*, 16(5), March 2019.

[144] Mandy M Salinas, Jason M Wilken, and Jonathan B Dingwell. How humans use

visual optic flow to regulate stepping during walking. *Gait & Posture*, 57:15–20, September 2017.

[145] Guang Zeng, Andreas Schadschneider, Jun Zhang, Shibo Wei, Weiguo Song, and Rui Ba. Experimental study on the effect of background music on pedestrian movement at high density. *Physics Letters. A*, 383(10):1011–1018, March 2019.

[146] Jing Qiao, Lishan Sun, Xiaoming Liu, and Jian Rong. Reducing the impact of speed dispersion on subway corridor flow. *Applied ergonomics*, 65:362–368, November 2017.

[147] Gustavo Hernandez-Mejia and Esteban A Hernandez-Vargas. When is sars-cov-2 in your shopping list? *Mathematical Biosciences*, 328:108434, October 2020.

[148] Miguel A Lopez-Carmona and Alvaro Paricio Garcia. Cellevac: An adaptive guidance system for crowd evacuation through behavioral optimization. *Safety science*, 139:105215, July 2021.

[149] Dirk Helbing, Anders Johansson, and Habib Zein Al-Abideen. Dynamics of crowd disasters: an empirical study. *Physical review. E, Statistical, nonlinear, and soft matter physics*, 75(4 Pt 2):046109, April 2007.

[150] John J Fruin. *Designing for pedestrians: A level-of-service concept*. Number HS-011 999. 1971.

[151] Steven Deere, Hui Xie, Edwin R Galea, David Cooney, and Peter J Lawrence. An evacuation model validation data-set for high-rise construction sites. *Fire Safety Journal*, 120:103118, March 2021.

[152] Milad Haghani and Majid Sarvi. Crowd behaviour and motion: Empirical methods. *Transportation Research Part B: Methodological*, 107:253–294, January 2018.

[153] Zhixiang Fang, Qiuping Li, Qingquan Li, Lee D. Han, and Shih-Lung Shaw. A spaceâ time efficiency model for optimizing intra-intersection vehicleâ pedestrian evacuation movements. *Transportation Research Part C: Emerging Technologies*, 31:112–130, 2013.

[154] Marc Goerigk, Kaouthar Deghdak, and Philipp HeÃ ler. A comprehensive evacuation planning model and genetic solution algorithm. *Transportation Research Part E: Logistics and Transportation Review*, 71:82–97, 2014.

[155] Marin Lujak and Sascha Ossowski. Evacuation route optimization architecture considering human factor. *AI Communications. The European Journal on Artificial Intelligence*, 30(1):1–14, March 2017.

[156] Marin Lujak and Stefano Giordani. Centrality measures for evacuation: Finding agile evacuation routes. *Future Generations Computer Systems: FGCS*, 83:401–412, June 2018.

[157] Hiroaki Yamada and Naoyuki Kamiyama. An information distribution method for avoiding hunting phenomenon in theme parks. In *Proceedings of the 19th International Joint Conference on Autonomous Agents and Multiagent Systems*, pages 2050–2052, 2020.

[158] Hitoshi Shimizu, Takanori Hara, and Tomoharu Iwata. Deep reinforcement learning for pedestrian guidance. In *International Conference on Principles and Practice of Multi-Agent Systems*, pages 334–342, 2020.

[159] Aravinda Ramakrishnan Srinivasan, Farshad Salimi Naneh Karan, and Subhadeep Chakraborty. Pedestrian dynamics with explicit sharing of exit choice during egress through a long corridor. *Physica A: Statistical Mechanics and its Applications*, 468:770–782, February 2017.

[160] Wenjing Yang and Patrick T I Lam. An experimental contingent valuation of users' attitudes towards a crowd management system. *Safety Science*, 121:231–239, 2020.

[161] Emiliano Cristiani and Daniele Peri. Robust design optimization for egressing pedestrians in unknown environments. *Applied Mathematical Modelling*, 72:553–568, August 2019.

[162] Chao Jiang, Zhen Ni, Yi Guo, and Haibo He. Learning humanâ robot interaction for robot-assisted pedestrian flow optimization. *IEEE Transactions on Systems, Man, and Cybernetics: Systems*, 49:797–813, 2019.

[163] Xiaomeng Shi, Zhirui Ye, Nirajan Shiwakoti, Dounan Tang, and Junkai Lin. Examining effect of architectural adjustment on pedestrian crowd flow at bottleneck. *Physica A: Statistical Mechanics and its Applications*, 522:350–364, 2019.

[164] Marina Gravit, Ivan Dmitriev, and Kirill Kuzenkov. Phased evacuation algorithm for high–rise buildings. *MATEC Web of Conferences*, 245:11012, 2018.

[165] Jeongin Koo, Yong Seog Kim, Byung-In Kim, and Keith M Christensen. A comparative study of evacuation strategies for people with disabilities in high-rise building evacuation. *Expert systems with applications*, 40(2):408–417, February 2013.

[166] Sai-Keung Wong, Yu-Shuen Wang, Pao-Kun Tang, and Tsung-Yu Tsai. Optimized evacuation route based on crowd simulation. *Computational Visual Media*, 3(3):243–261, 2017.

[167] Kalyanmoy Deb, Amrit Pratap, Sameer Agarwal, and TAMT Meyarivan. A fast and elitist multiobjective genetic algorithm: Nsga-ii. *IEEE transactions on evolutionary computation*, 6(2):182–197, 2002.

[168] A. Garcimartín, I. Zuriguel, J.M. Pastor, C. MartÃn-Gómez, and D.R. Parisi. Experimental evidence of the "faster is slower" effect. *Transportation Research Procedia*, 2:760–767, 2014.

[169] Frederik Styns, Leon van Noorden, Dirk Moelants, and Marc Leman. Walking on music. *Human Movement Science*, 26(5):769–785, 2007.

[170] Shigeyuki Ikeda, Takayuki Nozawa, Ryoichi Yokoyama, Atsuko Miyazaki, Yukako Sasaki, Kohei Sakaki, and Ryuta Kawashima. Steady beat sound facilitates both coordinated group walking and inter-subject neural synchrony. *Frontiers in Human Neuroscience*, 11:147, 2017.

[171] Inês A Ferreira, Maria Johansson, Catharina Sternudd, and Ferdinando Fornara. Transport walking in urban neighbourhoods—impact of perceived neighbourhood qualities and emotional relationship. *Landscape and Urban Planning*, 150:60–69, June 2016.

[172] Puay Ping Koh and Yiik Diew Wong. Comparing pedestrians' needs and behaviours in different land use environments. *Journal of Transport Geography*, 26:43–50, January 2013.

[173] Erica D Kuligowski and Dennis S Mileti. Modeling pre-evacuation delay by occupants in world trade center towers 1 and 2 on september 11, 2001. *Fire Safety Journal*, 44(4):487–496, May 2009.

[174] M F Sherman, M Peyrot, L A Magda, and R R M Gershon. Modeling pre-evacuation delay by evacuees in world trade center towers 1 and 2 on september 11, 2001: A revisit using regression analysis. *Fire Safety Journal*, 46(7):414–424, October 2011.

[175] A&A. Simtread. `https://www.aanda.co.jp/products/simtread/`. Accessed: 2021-10-18.

[176] PTV. Viswalk. `https://www.ptvgroup.com/en/solutions/products/ptv-viswalk/`. Accessed: 2021-10-18.

[177] Bentley. Legion. `https://www.bentley.com/en/products/brands/legion`. Accessed: 2021-10-18.

[178] Fire Safety Engineering Group. buildingexodus. `https://fseg.gre.ac.uk/exodus/exodus_products.html`. Accessed: 2021-10-19.

[179] Lachmi Khemlani. Designing for people. `https://prod-bentleycdn.azureedge.net/-/media/files/documents/white-papers/wp_designing_for_people_ltr_en_lr.pdf?la=it-it&modified=00010101000000`. Accessed: 2021-10-18.

[180] Hélène Macher, Tania Landes, and Pierre Grussenmeyer. From point clouds to building information models: 3d semi-automatic reconstruction of indoors

of existing buildings. *NATO Advanced Science Institutes Series E: Applied Sciences*, 7(10):1030, October 2017.

[181] András Sóbester, Alexander IJ Forrester, David JJ Toal, Es Tresidder, and Simon Tucker. Engineering design applications of surrogate-assisted optimization techniques. *Optimization and Engineering*, 15(1):243–265, 2014.

[182] Pierre-Elouan Réthoré, Peter Fuglsang, Gunner C Larsen, Thomas Buhl, Torben J Larsen, and Helge A Madsen. Topfarm: Multi-fidelity optimization of wind farms. *Wind Energy*, 17(12):1797–1816, 2014.

[183] Shusuke Shigenaka, Shunki Takami, Masaki Onishi, Tomohisa Yamashita, and Itsuki Noda. Estimating pedestrian flow in crowded situations with data assimilation. In *Proceedings of the 10th International Workshop on Optimization in Multi-Agent Systems Agents@ AAMAS (OptMAS)*, 2019.

[184] Andrey Rudenko, Luigi Palmieri, Michael Herman, Kris M Kitani, Dariu M Gavrila, and Kai O Arras. Human motion trajectory prediction: a survey. *The International Journal of Robotics Research*, 39(8):895–935, July 2020.

[185] Weichen Liao, Armel U Kemloh Wagoum, and Nikolai W F Bode. Route choice in pedestrians: determinants for initial choices and revising decisions. *Journal of the Royal Society, Interface / the Royal Society*, 14(127):20160684, February 2017.

[186] Ruggiero Lovreglio, Enrico Ronchi, and Daniel Nilsson. A model of the decision-making process during pre-evacuation. *Fire Safety Journal*, 78:168–179, November 2015.

[187] Stéphanie Cœugnet, Aurélie Dommes, Sabrina Panëels, Aline Chevalier, Fabrice Vienne, Nguyen-Thong Dang, and Margarita Anastassova. Helping older pedestrians navigate unknown environments through vibrotactile guidance instructions. *Transportation Research. Part F, Traffic Psychology and Behaviour*, 58:816–830, October 2018.

[188] Cagatay Catal, Akhan Akbulut, Berkay Tunali, Erol Ulug, and Eren Ozturk. Evaluation of augmented reality technology for the design of an evacuation training game. *Virtual Reality*, 24(3):359–368, 2020.

[189] Jing Lin, Lijun Cao, and Nan Li. Assessing the influence of repeated exposures and mental stress on human wayfinding performance in indoor environments using virtual reality technology. *Advanced Engineering Informatics*, 39:53–61, January 2019.

[190] Ruggiero Lovreglio, Vicente Gonzalez, Zhenan Feng, Robert Amor, Michael Spearpoint, Jared Thomas, Margaret Trotter, and Rafael Sacks. Prototyping virtual reality serious games for building earthquake preparedness: The auckland city hospital case study. *Advanced Engineering Informatics*, 38:670–682, 2018.

[191] G Keith Still. Crowd disasters. `https://www.gkstill.com/ExpertWitness/CrowdDisasters.html`. Accessed: 2021-2-11.

[192] Gabriele Bernardini, Silvia Santarelli, Enrico Quagliarini, and Marco D'Orazio. Dynamic guidance tool for a safer earthquake pedestrian evacuation in urban systems. *Computers, environment and urban systems*, 65:150–161, September 2017.

[193] Minji Choi and Seokho Chi. Optimal route selection model for fire evacuations based on hazard prediction data. *Simulation Modelling Practice and Theory*, 94:321–333, July 2019.

[194] Wenbo Huang, Yanyan Chen, Shushan Chai, and Huibo Bi. Dynamic guidance strategy for pedestrian travel in large-scale activity under harsh environment. *Journal of Advanced Transportation*, 2022, May 2022.

[195] Xinlu Zong, Shengwu Xiong, Zhixiang Fang, and Qiuping Li. Multi-objective optimization for massive pedestrian evacuation using ant colony algorithm. In *Advances in Swarm Intelligence*, pages 636–642. Springer Berlin Heidelberg, 2010.

[196] Mitko Aleksandrov, Cheng Cheng, Abbas Rajabifard, and Mohsen Kalantari. Modelling and finding optimal evacuation strategy for tall buildings. *Safety science*, 115:247–255, June 2019.

[197] Volodymyr Mnih, Koray Kavukcuoglu, David Silver, Alex Graves, Ioannis Antonoglou, Daan Wierstra, and Martin Riedmiller. Playing atari with deep reinforcement learning. December 2013.

[198] Gabriel Dulac-Arnold, Nir Levine, Daniel J Mankowitz, Jerry Li, Cosmin Paduraru, Sven Gowal, and Todd Hester. An empirical investigation of the challenges of real-world reinforcement learning. March 2020.

[199] M Reymond and A Nowé. Pareto-dqn: Approximating the pareto front in complex multi-objective decision problems. *ala2019.vub.ac.be*, 2019.

[200] Zhi-Hui Zhan, Lin Shi, Kay Chen Tan, and Jun Zhang. A survey on evolutionary computation for complex continuous optimization. *Artificial Intelligence Review*, 55(1):59–110, January 2022.

[201] Qi-Te Yang, Zhi-Hui Zhan, Sam Kwong, and Jun Zhang. Multiple populations for multiple objectives framework with bias sorting for many-objective optimization. *IEEE Transactions on Evolutionary Computation*, pages 1–1, 2022.

[202] Si-Chen Liu, Zong-Gan Chen, Zhi-Hui Zhan, Sang-Woon Jeon, Sam Kwong, and Jun Zhang. Many-objective job-shop scheduling: A multiple populations for multiple objectives-based genetic algorithm approach. *IEEE transactions on cybernetics*, PP, September 2021.

[203] Xin Zhang, Zhi-Hui Zhan, Wei Fang, Pengjiang Qian, and Jun Zhang. Multipopulation ant colony system with knowledge-based local searches for multiobjective supply chain configuration. *IEEE Transactions on Evolutionary Computation*, 26(3):512–526, June 2022.

[204] Jian-Yu Li, Xin-Yi Deng, Zhi-Hui Zhan, Liang Yu, Kay Chen Tan, Kuei-Kuei Lai, and Jun Zhang. A multipopulation multiobjective ant colony system considering travel and prevention costs for vehicle routing in covid-19-like epidemics. *IEEE Transactions on Intelligent Transportation Systems*, pages 1–15, 2022.

[205] Olive Niyomubyeyi, Petter Pilesjö, and Ali Mansourian. Evacuation planning optimization based on a multi-objective artificial bee colony algorithm. *ISPRS International Journal of Geo-Information*, 8(3):110, February 2019.

[206] Hitoshi Shimizu, Takanori Hara, and Tomoharu Iwata. Deep reinforcement learning for pedestrian guidance. In *PRIMA 2020: Principles and Practice of Multi-Agent Systems: 23rd International Conference, Nagoya, Japan, November 18–20, 2020, Proceedings 23*, pages 334–342, 2021.

[207] Yiran Xue, Rui Wu, Jiafeng Liu, and Xianglong Tang. Crowd evacuation guidance based on combined action reinforcement learning. *Algorithms*, 14(1):26, January 2021.

[208] Yongliang Yang, Bahare Kiumarsi, Hamidreza Modares, and Chengzhong Xu. Model-free λ-policy iteration for discrete-time linear quadratic regulation. *IEEE transactions on neural networks and learning systems*, PP, August 2021.

[209] Yongliang Yang, Hamidreza Modares, Kyriakos G Vamvoudakis, Wei He, Cheng-Zhong Xu, and Donald C Wunsch. Hamiltonian-driven adaptive dynamic programming with approximation errors. *IEEE transactions on cybernetics*, 52(12):13762–13773, December 2022.

[210] Yongliang Yang, Yongping Pan, Cheng-Zhong Xu, and Donald C Wunsch. Hamiltonian-driven adaptive dynamic programming with efficient experience replay. *IEEE transactions on neural networks and learning systems*, PP, October 2022.

[211] Diederik M Roijers, Peter Vamplew, Shimon Whiteson, and Richard Dazeley. A survey of multi-objective sequential decision-making. *The journal of artificial intelligence research*, 48(1):67–113, October 2013.

[212] Hossam Mossalam, Yannis M Assael, Diederik M Roijers, and Shimon Whiteson. Multi-objective deep reinforcement learning. October 2016.

[213] Diederik Marijn Roijers, Shimon Whiteson, and Frans A Oliehoek. Computing convex coverage sets for faster multi-objective coordination. *The journal of artificial intelligence research*, 52:399–443, March 2015.

[214] Diqi Chen, Yizhou Wang, and Wen Gao. Combining a gradient-based method and an evolution strategy for multi-objective reinforcement learning. *Applied intelligence*, 50(10):3301–3317, October 2020.

[215] Kristof Van Moffaert and Ann Nowé. Multi-objective reinforcement learning using sets of pareto dominating policies. *Journal of machine learning research: JMLR*, 15(107):3663–3692, 2014.

[216] Hisao Ishibuchi, Ryo Imada, Yu Setoguchi, and Yusuke Nojima. Reference point specification in hypervolume calculation for fair comparison and efficient search. In *Proceedings of the Genetic and Evolutionary Computation Conference*, GECCO '17, pages 585–592, New York, NY, USA, July 2017. Association for Computing Machinery.

[217] Carlos A Coello Coello and Margarita Reyes Sierra. A study of the parallelization of a coevolutionary multi-objective evolutionary algorithm. In *MICAI 2004: Advances in Artificial Intelligence*, pages 688–697. Springer Berlin Heidelberg, 2004.

[218] D Helbing and P Molnár. Social force model for pedestrian dynamics. *Physical review. E, Statistical physics, plasmas, fluids, and related interdisciplinary topics*, 51(5):4282–4286, May 1995.

[219] Shusuke Shigenaka Yusaku Kato and Masaki Onishi. Multi-fidelity optimization

for pedstrian route guidance. In *The 13th Workshop on Optimization and Learning in Multiagent Systems*, 2022.

[220] Akiko Ikenaga and Sachiyo Arai. Inverse reinforcement learning approach for elicitation of preferences in multi-objective sequential optimization. In *2018 IEEE International Conference on Agents (ICA)*, pages 117–118, July 2018.

[221] Koh Takeuchi, Ryo Nishida, Hisashi Kashima, and Masaki Onishi. Grab the reins of crowds: Estimating the effects of crowd movement guidance using causal inference. In *Proceedings of the 20th International Conference on Autonomous Agents and MultiAgent Systems*, AAMAS '21, pages 1290–1298, Richland, SC, May 2021. International Foundation for Autonomous Agents and Multiagent Systems.

[222] Song, Xiang, and Ph. D. Massachusetts Institute of Technology. *Personalization of future urban mobility.* PhD thesis, Massachusetts Institute of Technology, 2018.

[223] Mazen(mazen Salah) Danaf. *Online discrete choice models : applications in smart mobility.* PhD thesis, Massachusetts Institute of Technology, 2019.

[224] Himan Abdollahpouri, Gediminas Adomavicius, Robin Burke, Ido Guy, Dietmar Jannach, Toshihiro Kamishima, Jan Krasnodebski, and Luiz Pizzato. Multistakeholder recommendation: Survey and research directions. *User modeling and user-adapted interaction*, 30(1):127–158, March 2020.

[225] Yong Zheng. Multi-stakeholder recommendation: Applications and challenges. July 2017.

List of Publications

Journals

1. Ryo Nishida, Shusuke Shigenaka, Yusaku Kato, and Masaki Onishi. Recent Advances in Crowd Movement Space Design and Control using Crowd Simulation. *Transactions of the Japanese Society for Artificial Intelligence* (Japanese), 37 (2): J–LB1_1–16, 2022.

2. Ryo Nishida, Ryo Kanamori, Masaki Onishi, Itsuki Noda, and Koichi Hashimoto. Simulation Analysis on Benefits of Introducing Meeting Points into On-demand Shared Mobility Services *IEEE Access*, 2022.

Proceedings of International Conferences

3. Ryo Nishida, Masaki Onishi, and Koichi Hashimoto. Multiple Destinations Pedestrian Model using an Improved Social Force Model. *The 10th International Workshop on Agents in Traffic and Transportation (ATT)*, 2018.

4. Ryo Nishida, Masaki Onishi, and Koichi Hashimoto. Construction of a Route Choice Model for Application to a Pedestrian Flow Simulation. *International Workshop on Behavior analysis and Recognition for knowledge Discovery (BiRD)*, 2019.

5. Ryo Nishida, Ryo Kanamori, and Itsuki Noda. Modeling of a mode choice behavior toward agent-based Mobility as a Service simulation. *The 26th International Symposium on Artificial Life and Robotics (AROB)*, 2021.

6. Ryo Nishida, Ryo Kanamori, Masaki Onishi, Itsuki Noda and Koichi Hashimoto. Neural Choice Model for Representing Heterogeneous and Nonlinear Utility. *The 27th International Symposium on Artificial Life and Robotics (AROB)*, 2022.

7. Ryo Nishida, Masaki Onishi, and Koichi Hashimoto. Crowd simulation incorporating a route choice model and similarity evaluation using real large-scale data. *The 22th International Conference on Autonomous Agents and Multiagent Systems (AAMAS)*, 2023.

Others

8. (Submitted) Ryo Nishida, Yuki Tanigaki, Masaki Onishi, and Koichi Hashimoto. Multi-objective Deep Reinforcement Learning for Crowd Route Guidance Optimization.*Journal of Advanced Transportation.*

Awards

1. The 27th International Symposium on Artificial Life and Robotics (AROB2022) Young Author Award (Ryo Nishida, Ryo Kanamori, Masaki Onishi, Itsuki Noda and Koichi Hashimoto. Neural Choice Model for Representing Heterogeneous and Nonlinear Utility.)

2. The 18th ITS Symposium 2022 Best Poster Award, (Ryo Nishida, Ryo Kanamori, and Itsuki Noda. Analysis of an App usage data of MaaS experiment in Shizuoka City.) (Japanese)

3. The 64th Annual Conference of the Institute of Systems, Control and Information Engineers (SCI'20) Student Presentation Award, (Ryo Nishida, Masaki Onishi, Itsuki Noda, and Koichi Hashimoto. Improved reproducibility of large-scale pedestrian flow simulations with route choice modeling.) (Japanese)

Acknowledgments

First and foremost I would like to offer my sincerest gratitude to my supervisor, Professor Koichi HASHIMOTO, who has supported me throughout my Ph.D with his patience and knowledge. I attribute the level of my Ph.D degree to his encouragement and effort, and without him this dissertation would not have been completed or written.

I would like to thank to the other members of my thesis committee, Professor Takayuki OKATANI, Professor Takamasa IRYO, and Associate Professor Yusuke HARA for their comments and suggestions with their professional background.

I would also like to thank Masaki ONISHI at National Institute of Advanced Industrial Science and Technology (AIST), Itsuki NODA at Hokkaido University, Ryo KANAMORI at Nagoya University for the collaboration research. Their advices and comments from his professional knowledge always help for our research activity.

My experience as a graduate student has been much excellent thanks to all fellow members of AIST, Artificial Intelligence Research Center, Social Intelligence Research Team. For their friendship, and for many enlightening and edifying discussion and collaborations, I would like to thank particularly Shusuke SHIGENAKA, Yusaku KATO, and Yuki TANIGIAKI. I would also like to thank the secretaries, Mrs. Kaori ICHINOHE, Mrs. Akkiko KANAZAWA, Mrs. Sanae AMITA, and Mrs. Naomi NOGUCHI for all their supports.

In addition, the Systems Science of Bio-navigation project gave me the opportunity to discuss with a wide variety of researchers and laid the foundation for me to carry out my research with many researchers.

Last but not least, I dedicate this thesis to my family, especially my parents, who gave unconditional support and encouragement which made this work possible.